1-1-2007

Survival and proliferation of an opportunistic pathogen in mixed species biofilms

Mahtab Ghadakpour
Ryerson University

NOTE TO USERS

This reproduction is the best copy available.

SURVIVAL AND PROLIFERATION OF AN OPPORTUNISTIC PATHOGEN IN MIXED SPECIES BIOFILMS

By: Mahtab Ghadakpour

Bachelor of Science (Applied Chemistry and Biology), Ryerson University

A thesis presented to Ryerson University in partial fulfillment of the requirements for the degree of Master of Applied Science in the Program of Environmental Applied Science and Management

Toronto, Ontario, Canada, 2007

Author's Declaration

I hereby declare that I am the sole author of this thesis.

I authorize Ryerson University to lend this thesis to other institutions or individuals for the purpose of scholarly research.

I further authorize Ryerson University to reproduce this thesis by photocopying or by other means, in total or in part, at the request of other institutions or individuals for the purpose of scholarly research.

Abstract

Survival and Proliferation of an Opportunistic Pathogen in Mixed Species Biofilms

By: Mahtab Ghadakpour

Master of Applied Science
Environmental Applied Science and Management
Ryerson University, Toronto, 2007

The purpose of this study was to examine the interaction between an opportunistic pathogen and mixed community biofilms, in terms of integration, proliferation and subsequent release. *Pseudomonas aeruginosa* PAO1 was used as the test strain in conjuction with community biofilms obtained from sink drains. Confocal laser scanning microscopy (CLSM) analysis showed that PAO1 could successfully incorporate into the community. The relative abundance of PAO1 in the biofilms was dependant on the order of inoculation. Biofilm cell yield was studied using conventional plate counting, CLSM and flow cytometry, which revealed that PAO1 became a dominant community member. Cells were released from the biofilms in the form of single cells, duplets and aggregates of various sizes. Detached aggregates were often observed to contain PAO1 and community members. It was also determined that association with communities provided PAO1 with increased protection against EDTA but not against streptomycin, when applied at planktonic minimal inhibitory concentration.

Acknowledgements

I would like to express my gratitude to my supervisor Dr. Gideon Wolfaardt for his support, invaluable advice and constant encouragement. I would also like to thank my examining committee members Dr. Steven Liss and Dr. Ian Droppo for their interest in this research and their time and effort in reviewing this thesis.

My sincere thanks go to members of the Wolfaardt lab, especially Dr. Murray Gardner, Elanna Bester, Otini Kroukamp, and Andrew Sousa, for all their help and support and for making this experience an enjoyable one. I am grateful to Jag Sandhu and Mahban Ghadakpour for their help with the illustrations.

I am deeply indebted to my parents for their unconditional love, understanding, support and encouragement throughout my life. I am also grateful to all my family and friends for all the love and support, without which this work would not be possible.

Table of Contents

List of Tables

List of Figures

Abbreviations

BP	Band pass
CLSM	Confocal laser scanning microscopy
DNA	Deoxyribonucleic acid
EDTA	Ethylenediaminetetraacetic acid
EPS	Extracellular polymeric substances
GFP	Green fluorescent protein
LA	Luria agar
LB	Luria broth
LP	Long pass
MBEC	Minimal biofilm eradication concentration
MIC	Minimal inhibitory concentration
OD	Optical density
RFP	Red fluorescent protein
RNA	Ribonucleic acid
RPM	Revolutions per minute
SM	Streptomycin
SMEB	Sucrose magnesium electroporation buffer
TSA	Trypticase soy agar
TSB	Trupticase soy broth
UV	Ultra violet

CHAPTER 1 INTRODUCTION

1.1 Background

Biofilms are ubiquitous in the environment. They are responsible for many diseases and nosocomial infections. Most biofilms are highly resistant to antibiotics and often require high dosages and long-term treatments (Parsek et al., 2003). In industry, biofilms are responsible for billions of dollars in damages caused by biofouling and biocorrosion of products or damages to equipments (Lewandowski et al., 2002).

On the other hand, biofilms are beneficial in treating wastes such as sewage, industrial waste streams or contaminated ground waters (Freitas dos Santos et al., 1997). Biofilm forming microorganisms are also used in bioremediation of contaminated soil and aquatic sediments. In addition, bacteria attached to plant roots of most crops facilitate recycling of nutrients, resulting in higher profit yields (Sturman et al., 1995).

It is generally accepted that the presence of pathogens in biofilms give them certain advantages, making them difficult to treat. Biofilms, including associated extracellular polymeric substances (EPS), provide for higher levels of nutrient availability, and in the case of disease causing bacteria such as in cystic fibrosis, a protection against the host immune response (Parsec et al., 2003).

In the lungs of cystic fibrosis patients, pathogens exist as mixed communities, which give them an added advantage of quorum sensing. *In vitro* studies involving mixed biofilm communities have demonstrated the ability of *Burkholderia cepacia* to identify signals produced by *Pseudomonas aeruginosa,* which is believed to be a significant factor in their colonization of patients' lungs (Lens et al., 2003).

Although the advantages of opportunistic pathogens existing as parts of

community aggregates such as biofilms and flocs are recognized, most studies have focused on pure cultures as opposed to the more realistic conditions of mixed communities.

P. aeruginosa, an opportunistic pathogen, likely owes its success to existing as part of EPS protected biofilms. The biofilm provides for a well protected environment against biocides. Mixed species biofilms are also known to yield cells that will proliferate and colonize new surfaces. In cases where living conditions become harsh, planktonic cells die, while those that are a part of the biofilm survive (Baltch et al., 1994).

The research was designed to study the ability of a strain of *P. aeruginosa* to survive and proliferate in mixed communities of aggregates.

1.2 Hypothesis

This study tests the hypothesis that mixed communities provide a protective microenvironment in which pathogens such as *P. aeruginosa* improve their ability to survive and proliferate. It is believed that the environment created by the multi-species biofilms allow for protection against environmental stress. Furthermore, the test strain is transported as part of mixed-species aggregates following detachment from the biofilm.

1.3 Purpose

The main objective of this research was to study the interactions and integration for improved survivability and proliferation of an opportunistic pathogen in heterogeneous biofilm communities. In order to fulfill this objective, *P. aeruginosa* PAO1 was used as a test strain in the context of a mixed species biofilm sample obtained

from a sink drain. The study intended to determine whether incorporation of PAO1 into the drain community was stable and whether this association offered advantages to the test strain in terms of survivability within the biofilm as well as its subsequent release. The study of detached pathogenic cells from a biofilm is significant since through this process, the organism gains the potential to colonize other environments, including transplants and other surfaces in the human body.

Several techniques including plate counting, microscopy and flow cytometry were used to find whether the test strain detached from different scenarios with respect to the order of inoculation of the mixed community and the test strain. The experiments also intended to reveal the relative abundance of the test strain released from biofilms, and whether the detachment was in the form of single cells or as part of aggregates.

Mixed-species biofilms with incorporated PAO1 were disturbed by chemical, biological and physical means. The disturbance factors used in this study were the antibiotic streptomycin, the chelating agent EDTA and erosion caused by and an increase in the flow rate.

CHAPTER 2 LITERATURE REVIEW

2.1 Microbial Aggregates

A vast majority of microorganisms exist in the form of aggregates. 'Microbial aggregates' is a term which encompasses biofilms, flocs and sludges, which are accumulations of prokaryotic and eukaryotic unicellular organisms, extracellular polymeric substances, multivalent cations, inorganic particles, biogenic material as well as colloidal and dissolved compounds (Flemming et al., 2000b).

Although, the aggregation property of microbes is genetically inducible, environmental conditions can cause changes in the physiology resulting in a change from a dispersed to an aggregate state. Aggregation has been shown to be advantageous to microbes due to interaction between adjacent organisms (Kosaric et al., 1990).

2.2 Biofilms

Biofilms are the most common structural entity of microorganisms in both natural and industrial systems (Chandra et al., 2004). A biofilm is defined as a community of microbes embedded in an organic polymer matrix, adhering to a surface (Varnam et al., 2000). Fossil records as old as 3.3-3.4 billion years have confirmed the existence of biofilms as a primitive prokaryotic form of life (Hall-Stoodley et al., 2004). Most natural biofilms exist as mixed communities and are structurally and chemically heterogeneous.

Despite the history and ubiquity of biofilms, much of the work surrounding the study of bacteria has been on pure cultures and planktonic bacteria under artificial conditions in the laboratory. This may be due to the fact that pure culture bacteria growing in suspension are much easier to study than biofilms. Bacterial biofilms are

complex structures with numerous microenvironments and a concomitant number of distinct bacterial phenotypes and it has even been suggested that they should be studied as multicellular organisms (Marsh et al., 2000; Braxton et al., 2005).

2.2.1 Biofilm Formation

An explanation provided for existing in this form of growth is that biofilms provide a means of protection against harsh conditions of primitive earth, including extreme temperatures, pH, and exposure to ultraviolet light. Benefits to bacterial cells within a biofilm include the opportunity to develop complex interactions between individual cells that have led to signaling pathways and chemotactic motility (Stoodley et al., 2001).

Furthermore, the close cell to cell proximity and surfaces allow for nutrients to be more readily available (Stoodley et al., 2001). Nutrients usually absorb to surfaces and as a result they are often present at higher levels than in bulk solutions. It is partially due to this phenomenon that the rate of microbial metabolism is much higher in biofilms. Bacteria growing on surfaces are normally much greater in number and have higher activity compared to planktonic cells, due to adsorption effects. In some cases, the surface itself may be a nutrient, for instance a particle of organic matter, where attached microorganisms catabolize organic or inorganic nutrients directly from the surface of the particle (Madigan et al., 1997).

Other advantages to biofilms include protection against UV exposure, metal toxicity, highly acidic environments, dehydration and salinity, phagocytosis as well as antibiotics and other antimicrobial agents. The resistance of biofilms to biocidal agents

has been attributed to a number of mechanisms including one that involves the physiological state of biofilm organisms. Many cells within the deeper sections of the biofilm are physically shielded by those at the water interface layer. In addition, the existence of stationary phase dormant cells in biofilms plays an important role in resistance to antimicrobials such as β-lactams in Gram-positive bacteria (Stoodley et al., 2001).

A widely discussed explanation for antibiotic resistance is the barrier properties of the extracellular polymeric substances (EPS). This slime matrix is primarily responsible for protection against reactive agents such as bleach or superoxides, charged metals or large antimicrobial agents like immunoglobulin. These substances are either neutralized or bound and diluted by the EPS to sublethal concentrations. The EPS is also capable of protection against UV light, dehydration, and localization of enzymatic activity (Stoodley et al., 2001).

Despite the established notion of physical protection offered by the EPS and the biofilm matrix, Gilbert et al. (2002) have described this biofilm property as a means of delaying the death of cells within the community. Rather, they attribute antibiotic resistance to the existence of subpopulations of resistant phenotypes, known as persisters.

One hypothesis provided is that upon exposure to treatment agents, the majority of sublethally damaged cells commit suicide through apoptosis, while providing protection to the persisters, which survive, as they are suggested to be defective or repressed in apoptosis. Another proposed explanation for the existence of persisters is that application of stress on biofilms cause adoption of a viable, nonculturable state of quiescence, which is up-regulated in low nutrient level sections of the biofilm allowing

for survival against metabolically acting biocides. It has also been suggested that extracellular signals released from killed cells may be responsible for creation of a state of resistance. These signals, termed alarmones, result from premature death of peripheral cells and alert cells in the deeper sections of the biofilm into a resistant state (Gilbert et al., 2002).

2.2.2 Benefits of biofilms and the complications caused by them in the industry and medical environments

Biofilms are the cause of many diseases such as the development of kidney stones, bacterial endocarditis and Legionnaire disease. They are also responsible for a range of nosocomial infections in burn patients, cystic fibrosis patients and those with medical implants. Most biofilms are highly resistant to antibiotics and often require high dosages and long-term treatments (Parsek et al., 2003). Certain oral bacteria have the ability to store iodophilic polysaccharides or glycogen-like molecules that cause prolonged lactic acid formation resulting in decalcification of teeth (Phinny et al., 2004).

In industry, biofilms are responsible for billions of dollars in damages caused by contamination of products or damages to equipments. Biofouling and biocorrosion are often observed in water-based processes, pulp and paper manufacturing, as well as cooling tower operations (Lewandowski et al., 2002).

Although biofilm-forming microorganisms may be considered destructive entities in many cases, they do have the ability to break down certain suspended solids and soluble substances of organic and mineral origin, which is a property that makes them beneficial in treating wastes such as sewage, industrial waste streams or contaminated

ground waters (Capdeville et al., 1992; Freitas dos Santos et al., 1991).

Another property of certain biofilm-forming microorganisms that is of advantage is their ability to degrade soil contaminants. Bioremediation is currently used as an effective means of cleaning soil and aquatic sediments after accidental chemical spills such as chlorinated hydrocarbons. In addition, biofilms attached to plant roots of certain crops are used to recycle nutrients, resulting in higher profit yields (Sturman et al., 1995).

2.3 Mixed-species biofilms

Natural biofilms are comprised of multiple species of microorganisms enclosed in EPS. It is important to study these mixed community biofilms since they behave differently from pure culture biofilms due to the various interactions that exist among these complex cultures (Bryers, 1992).

Microorganisms existing in microbial communities enjoy benefits such as a broader habitat range for colonization, metabolic diversity and efficiency, as well as higher resistance to stressful conditions of the environment and host defense. In some cases pathogens in microbial communities also benefit from pathogenic synergism, which is an increased ability to cause disease (Marsh et al., 2000).

Bacterial cells, in a mixed community, may interact cooperatively or competitively. Synergic interactions have been shown to promote biofilm biomass as well as an increase in resistance to antibiotics and bacterial invasion (Burmølle et al., 2006). These positive interactions may also be used to explain the protection of certain bacterial biofilms against chlorinated alkaline solutions and other adverse environments (Leriche et al., 2003)

In addition to the positive interactions, bacteria in mixed-species biofilms may compete for resources. A study by Valle et al. (2006) showed an antagonistic effect on biofilms caused by bacterial interference via signaling polysaccharides and surface active compounds. Competitive interactions differ greatly between planktonic and biofilm communities. In planktonically grown bacteriocin-producing populations of two different species, it has been shown that one strain is always out-competed, while in the case of biofilms bacteriocin-producing and bacteriocin-sensitive strains are able to coexist (Tait et al., 2002).

In a study by Roa et al. (2005) the individuality of bacterial species has been used to demonstrate competitive dominance among mixed-species biofilms. In this case, two marine bacteria, namely *Roseobacter gallaeciensis* and *Pseudomonas tunicate*, proved to be superior competitors. The proliferation of these species has been attributed to their ability to rapidly form microcolonies and the production of antibacterial compounds.

The extent of interaction between the species of biofilm communities signifies the importance of recognizing the 'community lifestyle'. In fact, some researchers believe that these biofilm communities should be viewed as 'multicellular organisms' in which there exists a division of labour in terms of specific spatial organization and signaling networks between community members (Marsh et al., 2000).

As mentioned previously, mixed-species biofilms are ubiquitous in natural and engineered systems. For instance, marine biofilms, composed of bacteria and microaglae, are important factors in large-scale changes within intertidal systems. Heterotrophic bacteria are significant in transformations and remineralization of organic carbon, nitrogen and other nutrients throughout oceans while autotrophic eukaryotes, such as

diatoms are predicted to be primary producers in these systems (Decho, 2000).

2.3.1 Human diseases caused by mixed biofilms

Mixed-species biofilms are major contributors to nosocomial infections and drinking water related outbreaks of disease. Waterborne pathogens such as *Pseudomonas aeruginosa*, *Stenotrophomonas maltophilia*, *Chryseobacterium* species, non-tuberculosis mycobacteria, and *Legionella* species cause infections in healthcare facilities. Transmission of pathogens from water distribution systems may occur through contact, ingestion, aspiration, and aerosolization of potable water, or via hands of healthcare professionals (Squier et al., 2000).

Mixed-species biofilms cause infections associated with native and prosthetic valve endocarditis, vascular catheters, breast implants, urinary catheters, total joint replacements and otolaryngologic infections. In these infections the biofilm is often not as pathogenic as the inflammatory response of the host. For instance, the tissue damage in cystic fibrosis patients is caused by frustrated neurophils, which continuously fire oxidative bursts at biofilms that they cannot eliminate (Braxton et al., 2005).

Another example of biofilm communities is dental plaque. These biofilms have a structured architecture with a diverse composition of gram-positive and gram-negative bacteria. Plaque microorganisms have increased metabolic efficiency, high resistance to stress and enhanced virulence (Marsh, 2005).

Due to the fact that many practitioners are still unfamiliar with the concept of biofilms, most traditional pharmaceutical therapies and host defense mechanisms are aimed at treating planktonic bacteria and are thus largely ineffective against biofilm

bacteria. Characteristics of biofilms that account for the difficulty through which biofilms may be treated include the ability of bacteria to exist in an organized community surrounded by a slimy EPS, their high resistance to antibiotics, complications caused by the fact that when biofilms are cultured they are either undetected or underestimated, and their ability to release planktonic cells or clusters into other environments (Braxton et al., 2005).

2.4 Biofilm detachment and spread

Although not fully understood, attachment of microorganisms to surfaces and the physiological changes that biofilms undergo have been studied extensively. While a number of researchers have acknowledged the importance of biofilm detachment, this process has been largely overlooked (Moore et al., 2000).

Release of cells from a biofilm occurs continuously as well as through erosion and sloughing. Although increasing the rate of biofilm detachment has been used to prevent biofilm accumulation, this process has been shown to cause serious implications (Moore et al., 2000). Detachment provides an opportunity through which cells migrate from heavily colonized areas to areas of higher surface-adsorbed nutrient availability. The detached cells may be single cells or in the form of aggregates. In the case of infective endocarditis, a biofilm infection of the heart and valves, aggregates or single cells may be released into the bloodstream. Another example of complications caused by biofilm detachment is the case in which a pathogenic organism, with a low infective dose, in potable water biofilms is released into an environment that will allow contact with individuals (Donlan, 2002).

The process of shedding daughter cells by actively growing cells in a biofilm may

be explained by the changes in the surface hydrophobicity of newly divided cells. It has been demonstrated that hydrophobicity of newly detached cells in *Escherichia coli* and *P. aeruginosa* biofilms is lower than that of chemostat-intact biofilms and resuspended biofilm cells. Furthermore, surface hydrophobicity of these daughter cells steadily increases upon incubation and growth (Donlan, 2002).

There are four main processes through which aggregates are detached from a biofilm. The first is the continuous removal of small portions of the biofilm through erosion or shearing. The rate of erosion increases with biofilm thickness and fluid shear at the biofilm-bulk liquid interface. As the flow rate increases, the hydrodynamic boundary layer decreases, which causes turbulence and mixing along the biofilm surface. Another process is sloughing which is rapid and massive removal of the biofilm. Sloughing occurs randomly in situations of nutrient or oxygen depletion within the biofilm matrix and is often observed in thicker biofilms that have been developed in nutrient-rich environments. Detachment may also be caused by abrasion, a process that involves collision of the bulk fluid with the biofilm. This form of biofilm detachment is often seen in fluidized beds, filters, and particle-laden environments such as surface waters. The type of dispersal influences phenotypic characteristics of the released cells. Eroded and sloughed cells in the form of aggregates tend to retain biofilm phenotype, while released daughter cells are more likely to exhibit characteristics of planktonic cells (Donlan, 2002). Biofilm grazing by larger organisms may also be considered an indirect cause of detachment (Moore et al., 2000).

It has been observed that the shape of cells that form biofilms influences the form of detachment. Based on the shape of cells and biofilms produced by species, three main

mechanisms of biofilm dispersal has been suggested by Hall-Stoodley et al. (2005). These mechanisms include swarming dispersal, as seen in *Pseudomonas aeruginosa* biofilms, clumping dispersal in *Staphylococccus aureus* biofilms and surface dispersal in *Mycobacterium fortuitum.* As seen in figure 2.1, each of the three mechanisms can be divided into two modes depending on whether the dispersal occurs into an overlying fluid or onto a solid surface. Another means of dividing the dispersal mechanisms is with respect to the participation of the bacterial cells. Swimming, sliding and twitching dispersal mechanisms are caused by self-propelled locomotion, while clumping, rippling and rolling are fluid-driven. It should be noted that although the self-propelled dispersal mechanisms offer the bacteria a directional advantage, these cells no longer enjoy the advantages of existing as part of an aggregate. On the other hand, detached clusters from clumping, rolling and rippling have better protection in an aggregate environment but their movement is completely dependent on fluid motion.

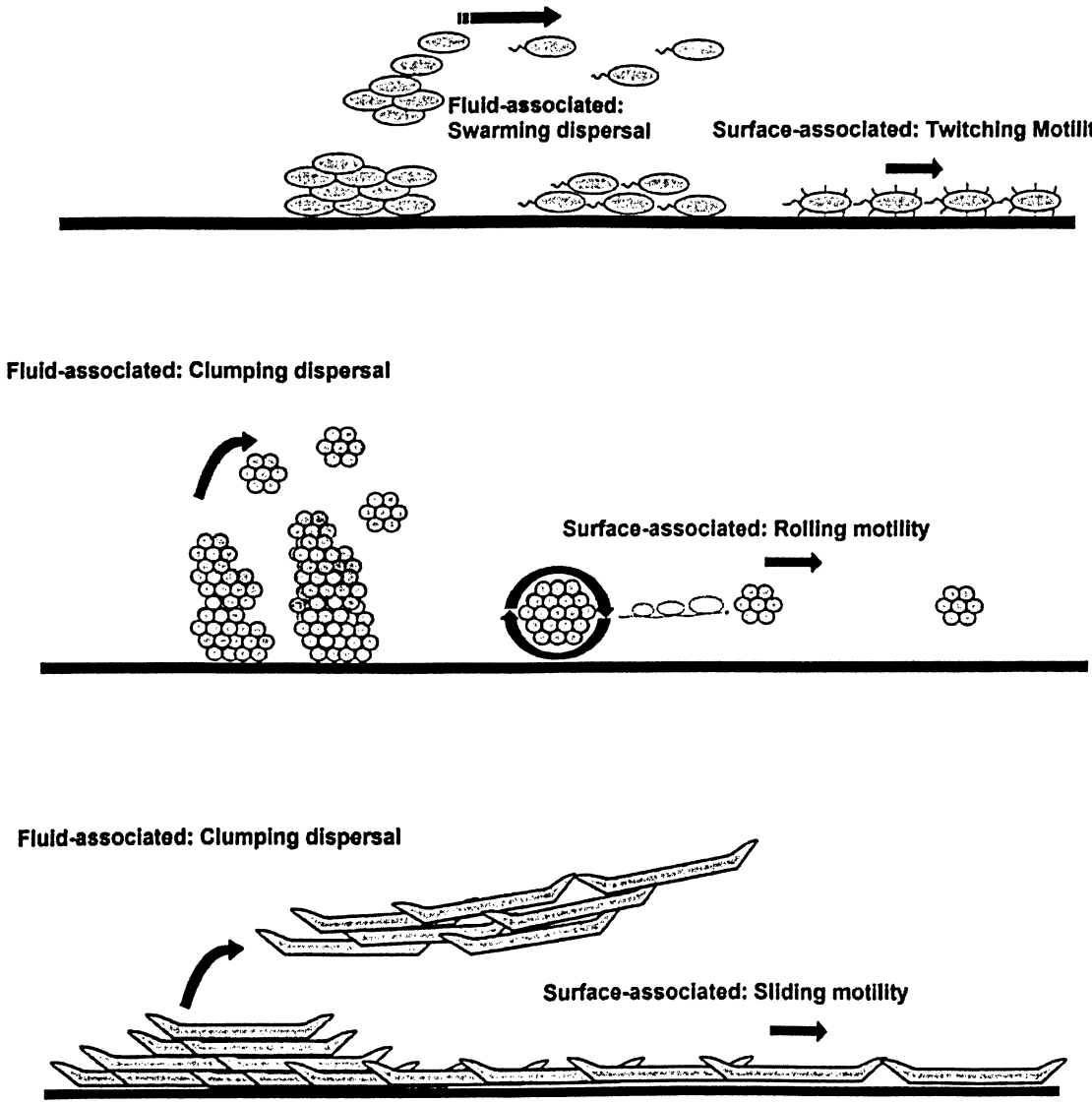

Figure 2.1. Schematic representation of biofilm dispersal mechanisms (Adapted from Hall-Stoodley et al., 2005).

Stoodley et al. (2001) investigated the release of cells from mixed-species biofilms through digital time-lapse microscopy and observed both single cells and clusters. The detached aggregates ranged from a few cells to those with approximately 500 μm in diameter. These researchers found a higher frequency of detachment of single

cells and small aggregates; however, the majority of detached cells were in the form of large clusters.

2.5 Extracellular Polymeric Substances

Extracellular polymeric substances (EPS) are accumulations of compounds of cellular origin that participate in the formation of microbial aggregates and are responsible for binding cells and other particulate materials together and to an environmental surface. It is also important to point out that intact cells may not be considered a part of EPS (Wingender et al., 1999).

Extracellular polymeric substances are a highly hydrated and often charged. They form a three-dimensional, gel-like matrix that surround and immobilize the cells in a biofilm (Wingender et al., 1999).

EPS can be divided in to two fractions, which can be separated by centrifugation. Bound EPS, also known as sheaths, capsular polymers and attached organic material, are more tightly bound to the cells, while soluble EPS consist of soluble macromolecules and colloids (Nielsen et al., 1999).

Certain bacterial EPS are of commercial interest in biotechnology and have a diverse range of industrial and biomedical applications. Commercially, certain extracellular polysaccharides including xanthan, gellan and cellulose, extracellular proteins such as enzymes from fungi and bacteria and some exoenzymes, for instance starch-hydrolyzing enzymes, proteases and cellulases have found various applications in the hydrolysis of macromolecules and for biosynthetic purposes. At the same time, they are significant virulence factors that are linked to infection processes in plants and

animals. As capsular and slime polysaccharides, certain types of EPS may serve as mediators in adhesion to surfaces and have a role in protecting the invading bacteria from host defense mechanisms (Wingender et al., 1999).

For instance, a major cause of death in cystic fibrosis patients is the invasion of lungs by opportunistic *Pseudomonas aeruginosa.* The infections caused by this biofilm forming bacterial pathogen usually persist even following long-term antibiotic therapy. Although it has been proposed that resistant *P. aeruginosa* variants are selected in the patient's respiratory tract by antimicrobial therapy, there is strong evidence suggesting that antibiotic resistance is the result of formation of a biofilm consisting of bacterial communities surrounded in an extracellular matrix (Drenkard et al., 2002).

Due to the fact that EPS acts as a mediator in biofilm formation and stability, it has gained attention in industrial and ecological settings. This slimy matrix is regarded as target structures for remedial actions to remove biofilms or prevent their formation. In other words, gaining control on EPS is a potential solution to biofouling and biocorrosion in industry as well as medicine (Wingender et al., 1999). Current infection control methods are either ineffective or not implemented until the antimicrobial biofilms have become epidemic. Moreover, most laboratory surveillance systems are designed for making patient treatment decisions as opposed to designing and implementing infection control and prevention interventions. Antimicrobial resistance processes are complex and controlling them requires a better knowledge of biofilms, EPS and their functions (Richet, 2000; Starkey et al., 2004).

2.5.1 EPS Composition

The main component of EPS is water, which comprises up to 97% of the slimy matrix. The most abundant macromolecules in the EPS are polysaccharides. Other major constituents of EPS include proteins, phospholipids, nucleic acids and other biological macromolecules. EPS may also contain non-polymeric substituents of low molecular weight as well as organic substituents such as acetyl, succinyl and pyruvyl groups as well as inorganic substituents, which affect their structure and physiochemical properties (Wingender et al., 1999; Flemming et al., 2000a).

2.5.2 EPS Origins

Extracellular polymeric substances may be a result of different processes such as active secretion, shedding of cell surface material, cell lysis, or absorption from the environment. Active secretion of EPS from live cells may be done via various biosynthesis pathways and discrete export machineries involving the translocation of EPS across bacterial membranes to the cell surface or into the surrounding medium have been described for bacterial proteins and polysaccharides. Bacteria produce and release DNA during growth. However, whether DNA is actively secreted or passively released is not fully understood (Flemming et al., 2003).

Spontaneous liberation of integral cellular components is another contributor to EPS. During normal growth of gram-negative bacteria, cellular components such as lipopolysaccharides may be released through formation of outer membrane-derived vesicles. This process is referred to as surface blebbing. Furthermore, metabolic turnover processes may be used to shed membrane components such as nucleic acids, enzymes,

lipopolysaccharides and phospholipids into the extracellular space (Flemming et al., 2003).

High-molecular weight cellular compounds present in EPS, usually originate from death and lysis of cells, which cause release of these compounds and their entrapment in the biofilm matrix. Compounds that become part of EPS in this way include intracellular organic polymers such as poly-β-hydroxyalkanoates or glycogen, cell wall components like peptidoglycan, as well as integral components of membranes like phospholipids and lipopolysaccharides (Wingender et al., 1999).

When EPS is shed from microbial aggregates, it may be absorbed in a different location. As a result of this, the location of original sites of synthesis, release and ultimate localization of EPS components often vary (Wingender et al., 1999).

2.5.3 Spatial Arrangement of EPS

Following production, there are many changes that EPS may be subjected to. Some of these changes are the result of biotic or abiotic degradation, modification or condensation processes. Therefore, composition and distribution of EPS in microbial aggregates may vary depending on spatial and temporal conditions affecting prevailing polymerizing, modifying, and degrading activities of the biofilm (Wingender et al., 1999).

EPS is located outside the cell wall or the pseudomurein layer of archaeobacteria, the peptidoglycan layer of Gram-positive eubacteria and the outer membrane of Gram-negative eubacteria. EPS-containing structures such as capsules are often tightly bound to the cell surface. Capsular EPS are normally attached to cell surfaces by non-covalent

interactions, although in some cases they may even be covalently bound to phospholipids or lipid-A molecules present on cell surfaces. This type of EPS is sometimes referred to as bound EPS (Nielson et al., 1999; Wingender et al., 1999).

Another category of EPS is the type that is loosely attached to the cell surface as peripheral capsules and may be shed into the environment in the form of a less organized and amorphous slime. This form of EPS is commonly referred to as soluble EPS. No matter what form EPS is in, those on the outmost surface layers of bacteria are formed as boundary structures that mediate contact and exchange processes with the surrounding environment (Morin, 1998; Wingender et al., 1999).

2.5.4 EPS Functions

Although the true purpose and functions of EPS are not fully understood, many properties of biofilms have been attributed to EPS production by the cells. Some of these properties include the formation of the gel-like matrix that holds the cells together, the ability of the cells to adhere to surfaces and other cells, the establishment of infections, as well as protection against noxious influences from the environment (Tsuneda et al., 2003).

Polysaccharides and proteins in the EPS are known to play fundamental roles in many functions of the EPS. Furthermore, certain extracellular surface-active polymers that contain lipid components appear to be linked to the interaction between bacteria and interfaces (Baty et al., 1996; Wingender et al., 1999).

2.5.5 EPS extraction

Various methods have been described for extracting EPS from cells in a biofilm. Some of these methods use physical means, such as ultrasonication, heating, steaming, and high-speed centrifugation. Other methods include the use of chemicals, such as NaOH, formaldehyde, EDTA, and cation exchange resin (Spaeth et al., 2000).

When selecting an extraction method, the ultimate goal of extraction should be considered. For instance, when the aim is to analyze polysaccharides, cell lysis does not affect the results, therefore chemical methods that do cause cell lysis would be more suitable. On the other hand, when a quantitative extraction of all EPS is the goal, methods that cause minimal cell lysis, such as centrifugation, should be used. Forces that hold the EPS components together include van der Waals forces, electrostatic interactions, hydrogen bonds, and hydrophobic interactions. Many chemical methods cause removal of water soluble components of the EPS by breaking electrostatic bonds (Nielsen et al., 1999).

The physical extraction method that involves high-speed centrifugation causes very little cell lysis, however, it usually results in a lower yield compared to chemical methods. Centrifugation is most effective in removal of the soluble EPS fraction, although the shear applied by this method also removes some bound EPS (Nielsen et al., 1999).

2.6 Biofilm Treatment and disruption

The ubiquity of biofilms in natural and engineered systems and their complexity has created an immense area of research in eradicating harmful biofilms, from

biocorrosion and biofouling in the industry, to implant and tissue colonization in medical fields. Cleaning biofilms may be performed through physical, chemical and biological means (Holah et al., 2000).

Biofilm removal from pipe and conduit surfaces has been performed through addition of corrosive chemicals such as chlorine or strong alkali solutions or through mechanical means (Davies, 1999) Although physical methods such as scrubbing of surfaces and the use of high pressure water sprays are particularly effective in biofilm removal, they also have the potential to disperse viable microorganisms over a large area (Holah et al., 2000). In medicine, often higher doses of antibiotics are required when dealing with cases involving biofilms (Davies, 1999).

2.6.1 Effect of chelating agents on biofilms

Chelating agents are multidentate complexes that bind metals through coordination or ionic bonds. Since these ligands bind metals in more than one place simultaneously, chelates are more stable than complexes involving unidentate ligands. Chelating agents that are found in natural waters and wastewaters contain a variety of functional groups that are able to donate electrons for bonding to metal ions. Examples of naturally occurring chelating agents include humic substances and amino acids, which are commonly found in water and soil. Synthetic chelating agents such as sodium tripolyphosphate, sodium ethylenediaminetetraacetate, sodium nitrilotriacetate and sodium citrate are commonly used in industrial water treatment and food preparation (Manahan, 2005).

Ethylenediaminetetraacetic acid (EDTA) is a chelating agent which binds to

metals such as manganese, copper, iron and cobalt via its carboxylate and amino groups. EDTA has been shown to induce biofilm detachment from surfaces through chelation of calcium and magnesium ions, which causes the destabilization of the biofilm matrix (Chen et al., 2000; Holah et al., 2000).

EDTA has often been used in combination with other treatment methods in order to ensure maximal removal efficiency. Oulahal et al. (2004) combined ultrasonication with EDTA application and found a synergic effect on biofilm removal. In other studies EDTA has been paired with antibiotics. Raad et al. (2002) demonstrated that a combination of EDTA with minocycline was effective in eradicating catheter surface biofilms.

2.6.2 Effect of antibiotics on biofilms

From the time English microbiologist Alexander Fleming discovered penicillin in 1928, antibiotics have played a significant role in fighting diseases and infections caused by bacteria. However, it did not take very long for complications caused by bacterial resistance to antibiotics to become obvious (Mulcahy, 1996).

As mentioned previously, existing as part of biofilms allows for protection of the bacterial cells from antibiotics. Traditionally, antibiotic dose has been determined with respect to the minimal inhibitory concentration (MIC) of an antibiotic for a specific strain. It has been proposed, however, that due to the altered level of susceptibility in biofilms a minimal biofilm eradication concentration (MBEC) should be used instead. A verity of antibiotics used in biofilm infections, including Cefazolin, Cloxacillin, Clindamycin, and Ceftazidine, have been shown to have significantly higher MBECs

than MICs when tested on *Staphylocpccus aureus* biofilms (Ceri et al., 2005).

Streptomycin is an antibiotic that inhibits bacterial growth by binding directly to specific sites of the 16S RNA, which causes the formation of altered proteins (Lancini et al., 2003). This aminoglycoside antibiotic has also been shown to cause cell membrane damage, inhibit respiration, stimulate RNA synthesis, and cause misreading or miscoding of the genetic code (Zhang et al., 2005).

Streptomycin, in combination with penicillin G or ampicillin, has been shown to synergically facilitate the uptake of aminoglycoside, making it an effective bacteriocide (Antonios et al., 2005). On the other hand, bacteria that survive chlorination during water supply treatment processes are frequently found to be resistant to streptomycin. However, the reason for this common occurrence is not known (Geldreich, 1996).

2.6.3 Effect of increased flow rate on biofilms

Higher flow conditions, depending on frequency and magnitude, cause erosion or detachment of a biofilm. If changes in stress are not frequent, the biofilm may have the opportunity to repair itself. On the other hand, constant fluctuation of the flow rate may result in a reduction in biofilm thickness. Furthermore, it is generally accepted that biofilms growing under high flow rates are much stronger and smoother than those formed under low-flow conditions (Moore et al., 2000).

2.7 Methods for studying detached cells

Methods that may be used to quantify cells released from biofilms include conventional plate-counting, microscopy and Flow Cytometry.

Flow Cytometry is a method used to make multiple objective simultaneous measurements at the single cell level at rates of up to 5000 cells per second. During the 1930s Caspersson and colleagues projected stained images onto a wall and they quantified the amount of light that was absorbed in different areas of the images with primitive photodetectors. This method was also used to study nucleic acid metabolism in *Drosophila melanogaster* salivary gland chromosomes (Watson, 1991).

Modern Flow Cytometers have evolved over the past thirty years. Today these instruments have fluidic, optical, electronic, and computational features. The fluidic component uses hydrodynamic focusing to create a stable particle stream in order for the particles to be aligned in single file surrounded by sheath fluid. The optical components are responsible for the illumination of particles by one or multiple lasers, causing light to be scattered. The scattered light, along with multiple fluorescence signals, is resolved and routed to individual detectors. The main function of the electronics component is to coordinate the named functions, from the acquisition of the signals to making sort decisions. The computation components perform post-acquisition functions such as data display and analysis (Sklar, 2005).

Due to the relatively small sizes of microbial cells, researchers utilizing flow cytometry have been more successful when studying mammalian cells. Despite the fact that the majority of studies in this area have been on clinical studies of mammalian cells, this method has been used to study bacterial cells as early as the late 1970's. For instance, Steen et al. (1980) studied the different phases of growth for *Escherichia coli* K-12 through measurement of DNA-associated fluorescence using a microscope-based flow cytometer. There have been many attempts on optimizing this method for use with

bacteria. Davey et al. (1997) used the Skatron Argus devised by Steen and colleagues to study optical properties of individual bacterial cells using UV-excited fluorescent whitening agents. The Skatron Argus flow cytometer has also been used to monitor damage caused to bacterial cells through antibiotic exposure (Suller et al., 1999).

New generation flow cytometers are able to detect objects between 0.2 to 50 μm in diameter and plot them as events based on relative size, granularity or inner complexity and fluorescence. Two types of photodetectors commonly used in flow cytometers are photodiodes, which are less sensitive and responsible for forward scatter detection, and photomultipliers, which detect side scatter and fluorescence. Detector amplifiers may be set to linear, for scatter signals, and to log, for fluorescent signals.

2.8 Visualizing biofilms

Due to the fact that biofilms containing EPS that is up to 97% water, it is not easily observed using conventional optical microscopy methods. This is because the three-dimensional structure collapses when the biofilm is dehydrated during sample preparation. More recent microscopy methods include confocal laser scanning microscopy and fluorescent microscopy, which utilize fluorescent chemical probes and allow for examination of the three-dimensional structure of biofilms. These techniques and related fluorescent probes are briefly discussed below.

2.8.1 Fluorescent microscopy

Since in traditional light microscopy an image is produced as light passes through a specimen, it requires relatively dense samples. On the other hand, fluorescent

microscopy is based on capturing light emission from the specimen. Therefore, fluorescent microscopy is better suited for visualizing biofilms and cells that are released by them. When a fluorescent sample is exposed to ultraviolet, violet or blue light, it emits energy at a longer wavelength than the absorbed energy. This emission is used to create an image (Beech et al., 2000).

2.8.2 Confocal Laser Scanning Microscopy

Confocal laser scanning microscopy (CLSM), originally described by Minsky in 1957, has been called the most revolutionary development in optical microscopy. It has been used for visualization of both fluorescent and non-fluorescent signals. The CLSM system contains a viable pinhole with modifying scan angles, which allow for the adjustment of magnification (Matsuno et al., 2001).

The scanner focuses the laser light through the tube lens and objective. This causes illumination of a small area in the specimen. A scanner directs light emitted from the focal plane and the planes above and below to the dichroic beam splitter. The emitted light is then directed onto a photomultiplier detector (Matsuno et al., 2001).

CLSM is a suitable method for the study of biofilms, since it is nondestructive and can be used on thick samples (Takenaka et al., 2001). Furthermore, this method allows for analysis of the three dimensional structure of fully hydrated microbial biofilms with the use of its sectioning feature (Lawrence et al., 1991).

2.8.3 Fluorescent probes

Stains used in microscopy are dyes that bind to cells or cell components and are mainly used to make microorganisms and the components of their cells easier to visualize. Staining is often required because cells have poor contrast and their structures are difficult to see. Staining is also used for classification and taxonomic identification of microorganisms.

The different types of stains include simple stains, such as methylene blue, which are single dyes that are used to stain cells. Others are known as differential stains, which consist of two or more dyes used to distinguish between different groups of bacteria, such as gram stain, which stains gram positive bacteria purple and gram negative bacteria red. Another example of a differential stain is an acid-fast stain, which is a differential stain that stains mycobacteria red and non-acid-fast bacteria blue. There are other types of stains called special stains used to visualize specialized cell structures and include endospore stain for spores inside cells, flagella stain, and negative stain to visualize the capsules surrounding cells (Talaro et al., 2003). An alternative to staining is the use of fluorescent proteins, such as green fluorescent protein (GFP) and red fluorescent protein (RFP), which can be expressed by the cells.

2.8.3.1 Green Fluorescent Protein

Prior to the discovery of the GFP, most of the compounds used to visualize living cells were either radioactive or toxic. Furthermore, the methods used to insert the compounds into the cells were destructive. Therefore, most studies were conducted on

fixed or dead cells. In order to study various activities within the cell, a nondestructive method of visualization had to be developed that would involve a naturally occurring protein that could be expressed in a wide range of cell types (Micklos et al., 2003).

The crystal structure of GFP, shown below, is shaped like a can and consists of eleven beta-strands that make up the beta-barrel and an alpha-helix which runs through the centre. The structure shown in the middle is the chromophore (Zhang et al., 2002). The molecular structure of the chromophore, which is responsible for GFP's fluorescence, is shown in figure 2.2.

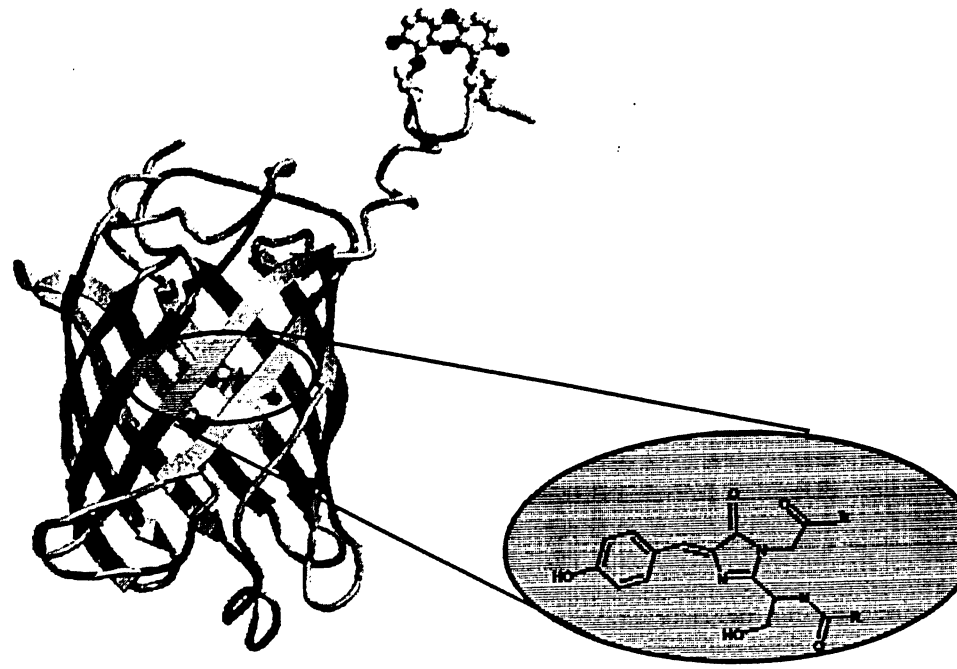

(a) (b)

Figure 2.2. (a) The can-shaped structure of GFP and (b) the molecular structure of the GFP chromophore.

2.8.3.1.1 Tagging of bacterial cells with GFP

One of the most common methods used to introduce plasmids into microbial cells is triparental mating. This method requires the use of a helper strain, which carries the genes that code for conjugation and DNA transfer, a donor strain, which carries the plasmid and the bacterial cell into which the plasmid is aimed to be inserted.

A disadvantage of this method is that five to seven days are required before a successful mating can be confirmed. Furthermore, this method is not suited for all strains of bacteria. An alternative to triparental mating is the use of electroporation, a highly efficient method that does not require the presence of donor or helper strains, which greatly reduces the chances of contamination (Sá-Correia et al., 2000).

Strong electric field pulses, when applied to living cells and tissue, are known to cause rearrangement of the cell membrane. In some cases this rearrangement may be in the form of temporary aqueous pathways, known as pores. The electronic field plays the dual role of creating the pore as well as providing a driving force that pushes ions and molecules through the pores into the cell. Electroporation provides a means for tagging bacterial cells with fluorescent proteins such as GFP. It may also be used for insertion of enzymes, antibodies, viruses, and cellular macromolucules (Weaver, 1995).

The mechanism of electroporation is based on the universal bilayer membrane phenomenon. Short electric field pulses cause the transmembrane voltage to rise to about 0.5 to 1.0 volts, resulting in electroporation. In the case of isolated cells, the necessary single electric field pulse amplitude depends on cell size and is in the range of $10^3 - 10^4$ V/cm (Weaver, 1995).

The application of an electromagnetic pulse is followed by reversible electrical

breakdown along with greatly enhanced transport of molecules across the membrane, which also triggers a rapid membrane discharge. The transmembrane voltage returns to small values after the pulse ends. It should be noted, however, that the membrane takes much longer to recover. Cell survival throughout the process depends upon the cell type, the extracellular medium composition and the ratio of intracellular to extracellular volume (Weaver, 1995).

The outlined mechanism for the function of the electroporator is based on the hypothesis that pores are microscopic membrane perforations, which allow for a hindered transport of ions and molecules across a membrane (Weaver, 1995). Figure 2.3 illustrates the structure of both transient and meta-stable membrane conformations that are possibly involved in electroporation. According to the transient aqueous pore model assumes the occurrence of transitions A, B and C or A, B and D, with increasing frequency. Type E may only occur in case of entry of a tethered macromolecule during the time that the transmembrane voltage is high.

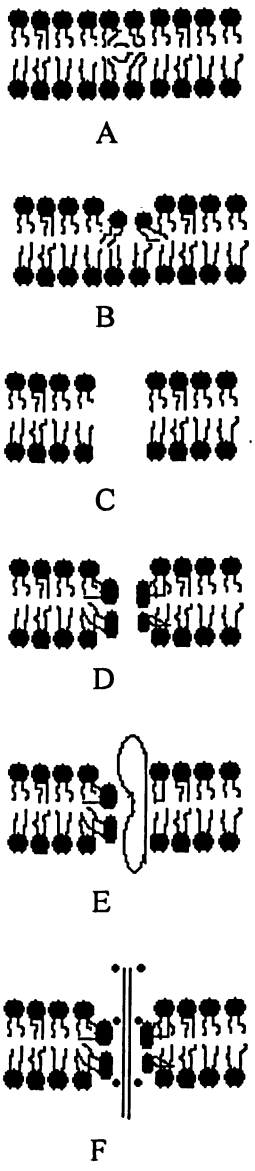

Figure 2.3. Hypothetical structures of both transient and meta-stable membrane conformations (adapted from Weaver, 1995)

Strains that have previously been successfully electroporated include *P. aeruginosa* and *P. putida.* During the process of electroporation, large numbers of the cells are killed. If the electric field strength does not exceed the critical level, some cells do survive and undergo reversible permeability (Nickoloff, 1995).

2.8.3.2 Nile red

Visualization of biofilms may also be performed by staining the cells with dyes such as 9-dimethylamino-5H-benzo[α]phenoxazine-5-one. This intensely fluorescent dye is more commonly known as Nile Red. The chemical structure of Nile Red is shown in figure 2.4. This uncharged heterocyclic molecule, when dissolved in hydrophobic solvents such as phospholipids, fluoresces red. Thus the outer hydrophobic regions of the bacterial cells will fluoresce while in the surrounding EPS, which consists mainly of water, the stain is almost entirely quenched (Fowler et al., 1985).

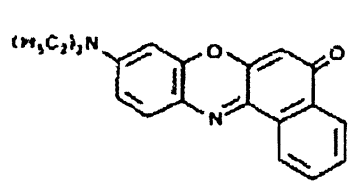

Figure 2.4. Chemical structure of Nile Red (Greenspan et al., 1985)

Nile Red was originally prepared by dissolving Nile Blue into dilute sulfuric acid and boiling it for two hours, and thus in some older literature it is referred to as Nile Blue A-oxazone. The fluorescence of this dye varies from deep red to a golden yellow, depending on the hydrophobicity of the solvent. Another property of Nile Red, which makes it an ideal stain for biofilm visualization, is the fact that it binds only to the outer, hydrophobic regions of the cell and does not penetrate the cells. This property allows for visualization of the biofilm at different times throughout its growth, without interruption of cell growth (Greenspan et al., 1985). Excitation and emission spectra of Nile Red are shown in figure 2.5.

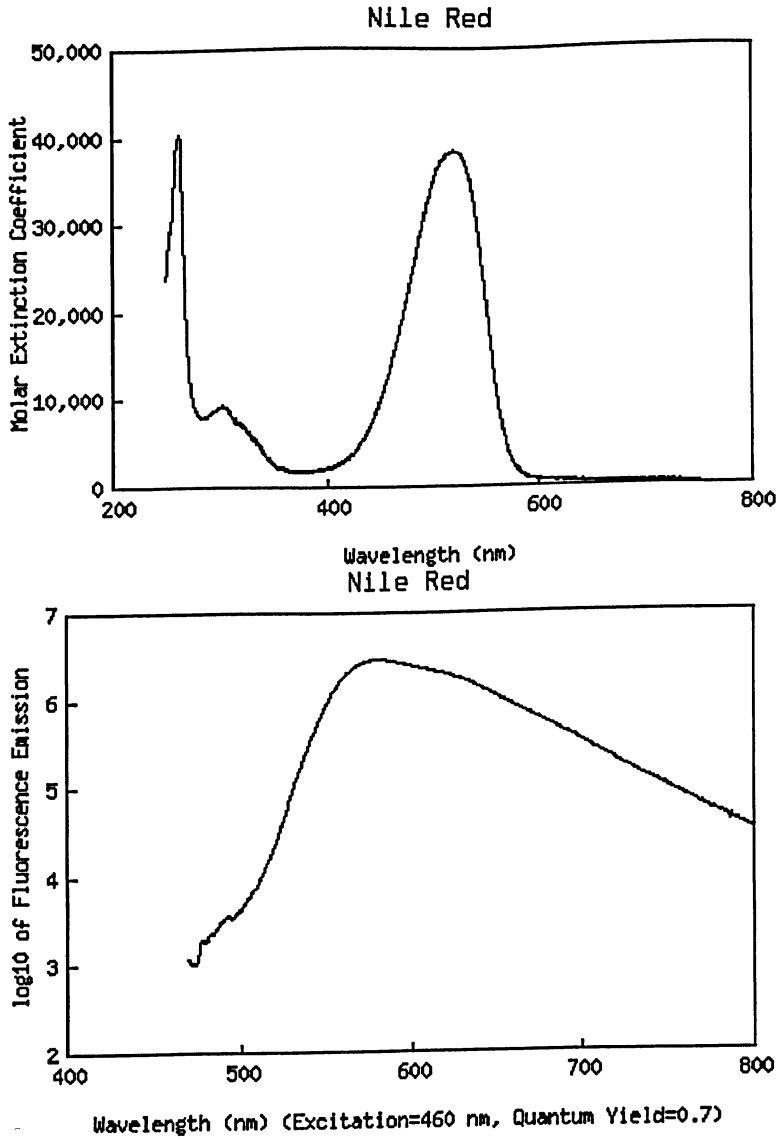

Figure 2.5. Emission and excitation spectra of Nile Red (Fuh et al., 1998).

2.8.3.3 FM 4-64

The red stain, *N*-(3-triethylammoniumpropyl)-4-{6-[4-(diethylamino) phenyl]-hexatrienyl} pyridinium dibromide commonly known as FM 4-64, is hydrophobic and thus stains cell membranes. Although, FM 4-64 has been referred to as a vital stain (Vida et al, 1995), it has been shown to effectively stain dead cells of *Hordeum vulgare* (Fath et

al, 2001). According to the absorption and emission spectra of FM 4-64, shown in figure 2.6, a suitable excitation laser for this stain is Ar 488nm.

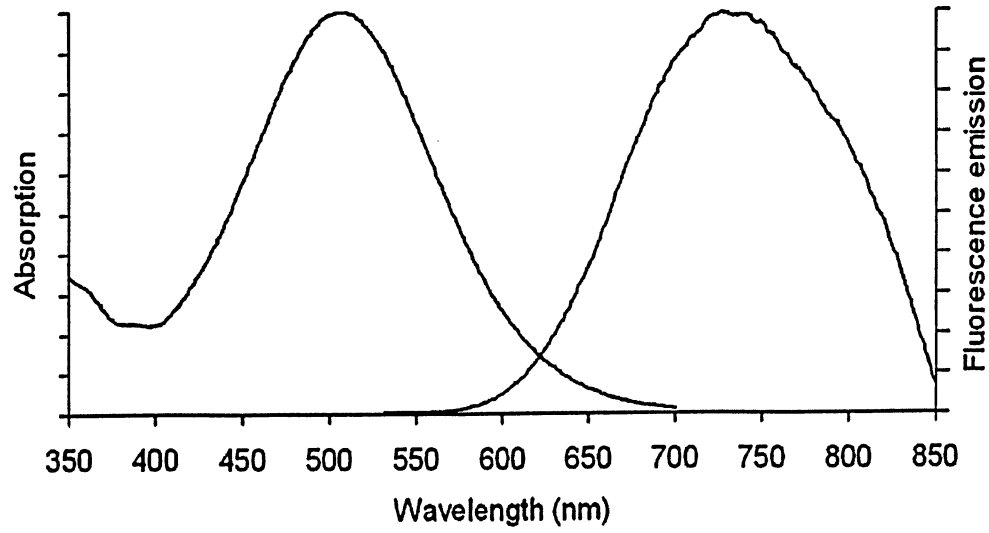

Figure 2.6. Absorption and fluorescence emission spectra of FM 4-64 (Invetrogen™ http://probes.invitrogen.com/servlets/spectra?fileid=3166ch2)

2.8.3.4. Propidium iodide and Syto 9

A combination of propidium iodide and Syto 9 is often used to distinguish between live and dead cells. Syto 9 fluorochrome is a small molecule that penetrates intact plasma membranes and stains nucleic acids in both live and dead cells green. On the other hand, the propidium iodide fluorochrome, which is larger, is only able to penetrate compromised membranes and stains dead cells red (Alonso et al., 2002). The excitation and emission maxima for Syto 9 are 480 nm and 500 nm respectively (Figure 2.7). In the case of propidium iodide, the excitation maximum is similar to that of Syto 9, at about 490 nm, while its emission maximum is at about 635 nm (Figure 2.8).

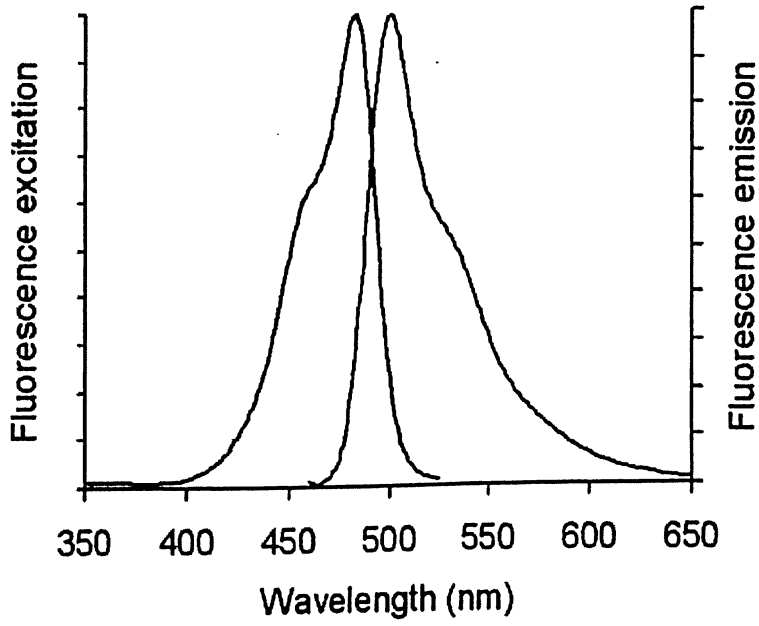

Figure 2.7. Excitation and emission spectra of Syto 9 fluorescent nucleic acid bound to DNA. (Invetrogen™ http://probes.invitrogen.com/servlets/spectra?fileid=34854dna)

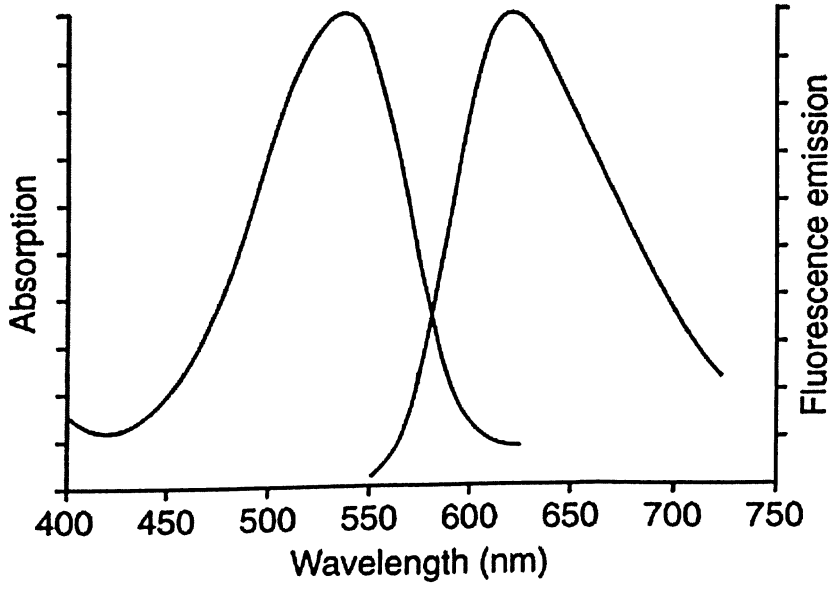

Figure 2.8. Excitation and emission spectra of propidium iodide bound to DNA. (Invetrogen™ http://probes.invitrogen.com/servlets/spectra?fileid=1304dna)

2.9 Laboratory strains in biofilm research

A range of bacterial strains, which are well understood, are often used in laboratory studies. Among bacterial strains that are commonly used in the study of biofilms, *Aeromonas hydrophila* (Gavín et al., 2002; Lynch et al., 2002), *Serratia marcescens* (Gandhi et al., 1993; Rice et al., 2005), *Staphylococcus aureus* (Cramton, et al., 1999; Beenken et al., 2003), *Staphylococcus epidermidis* (Heilmann et al., 1996; Mack et al., 1996), *Pseudomonas aeruginosa* (Nickel et al., 1985; Sauer et al., 2002), *Pseudomonas fluorescens* (Allison et al., 1998; O'Toole et al., 1998), *Pseudomonas putida* (Moller et al., 1996), and *Escherichia coli* (Pratt et al., 1998; Danese et al., 2000) are a few examples. The most frequently used pseudomonad is probably *P. aeruginosa.*

2.9.1 *Pseudomonas aeruginosa*

Bacteria belonging to the genus *Pseudomonas* are motile, Gram-negative and rod shaped. They are aerobic and able to utilize acetate for carbon and ammonium sulfate for nitrogen. Some species of this genus are resistant to high concentrations of salt, dyes, weak antiseptics and many antibiotics. These properties have given these bacteria the advantage of being able to survive in conditions where few other organisms can tolerate. Moreover, the EPS that they produce allows them to become resistant to phagocytosis. These characteristics have made *Pseudomonas* species major causes of hospital-acquired or nosocomal infections (Cabral et al., 1987).

Although device-related and other chronic infections are most commonly caused by autochthonous skin bacteria, such as *Staphylococus epidermidis*, in many cases *P. aeruginosa* have been observed on vascular catheters, peritoneal catheters, urinary

catheters, nasogastric tubes, nephrostomytubes, orthopedic and other devices and prostheses (Costerton et al., 1994).

These opportunistic pathogens cause death in many cystic fibrosis patients, burn victims and other immunocompromised individuals. They can also infect many different sites of the body and cause urinary tract infections, sepsis, pneumonia and pharyngitis. However, *Pseudomonas* is rarely found as an infectious agent in healthy individuals due to its non-invasive nature (Mitchell, 1992).

2.9.1.1 *Pseudomonas aeruginosa* PAO1

Pseudomonas aeruginosa PAO1 is a strain commonly used in laboratory settings for biofilm studies. This strain was first isolated from a burn wound in 1955, from which subcultures have been preserved growing on laboratory media over the past few decades. PAO1 has become a popular laboratory strain because it is a common human pathogen, with the capacity to grow persist and proliferate in many different environments (Lee et al., 2005). As a result of numerous studies on PAO1, it is relatively well understood and its entire genome, consisting of 6.3 million base pairs, has been sequenced (Stover et al., 2000).

Although, PAO1 is a convenient strain to use in laboratory settings, it does have some notable disadvantages. Because subcultures of this strain have been used in laboratories over the last three decades there have been significant changes in its genome. For instance, many genes that were not advantageous in the laboratory environment may have been progressively deleted. Conversely, in laboratory strain PAO1 a number of pathogenicity islands have been detected, which were not present originally.

Furthermore, phenotypic comparison of PAO1 with strains derived from cystic fibrosis patients have shown that natural strains tend to express reduced planktonic growth *in vitro* and form more efficient biofilms (Fux et al., 2005).

2.10 Sources of inocula for biofilm research

Despite pure cultures being the most popular choice from biofilm studies in laboratory settings, many naturally occurring biofilms have been used as inocula for biofilm research. These sources include environmental sources such as groundwater communities (Cho et al., 2005), sludge (Pai et al., 2004), contaminated soil (Abraham et al., 2003), water distribution systems (Hu et al., 2005) and biological sources such as infected lungs (Lam et al., 1980), tongue (Spencer et al., 2007) and teeth (Lee et al., 2004).

Biofilms may also form in water distribution systems, where they can cause pipe corrosion and water quality deterioration. They are usually seen in cases of low residual chlorine levels, when ozone is used as a treatment process, and when high concentration of carbon is available as it usually is the controlling nutritional parameter. Growth of biofilms in water distribution systems occurs in pipes due to their large surface to volume ratio. In excess of 95% of the biomass is found on walls while the rest exist in the water (Hu et al., 2005).

Although, drains may not be deemed very convenient environments for biofilm growth due to presence of detergents, disinfectants and other cleaning products, several

studies have shown biofouling of drains caused by biofilms. Biofilms in sink drains within medical-surgical intensive-care wards and cystic fibrosis units have been proven to be the cause of infections. In domestic drains, pathogens have been identified in kitchens and bathrooms (McBain et al., 2003).

McBain et al. (2003) studied drain biofilm composition and found that certain species were specific to the tested drain. They also found a significant number of opportunistic pathogens including aeromonads and pseudomonads, pathogens such as *L. pneumophila* and non-intestinal coliforms, as well as protozoa as part of drain biofilms.

CHAPTER 3 Materials and Methods

3.1 Strain selection

In order to study the incorporation of an opportunistic pathogen into naturally existing mixed-species biofilm, *Pseudomonas aeruginosa* PAO1 was chosen as the test strain. PAO1 was tagged with gfp to make it possible to distinguish between this strain and other community members.

3.1.1 GFP tagging of PAO1 using triparental mating

Triparental mating was performed in order to tag *P. aeruginosa* PAO1 with gfp3 (AKN 67). The helper strains used contained pUX BF13 and pRK 600. Overnight cultures of the recipient strain was inoculated into sterile Luria Broth (LB) medium and incubated at 30°C for 7 hours. Fresh inoculations of the donor and helper strains were also incubated at 37°C for 4 hours. The donor and helper strains were washed with LB and centrifuged at 8,000 g for 30 seconds.

A mixture of 100 µl of each strain was filtered through a 0.2 µm filter. The filter paper was then placed on a Luria Agar (LA) plate to grow overnight at 30°C.

3.1.2 GFP tagging of PAO1 using electroporation

3.1.2.1 Plasmid extraction

Using the *Genopure Plasmid Midi kit* (Roche Molecular Biochemicals) plasmid DNA was isolated from *E. coli* strain XL1-Blue (AKN 66, gfp-2), which is a high copy number plasmid and *E.coli* SM10:lambda pir (AKN 68, pUX-BF13), which is a low copy number plasmid.

3.1.2.2 Reagent preparation

Sucrose Magnesium Electroporation Buffer (SMEB):

In order to prepare 500 ml of the SME buffer 1 ml 0.5 M HEPES (pH 7), 0.5 ml 1M $MgCl_2$ and 51.3 g sucrose were dissolved in the required volume of water and autoclaved.

SOB solution:

In order to prepare SOB, 1 g tryptone peptone, 0.25 g yeast extract, 0.1 ml 5 M NaCl, and 0.125 ml 1 M KCl were dissolved in 50 ml water, the pH was adjusted to 7 and autoclaved. Then, 0.5 ml sterile 1M $MgCl_2$ and 0.5 ml sterile 1M $MgSO_4$ were added to the solution.

SOC solution:

In order to prepare the SOC solution, 1 ml filter sterilized 1 M glucose was added to 50 ml SOB.

3.1.2.3 Preparation of electrocompetent cells

Pseudomonas aeruginosa PAO1 was inoculated into 5 ml LB in a test tube and incubated overnight at 37°C while shaking at 300 RPM. From the overnight culture 0.5 ml was inoculated into 250 ml flask containing 50 ml sterile LB. The flask was then incubated at 37°C while shaking at 300 RPM until an optical density of 0.5 was reached at 600 nm. The flask was chilled on ice for 10 minutes then transferred into two chilled, sterile centrifuge tubes. The tubes were centrifuged at 4°C for 10 minutes at 4400 RPM

in an Eppendorf 5415D centrifuge at 2300 x g. The pellets were resuspended in 25 ml sterile, 0 °C SMEB buffer.

3.1.2.4 Electroporation

The solution of the electrocompletent PAO1 cells and a high concentration of gfp plasmid were prepared. Bio-Rad Gene Pulser Xcell electroporation was used to facilitate gfp insertion into PAO1 cells. These cells were then placed in a medium of very high nutrient level, SOC, and incubated in a water bath at 37°C for 3 hours before being plated on 10% TSA agar plates, which were incubated at 37°C overnight. Using the 10x objective on an epifluorescent microscope, colonies formed on the plates that fluoresced green under UV light were re-streaked onto 10% TSA plates in order to ensure stable insertion of gfp.

3.1.3 PAO1 Growth Curves

In order to determine if the GFP insertion affected metabolic performance of PAO1 growth curves of untagged PAO1 was compared to that of PAO1:GFP through growth curve construction.

Overnight cultures of PAO1 and PAO1:GFP were inoculated into flasks of sterile 10% TSB media, and growth was measured by changes in the optical density, using an Eppindorf Bio-Photometer at OD_{600} for 11 hours.

3.2 Interaction of PAO1::GFP with a heterogeneous biofilm community

3.2.1 Cultivation of heterogeneous biofilm communities

Two mixed microbial communities were used to study the behaviour of PAO1:GFP, as an example of an opportunistic pathogen, in a community context. The first community was cultivated by obtaining a swab from a drain in the sink of a public washroom. In the discussion, this community is referred to as 'community 1'. The other community sample, referred to as 'community 2', was cultivated in the same manner from a washroom sink at a local hospital. It should be noted that the sink from which community 2 was obtained, had been chemically treated with antimicrobial substances unknown to the author several days prior to sampling.

3.2.2 Flow cell experiments to evaluate the potential protection of PAO1:GFP by association with a mixed community

Biofilms were cultivated in conventional flow cells (Bester et al, 2005). Sterile silicon tubes of 1.6 mm diameter were then attached to both sides of the flow cell chambers. The volume of each chamber of the Flowcell was 450 mm^3. Flow cells and related tubing were sterilized with 5% sodium hypochlorite (v/v) which was pumped through the system for one hour, followed by washing with deionized water over-night. Figure 3.1 illustrates the experimental setup in which the flow cells were used.

Inoculation of the flowcells was performed by injecting 100 µl of an overnight culture directly into the flow chambers. The pump was stopped for 1 hour to allow the newly added cells to adhere to the glass surface. The pump was then started and run

throughout the experiment at a flow velocity of 1.08 m/h with 1% TSB medium. The flowcells were run for up to 10 days following inoculation.

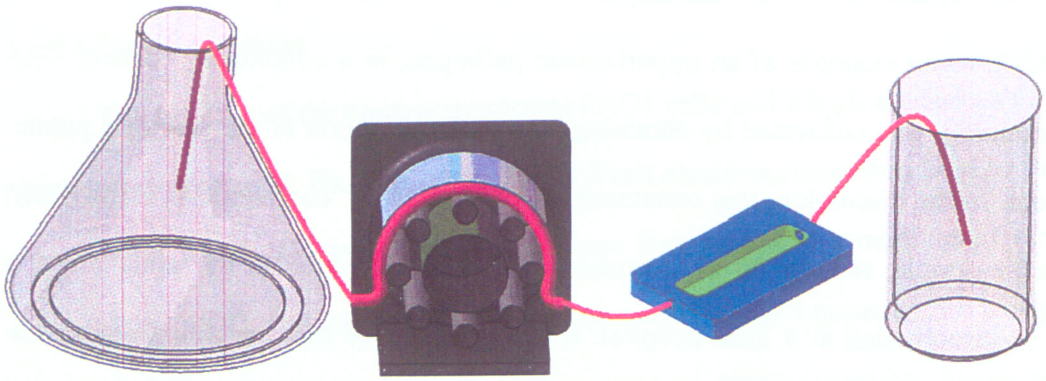

Figure 3.1. Experimental setup used for the flow cell. Flow direction in this diagram is from left to right. A peristaltic pump is used to provide continuous flow from growth medium in a flask into the flow cell, which is connected to a waste container.

Three scenarios of pathogen and mixed community combinations were simulated, namely 1) where an established biofilm of the pathogen was challenged with a mixed community, 2) where the pathogen was co-inoculated with the community, and 3) where the pathogen was introduced to an established mixed biofilm community. These experiments were conducted as follows:

Scenario 1: PAO1:GFP was inoculated into the flowcell and allowed to grow for 72 hours before the drain cultures were added.

Scenario 2: PAO1:GFP and the drain cultures were inoculated into the flowcell simultaneously.

Scenario 3: PAO1:GFP was inoculated into a biofilm of drain cultures that had been growing for 72 hours.

Integration of PAO1:GFP in the mixed community was studied using microscopic observation of the flowcells as well as flowcell effluent. Samples were obtained by

disconnecting the out-flowing tube and collecting 1 ml of the effluent directly downstream of the chamber in an eppendorf tube.

The numbers of total cells as well as the relative numbers of PAO1:GFP cells to drain cells that were released from the biofilms at different stages of growth were determined through conventional plate-counting method for the three scenarios of mixed-community biofilms.

3.2.2.1 Microscopy

Comparison of the biofilms in different scenarios was done by visualization using an epifluorescent microscope and a confocal laser scanning microscope. Images were obtained from biofilm effluent samples at various times during the cultivation period, and of biofilm *in situ* following the final effluent sampling.

3.2.2.1.1. Confocal laser scanning microscopy

A CARL ZEISS 510 laser scanning microscope was used to visualize effluent samples and biofilms. The objectives used included water immersion objectives 63X 1.2 N. A. and 20X /0.75 N. A.

For purposes of imaging sample containing green fluorescent cells that were stained with a red dye, either Nile Red or FM 4-64, two channels were employed, one with a band-pass filter at about 500 – 550 nm and the other with a long – pass filter at 650 nm. In order to image gfp-labelled samples a single channel and an LP 505 filter were employed, while for samples that fluoresced red, the LP 650 filter was chosen. The

excitation lasers used were 488 nm for gfp and 543 nm for Nile Red and FM 4-64. For further details on the configurations and the filters used refer to Appendix A.

3.2.2.1.2 Epifluorescent microscopy

A Leica DM 5000B epifluorescent microscope with an excitation wavelength of 488 nm was used to image effluent samples and count fluorescent colonies on agar plates. For imaging purposes the oil-immersion objective 63 x 1.4-0.6 was used in combination with the GFP, RFP and I3 filters. Images were captured using a Leica DC 300F camera.

3.2.2.2 Enumeration

Changes in the number of cells released by these biofilms over time were determined through plate counting. Effluent samples, collected in eppendorf tubes, were vortexed at high speed for 60 s in order to break apart clusters. Dilution series of the effluent samples were prepared in saline solution and plated onto 10% TSA plates. Colonies grown overnight were counted using a 10x objective on an epifluorescent microscope, where PAO1:GFP colonies were distinguished using UV light and a GFP filter.

3.3 Response to antibiotic treatment in a community setting

The minimal inhibitory concentration (MIC) of streptomycin, which is the lowest concentration of the antibiotic that results in inhibition of visible growth of planktonic cells, was determined for PAO1.

An overnight culture of PAO1::GFP was grown in 10% TSB and 10μg/ml gentamycin. From this culture, 100 μl was added to test tubes containing 5 ml 10% TSB. A series of concentrations of streptomycin was created in these test tubes in triplicate and allowed to grow over night. The test tubes containing the lowest concentration of streptomycin in which no growth was observed, was considered to be the MIC.

Antibiotic susceptibility of PAO1:GFP in biofilms under the different scenarios was tested in order to determine the potential protection of PAO1:GFP by community members. This was tested by irrigating the flowcells with 1% TSB medium containing 8 μl/ml streptomycin (slightly higher than MIC, see section 4.3) for 2 hours. A reference biofilm containing a pure culture of PAO1:GFP was cultivated in parallel.

In order to determine the effect of antibiotic treatment on biofilm cell yield, changes in the number of cells released from the biofilms were monitored by plating the flowcell effluent on 10% TSA plates, as described in section 3.2.2.2. Counting green fluorescent colonies, representing PAO1: GFP cells, and non-fluorescent cells, attributed to the mixed community biofilm, enabled the determining of relative numbers of PAO1:GFP released cells. For qualitative monitoring of the biofilms and their effluent, epifluorescent and confoccal laser scanning microscopy were used, as described in sections 3.2.2.1.1 and 3.2.2.1.2.

3.4 Response to a chelating agent in a community setting

In order to determine the possible protection of PAO1 in a community setting against a chelating agent, 40 mg/ml EDTA dissolved in 1% TSB was run through flowcells containing 72 hour scenario 2 biofilms over a 15 hour period. A flow cell

containing a pure culture of PAO1:GFP was cultivated as reference in parallel and was subjected to the same conditions.

Effluent sampling was performed at 1, 5, and 15 hours following the initiation of EDTA exposure. The samples were plated as described in section 3.2.2.2. Light microscopy was used to monitor possible changes in the biofilm structure during the initial 75 minutes of EDTA exposure.

3.5 Biofilm erosion by increased flow rate

In order to test the effects of physical disruption of a mixed community on the spread of an embedded opportunistic pathogen, shear was applied to 72 hour scenario 2 biofilms, by increasing the peristaltic pump flow velocity from 1.08 m/h to 30.0 m/h for 9 seconds. Effluent plate counts and microscopy were performed as described in sections 3.2.2.2 and 3.2.2.1 respectively.

3.6 EPS analysis

In order to investigate whether the volume of EPS in the mixed community and PAO1:GFP played a role in protection against environmental stress, EPS was extracted from Community 1 and PAO1:GFP biofilms. This was done because it was often observed that there appeared to be a difference in EPS volumes in colonies of PAO1:GFP and community members when grown on agar.

The volume of EPS was measured by growing the biofilms in tube reactors followed by EPS extraction using high-speed centrifugation. The experimental setup for biofilm growth was similar to that of flowcells (section 3.2.2) with the replacement of the

flowcells with silicone tubes with an inner diameter of 5 mm and 30 cm in length.

Following 14 days of growth, the biofilms produced in the tubes were harvested by carefully draining the aqueous phase followed by squeezing the tube in order to minimize the volume of growth medium in the sample.

In order to separate the EPS, 2 mL of the biofilm sample was centrifuged at 6,000 RPM for 10 minutes. The supernatant was transferred into a new eppendorf tube through a 0.2 μm filter. The pellet was resuspended in 1 mL of deionized water using a vortex. The suspension was then centrifuged at 13,000 RPM for 30 minutes. Once again the supernatant was transferred through a 0.2 μm filter into a new tube (figure 3.2). It was assumed that the first centrifugation step had removed the loosely bound EPS, while the second round of centrifugation removed the more tightly bound EPS (Zhang et al., 1999).

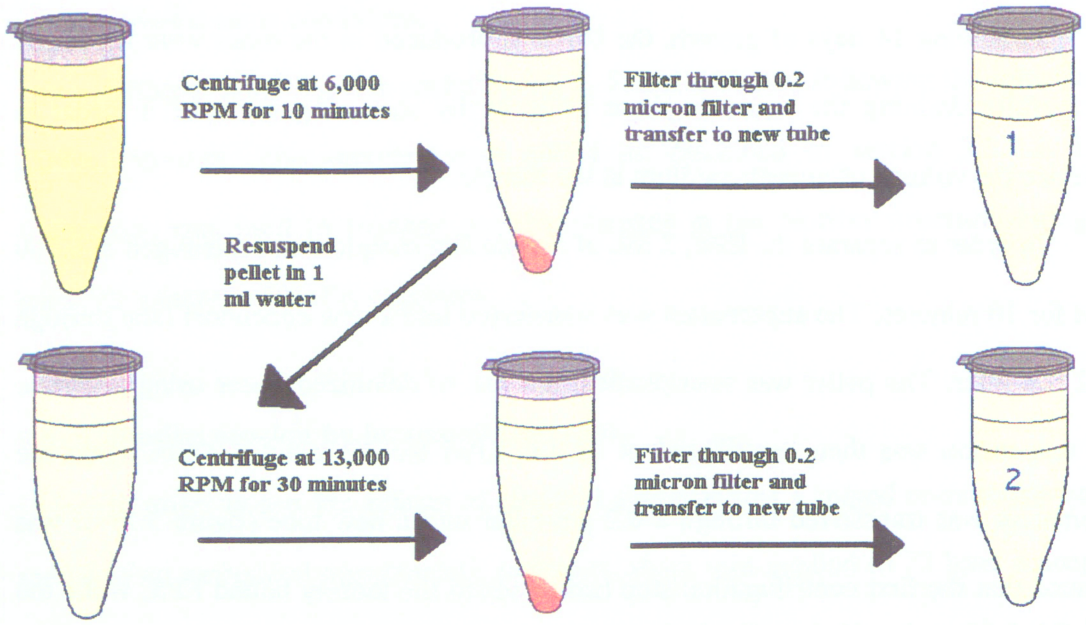

Figure 3.2. EPS extraction method employed. The procedure involves two rounds of centrifugation that aims to extract both soluble and capsular EPS.

Light microscopy images, using a 10x objective, from colonies of PAO1:GFP and various strains from Community 1 grown on 10% TSA plates, as well as CLSM images, using 63x 1.2 objective, were obtained from biofilms of a pure culture of PAO1:GFP and Community 1 were obtained to further compare the EPS matrix of the two types of biofilms.

3.7 Flow Cytometry

A BD FACSCalibur™ flow cytometer was used to find the ratio between PAO1:GFP cells to those of drain strains released from a scenario 2 biofilms. This was achieved by staining the flowcell effluent with FM 4-64 red stain, which would cause the mixed community cells to fluoresce red, while the PAO1 cells fluoresced green. Two

lasers were used for excitation of FM 4-64 and gfp fluorescence, 488 nm (blue) and 635 nm (red).

Sample pressure was set to 'HI', which results in a flow rate of 1200 events/sec. In order to ensure 'events' in flow cytometer plots account for cells only, the medium and saline solution were filtered through 0.2 μm filters. In addition, filtered saline solution, PAO1:GFP cells and FM 4-64 stained cells were sampled by the flow cytometer to provide a means of correction for the presence of small debris, unstained drain cells, and non-fluorescent PAO1:GFP cells respectively.

The samples were diluted in filtered saline to a concentration of $2x10^5 - 2x10^7$ cells/ml which would result in readings of fewer than 1500 events/second. The instrument settings used for samples containing red and green cells are shown in Appendix B.

Samples analyzed by flow cytometry were plated, as described in section 3.2.2.2, for quantitative comparison of the methods.

3.7.1 Live/dead staining

In order to monitor changes in the ratio of live to dead cells released from the biofilms, *Bac*Light bacterial viability kit was used for staining and an epifluorescent microscope was used for imaging. The concentrations of stains used were 2 μl/ml of Syto 9 and 3 μl/ml of propidium iodide.

Effluent samples were collected, as described in section 3.2.2, stained for 30 minutes and diluted in sterile deionized water. The dilution step was performed in order for each image obtained by the microscope to contain 20-50 cells. The diluted samples

were filtered through a 2 μm filter, upon which microscopy was carried out. The 63x objective on an epifluorescent microscope in combination with GFP and RFP filters were used for imaging. A minimum of 40 images were obtained for each sample. Image analysis was done using Scion Image.

CHAPTER 4 RESULTS AND DISCUSSION

4.1 GFP labeling of PAO1

4.1.1 Tri-parental mating

Several attempts at tagging *P. aeruginosa* PAO1 with gfp, using triparental mating were unsuccessful. Triparental mating is the traditional method of insertion of plasmids into bacteria, but has numerous disadvantages including high probability of contamination due to the presence of the helper and donor strains, as well as the fact that it requires five to seven days in order to ensure successful insertion of the plasmid into the new bacterial cells. Therefore, electroporation was subsequently evaluated as a method to tag PAO1. This method has been described as faster and potentially more efficient (Lin, 1995).

4.1.2 Electroporation

Following overnight growth of the electroporated cells, green fluorescent colonies of PAO1 observed on the agar plates, which were re-streaked onto LA plates and retained their green fluorescence, were confirmed to be PAO1 with stable GFP insertion (PAO1:GFP).

4.1.3 PAO1 growth curves

Figure 4.1 shows the growth of PAO1 and PAO1:GFP by plotting changes in optical density over a period of 11 hours. These curves demonstrate that the GFP insertion into the PAO1 genome does not impact its growth, and therefore most probably its metabolic rate. The maximum specific growth rate, μ_{max}, of untagged PAO1 and the

GFP tagged strain were found to be $1.01 \pm 0.11\ h^{-1}$ and $1.06 \pm 0.12\ h^{-1}$ respectively.

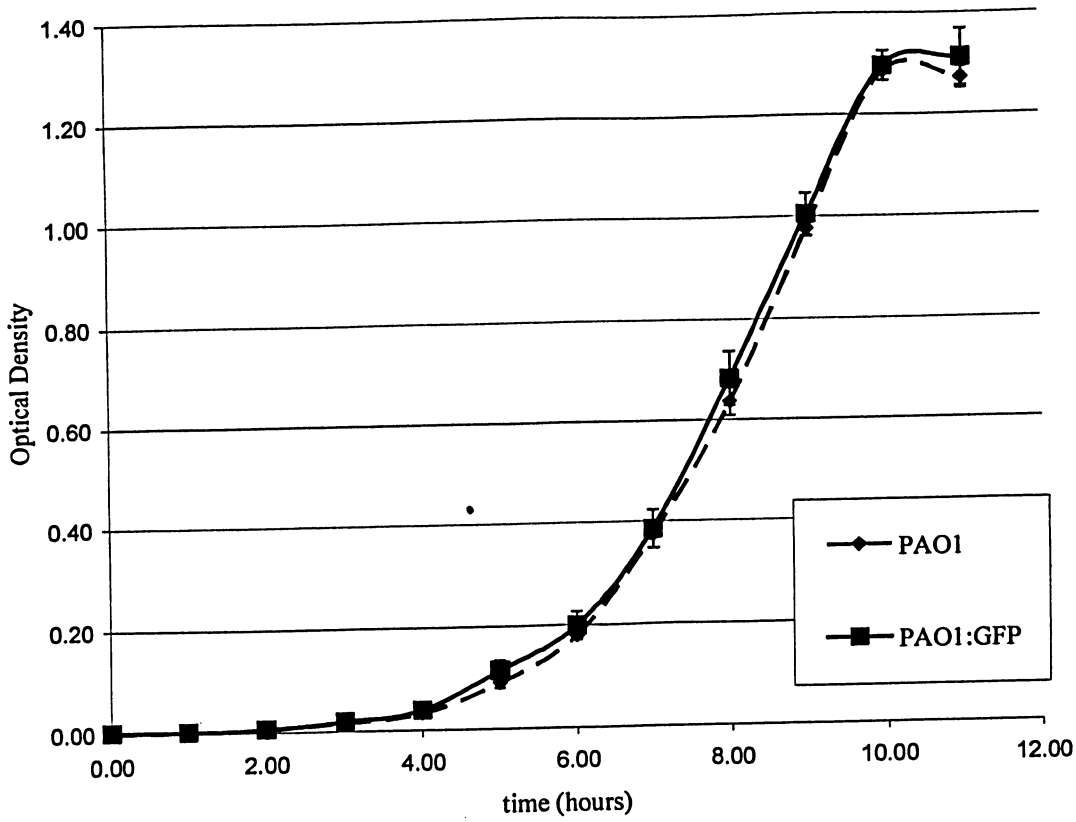

Figure 4.1. Growth curves of PAO1 and PAO1:GFP as determined by OD_{600} measurements.

4.2 Interaction between PAO1 and community 1 when introduced in different sequence

Three scenarios were selected in which the order of inoculation of PAO1 and the mixed community was varied. In scenario 1 PAO1 was inoculated first, in scenario 2 PAO1 and the mixed community were inoculated simultaneously, and in scenario 3 the mixed community was inoculated first. For a more detailed description of the procedure refer to section 3.2.2.

4.2.1 Microscopy

4.2.1.1 PAO1:GFP Biofilms

Confocal laser scanning microscopy on flow cells containing PAO1:GFP biofilms, revealed microcolonies in the form of mushroom-like structures, in biofilms that had been growing for 7 days. Figure 4.2 shows the top-view and a side-view of these structures.

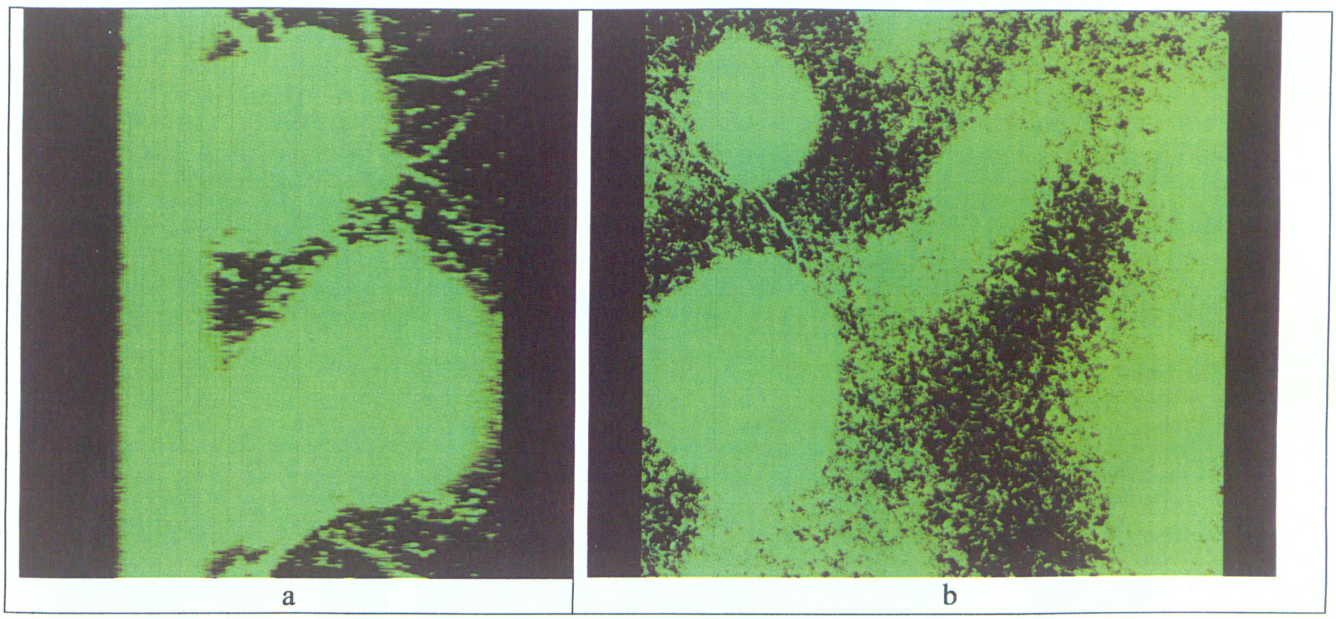

Figure 4.2. Side-view (a) and top-view (b) of microcolonies of a 7 day PAO1:GFP biofilm, obtained by a confocal laser scanning microscope, using a 63x 1.2 objective.

4.2.1.2 Community 1 and PAO1:GFP biofilms

Images shown in figures 4.3 and 4.4 are examples of scenario 1 biofilms (PAO1:GFP inoculated first), using community 1 as a mixed species biofilm. These images were obtained from biofilms that had been grown for 7 days.

As seen in figures 4.3.a and 4.4.a, PAO1:GFP cells appear to be evenly distributed horizontally. A striking observation made from figure 4.3.b, is that while most PAO1:GFP cells appear to be located closer to the attachment surface, as would be

expected considering the fact that this strain was inoculated first, some green cells are seen on the outer regions of community 1 microcolonies. This can also be seen in figure 4.3.b, as pointed out by the white arrows.

These observations may help understand survivability and proliferation of PAO1:GFP as part of a mixed community biofilm. Existence of PAO1:GFP at the biofilm-water interface may allow for these opportunistic pathogens to readily detach from the biofilm through erosion or other means of dispersion.

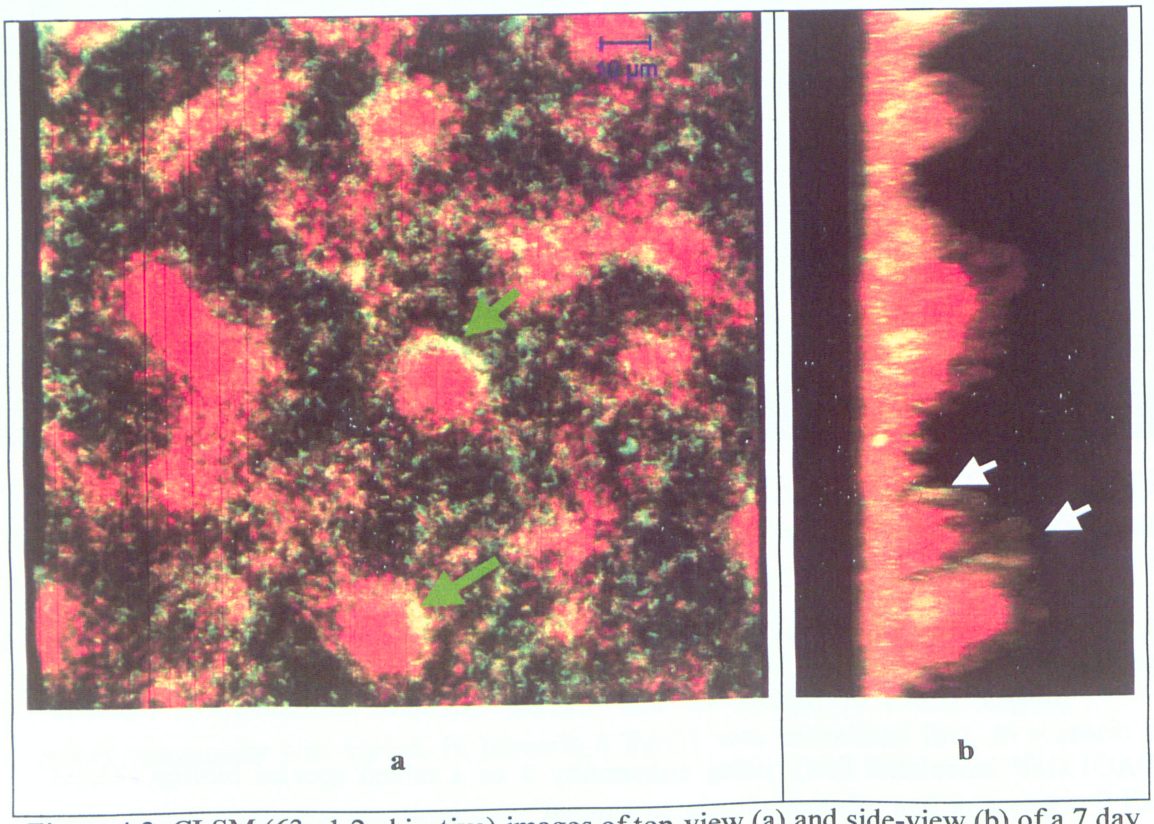

Figure 4.3. CLSM (63 x1.2 objective) images of top-view (a) and side-view (b) of a 7 day scenario 1 biofilm, showing the distribution of PAO1:GFP (green) cells within the community 1 stained with FM4-64 (red) cells. The arrows point to PAO1:GFP growth surrounding microcolonies from community members.

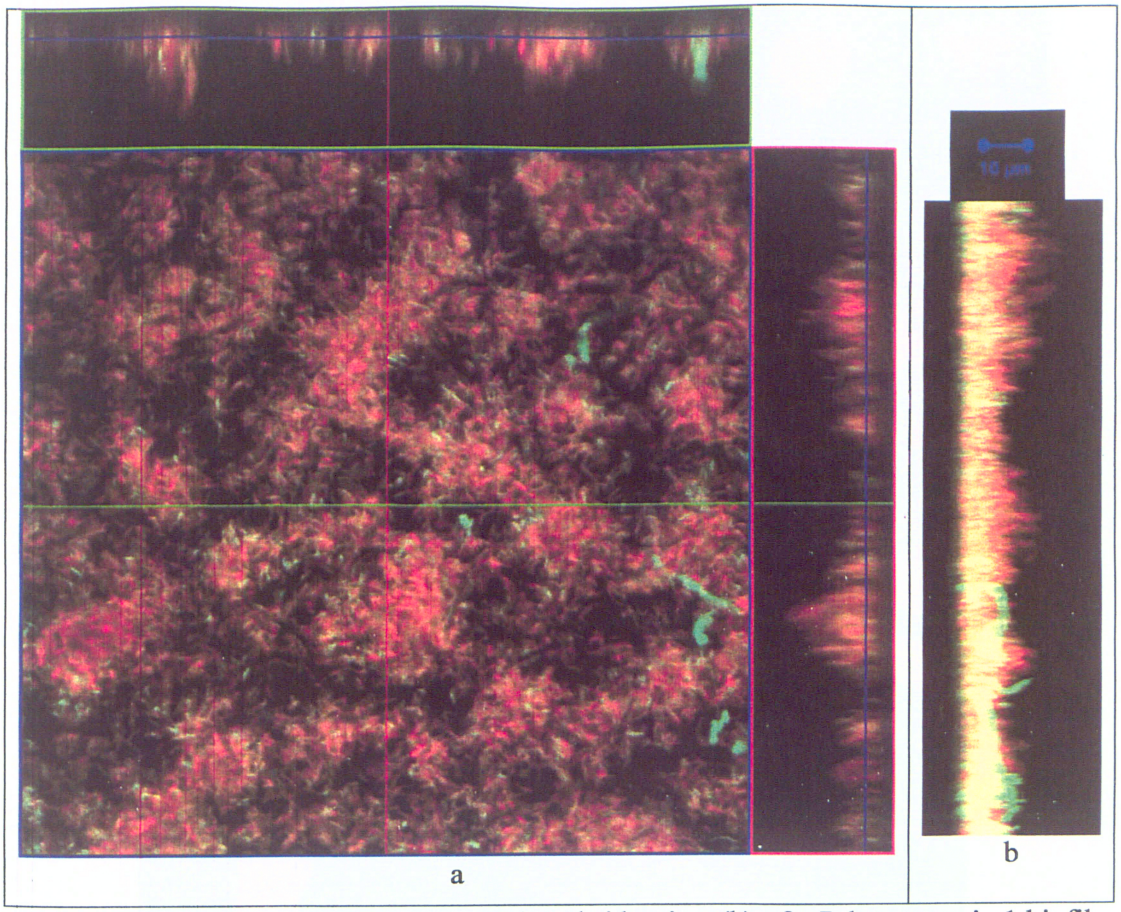

Figure 4.4. CLSM images of top-view (a) and side-view (b) of a 7 day scenario 1 biofilm, using a 63 x 1.2 objective, showing the positioning of PAO1:GFP (green) cells and community 1 (red) cells stained with FM4-64.

The biofilm images obtained from scenario 2 biofilms, using confocal laser scanning microscopy, show the complex structures of these systems (Figures 4.5 and 4.6). A notable observation made from these images is that the PAO1:GFP cells are mainly positioned at the lower layers of the biofilm, even though PAO1:GFP and community 1 were inoculated simultaneously.

Based on these images, it may be speculated that the mixed community provides a certain degree of protection to the PAO1:GFP. The issue that is raised by these observations is whether the physical shielding of the PAO1:GFP limits its detachment.

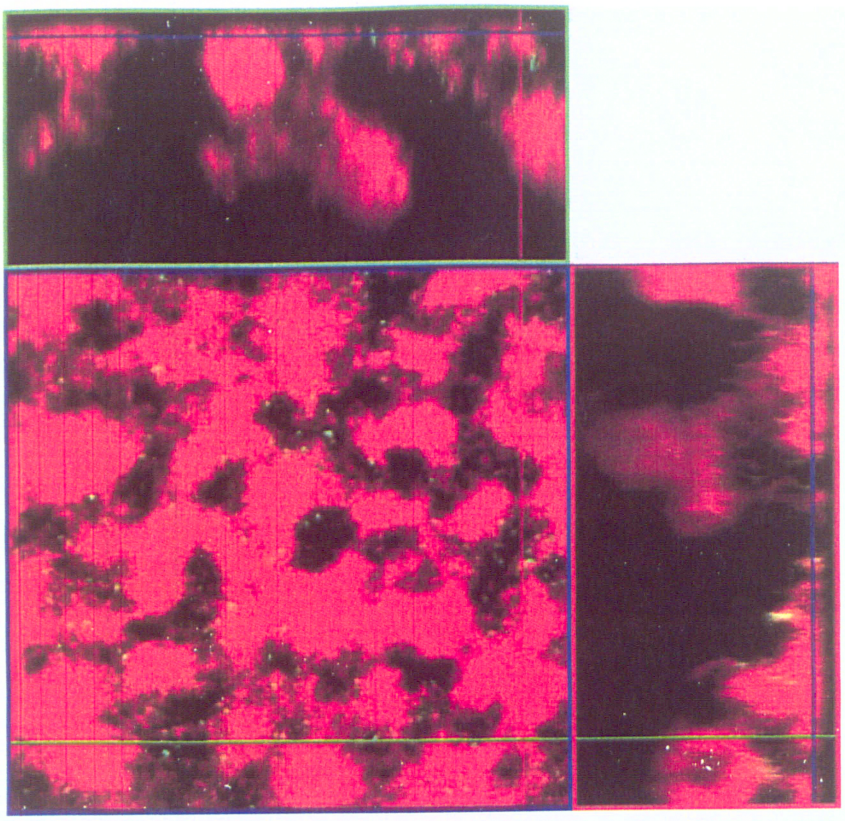

(a)

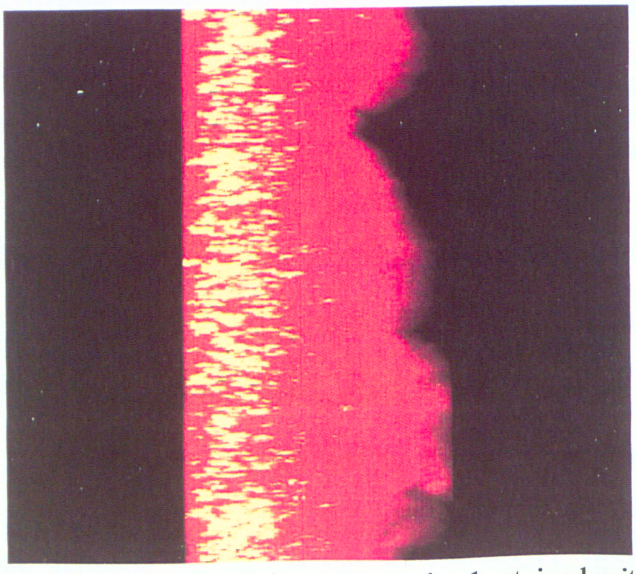

(b)

Figure 4.5. A scenario 2 biofilm showing community 1, stained with FM 4-64 (red) and PAO1:GFP (green) grown for 7 days. (a) The xy-projection image (bottom left) shows that even though PAO1 has a relatively even horizontal distribution, the xz- and yz-projections suggest that PAO1 appears to be found more frequently in the regions closer to the attachment surface. (b) A side-view cross section of the biofilm, demonstrating the accumulation of PAO1 in the regions closest to the biofilm base.

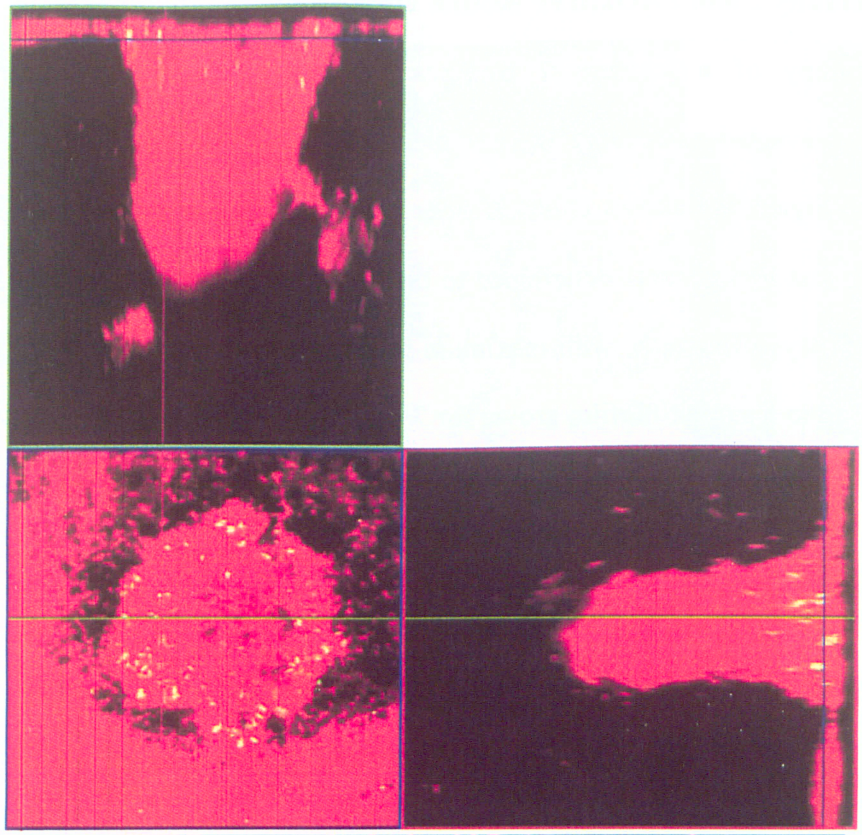

(a)

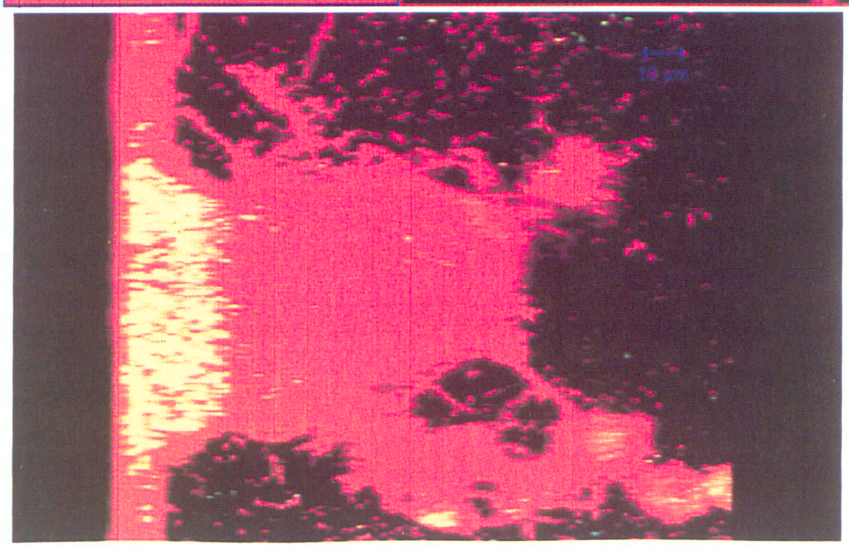

(b)

Figure 4.6. CLSM (63 x 1.2 objective) images of a microcolony of a 7 day old scenario 2 biofilm. Community 1 cells stained with FM 4-64 (red) and PAO1:GFP (green). (a) The xy-projection image (bottom left) shows that even though PAO1 has a relatively even horizontal distribution, the xz- and yz-projections suggest that PAO1 appears to be found more frequently in the regions closer to the base of the microcolony. (b) A side-view cross section of the biofilm, demonstrates PAO1 accumulation in certain parts of the microcolony, mainly close to the attachment surface.

4.2.1.3 Community 2 and PAO1:GFP biofilm microscopy

Microscopy of a scenario 1 biofilms (PAO1:GFP inoculated first), using community 2, revealed noticeably thinner biofilms than those seen in the case of community 1. Figure 4.7 shows confocal laser scanning microscope images obtained from a section that was visually determined to be one of the thickest part of a scenario 1 biofilm after 8 days of growth, with maximum thickness of about 10μm (figure 4.7.b). When compared to a similar biofilm grown for 7 days using community 1, a thickness of more than 30 μm was observed. Furthermore, cell distribution appears to be even across the attachment surface, unlike the structures seen in thicker scenario 1 biofilms seen in the case where community 1 was used (figure 4.3.b)

Figure 4.7 illustrates a bilayered biofilm, with PAO1:GFP cells growing closer to the biofilm base, while community 2 cells are mainly observed closer to the biofilm interface. This observation is consistent with the order of inoculation.

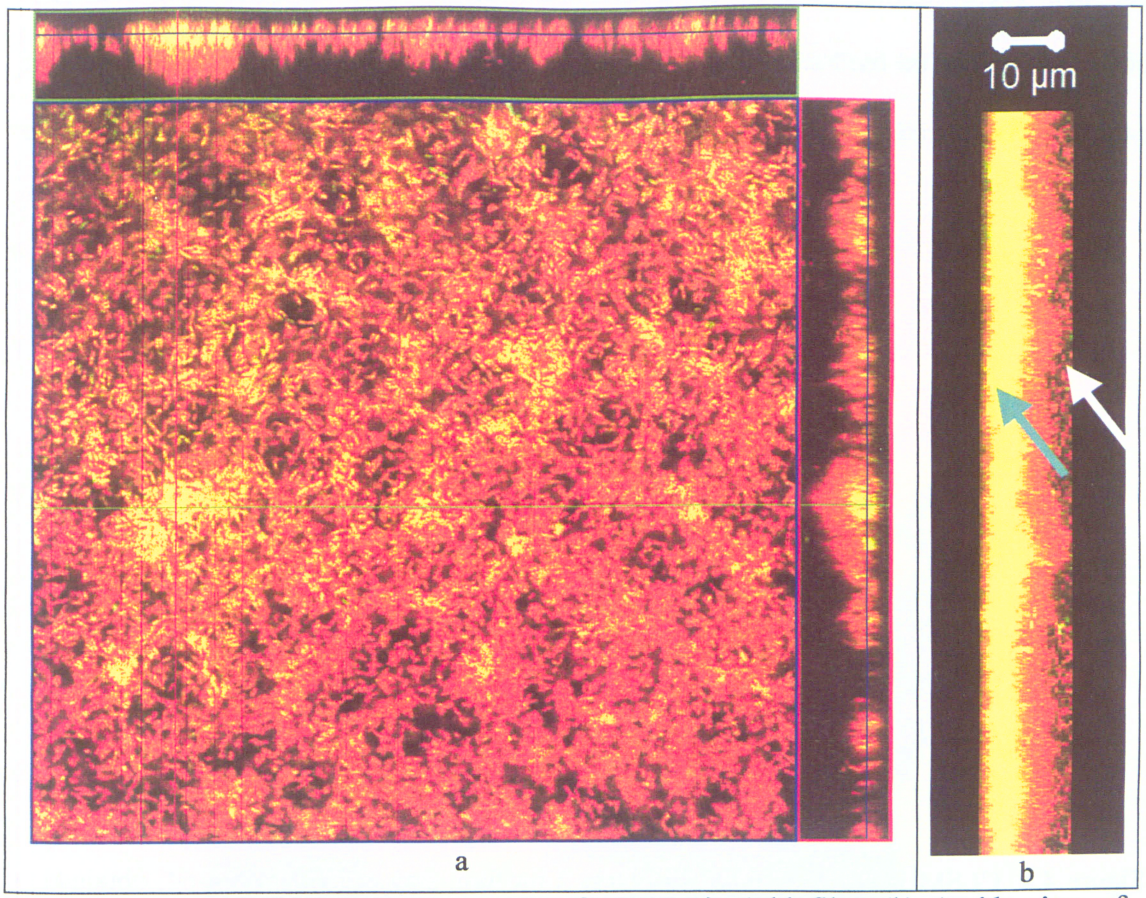

Figure 4.7. (a) An orthogonal sectioning of a scenario 1 biofilm. (b) A side-view of CLSM images obtained using a 63 x 1.2 objective, from a scenario 1 biofilm grown for 7 days, stained with FM4-64. Red cells represent community 2 cells and PAO1:GFP cells are shown in green, showing the bi-layered organization of this biofilm. The arrows point out these layers, white: community 2 layer, and blue: PAO1:GFP layer.

Confocal laser scanning microscopy images obtained from a scenario 2 biofilm, at a magnification of 20x (figure 4.8), illustrate relatively large microcolonies from community 2 strains surrounded by PAO1:GFP growth.

Although, as shown in figure 4.2, pure culture biofilms of PAO1:GFP have been shown to readily form mushroom-like structures, when grown in a community, this strain is less likely to form such microcolonies. A previous study by Lee et al. (2005) has shown that *P. aeruginosa* does not form mushrooms in the lungs of cystic fibrosis

patients. These finding suggest that a study on the structure of pure culture PAO1 biofilms may not be used as an accurate representation of the behaviour of this strain in natural environments.

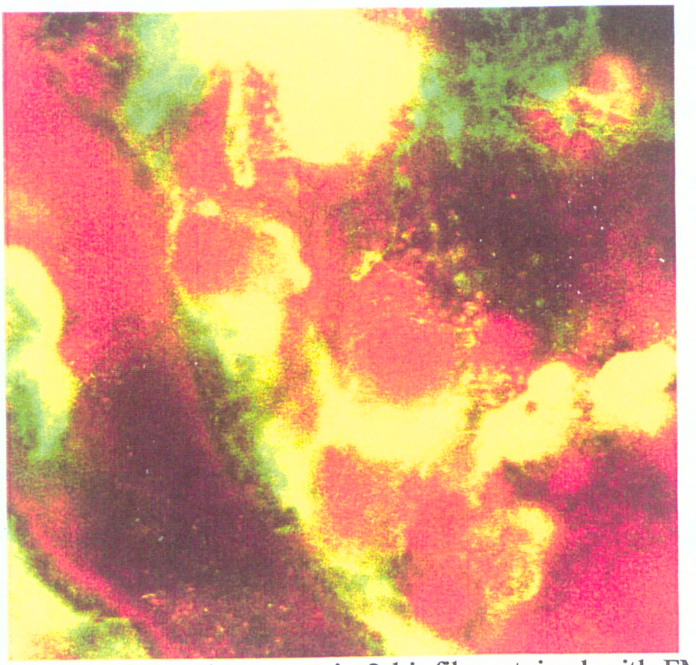

Figure 4.8. CLSM image of a 7 day scenario 2 biofilm, stained with FM 4-64, obtained by 20x objective, showing sectioning within the biofilm between PAO1:GFP cells (green) and community 2 cells (red)

Figures 4.9 and 4.10 show examples from the scenario 2 biofilms at a higher magnification (63x). These images show PAO1:GFP growth embedded in community 2 cells. In figures 4.9.b and 4.10.b a layered growth is seen, as was the case when community 1 was tested (figures 4.5 and 4.6).

Although, unlike in community 1, cells closest to the biofilm base appear to be from the mixed community, PAO1:GFP cells still seem to be protected underneath a relatively thick layer of community members. Figure 4.10 shows a section of the biofilm (pointed out with an arrow in figure 4.10.b), consisting mainly of community 2 cells

subjected to sloughing. This image reveals that cells are in fact released from the biofilm as part of aggregates. This form of dispersal provides for the detached cells to continue to enjoy advantages of existing as part of an aggregate when colonizing new surfaces.

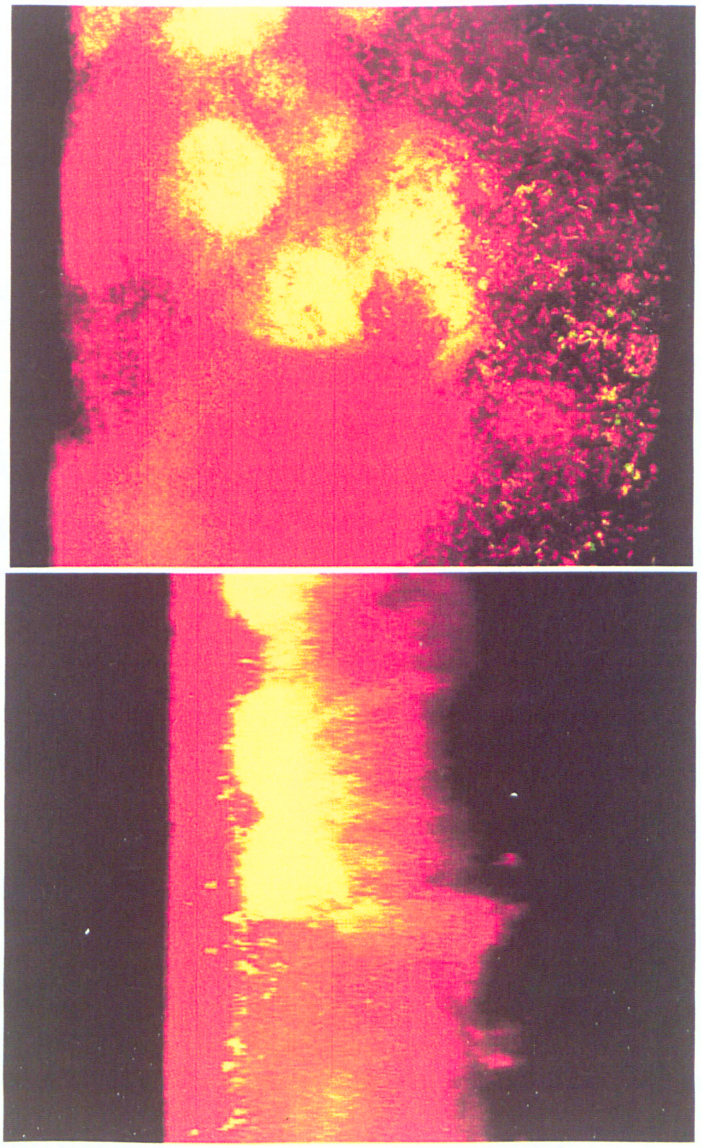

Figure 4.9. (a)Top-view and (b) through-view of a 7 day scenario 2 biofilm stained with FM 4-64, obtained by confocal laser scanning microscopy (63 x 1.2 objective) showing positioning of PAO1:GFP cells (green) among community 2 cells (red).

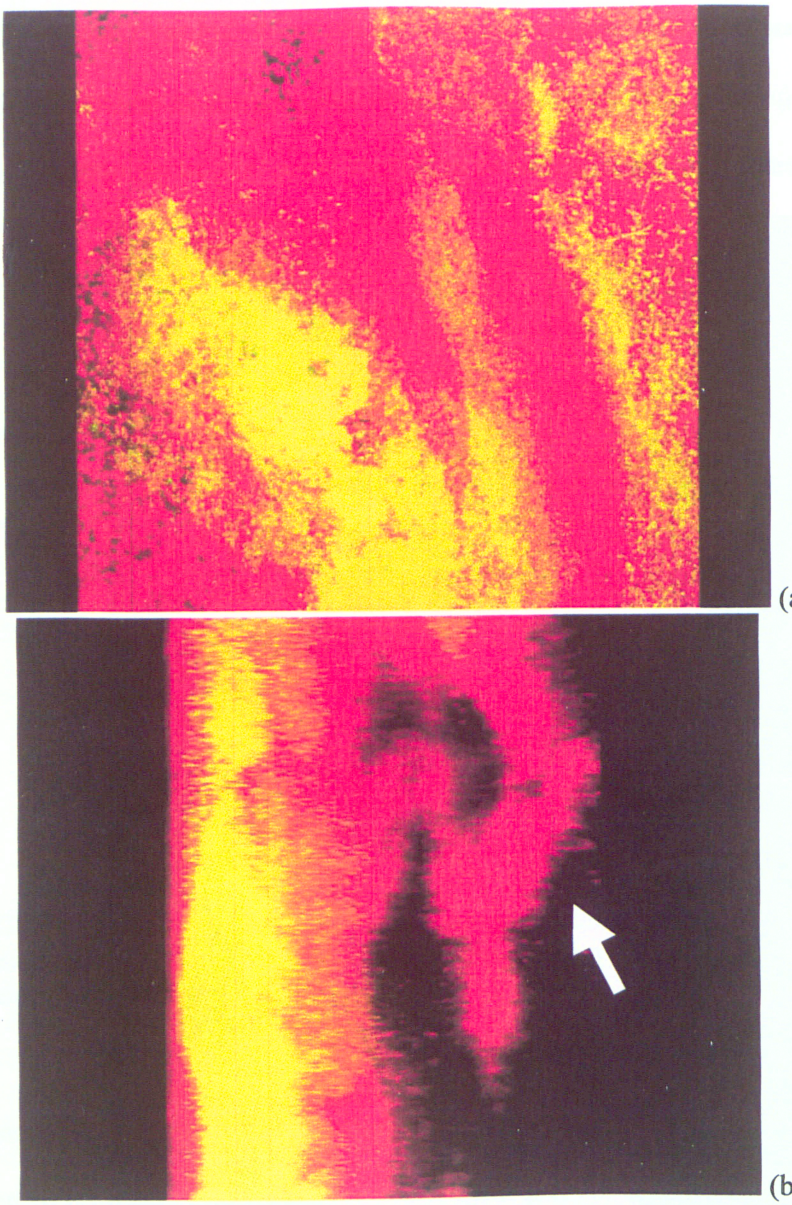

Figure 4.10. (a)Top-view and (d) through-view of a 7 day scenario 2 biofilm stained with FM 4-64, obtained by confocal laser scanning microscopy (63 x 1.2 objective) showing that sloughing of a section of the biofilm consisting mainly of community members.

Images obtained by confocal laser scanning microscopy from a scenario 3 biofilm (community 2 inoculated first), show PAO1:GFP growth surrounding microcolonies of strains from community 2. This can be seen under both 20x (figure 4.11) and 63x (figure 4.12) magnifications. Just the same, as seen in figure 4.12.b, PAO1:GFP is also

distributed inside the biofilm and thus is likely to be protected, in part, through this community association.

Considering the fact that this scenario is the most likely of the three to occur, it is important to note that the positioning of PAO1:GFP cells on the biofilm interface provides for little physical protection against environmental stress and therefore it does increase the potential for detachment and spread to other environmental surfaces.

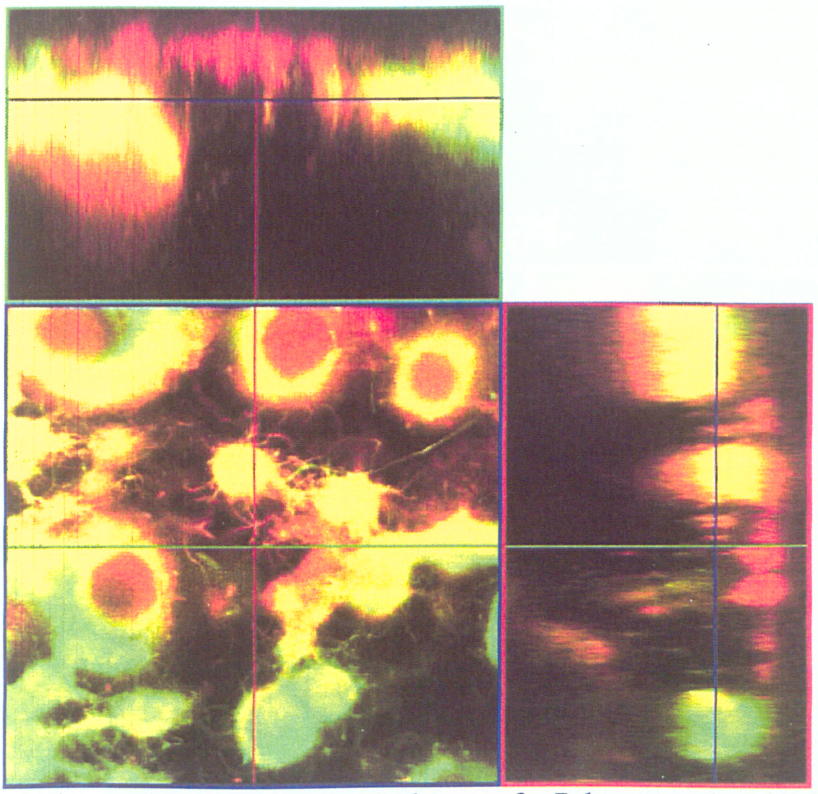

Figure 4.11. Orthogonal sectioning of a 20x image of a 7 day scenario 3 biofilm, stained with FM 4-64, obtained by confocal laser scanning microscopy shows microlonies of community 2 (red) surrounded by PAO1:GFP growth (green).

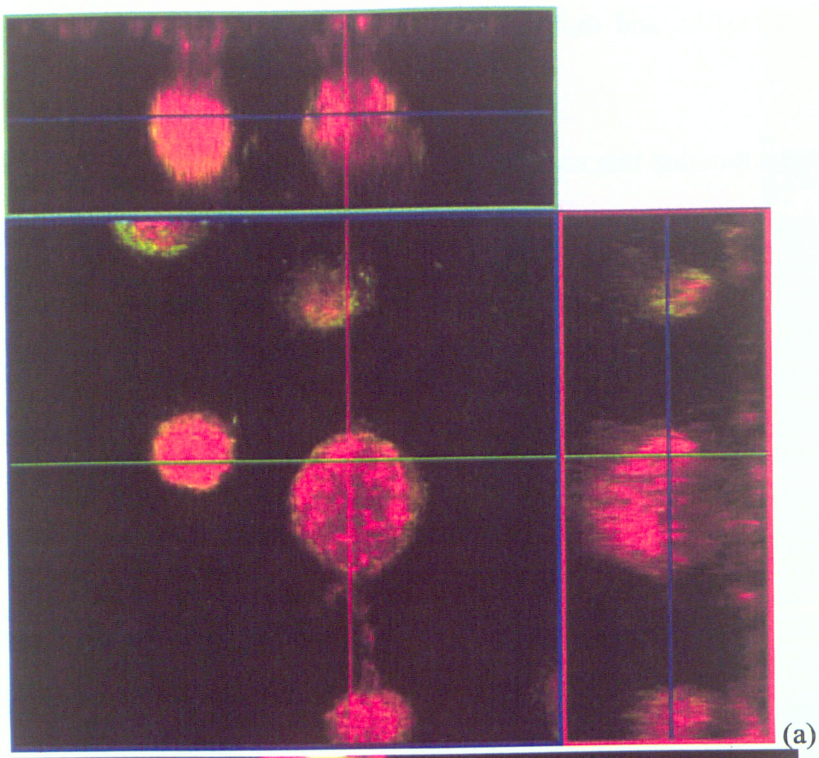

(a)

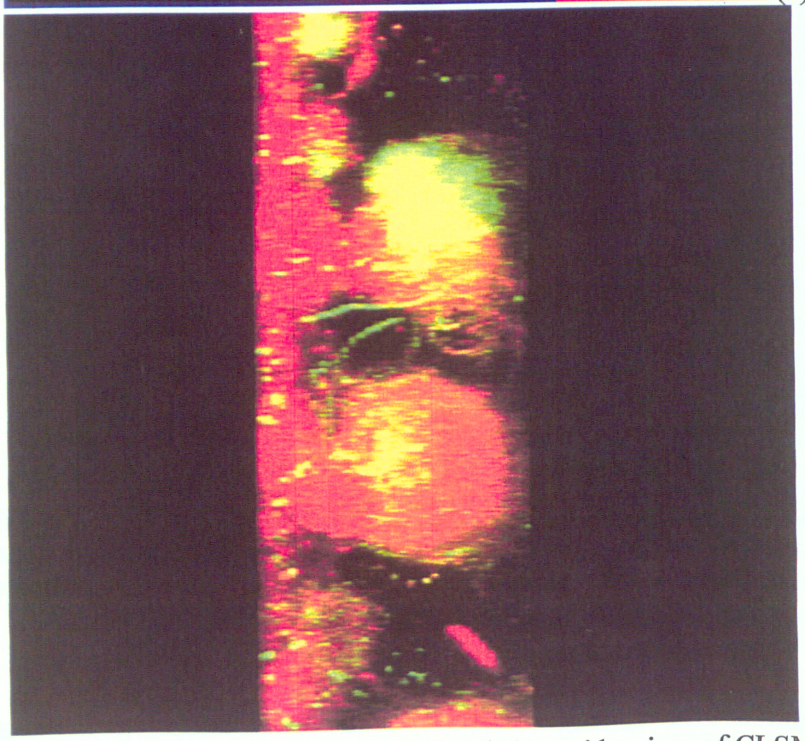

(b)

Figure 4.12. (a) An orthogonal sectioning and (b) a side-view of CLSM images obtained using a 63 x 1.2 objective, from a scenario 3 biofilm grown for 7 days, stained with FM4-64. Red cells represent community 2 cells while PAO1:GFP cells are shown in green.

4.2.1.4 Biofilm-to-planktonic cell dispersion

Epifluorescent microscopy and confocal laser scanning microscopy were used to study the effluent collected from PAO1:GFP biofilms, in order to determine the nature of cells (single or aggregates) released from the biofilms.

As seen in figure 4.13, cells are released from these biofilms as single cells, duplets, and clusters in various sizes. The presence of high numbers of duplets in the biofilm effluent, indicate that cell detachment occurs from metabolically active regions of the biofilm.

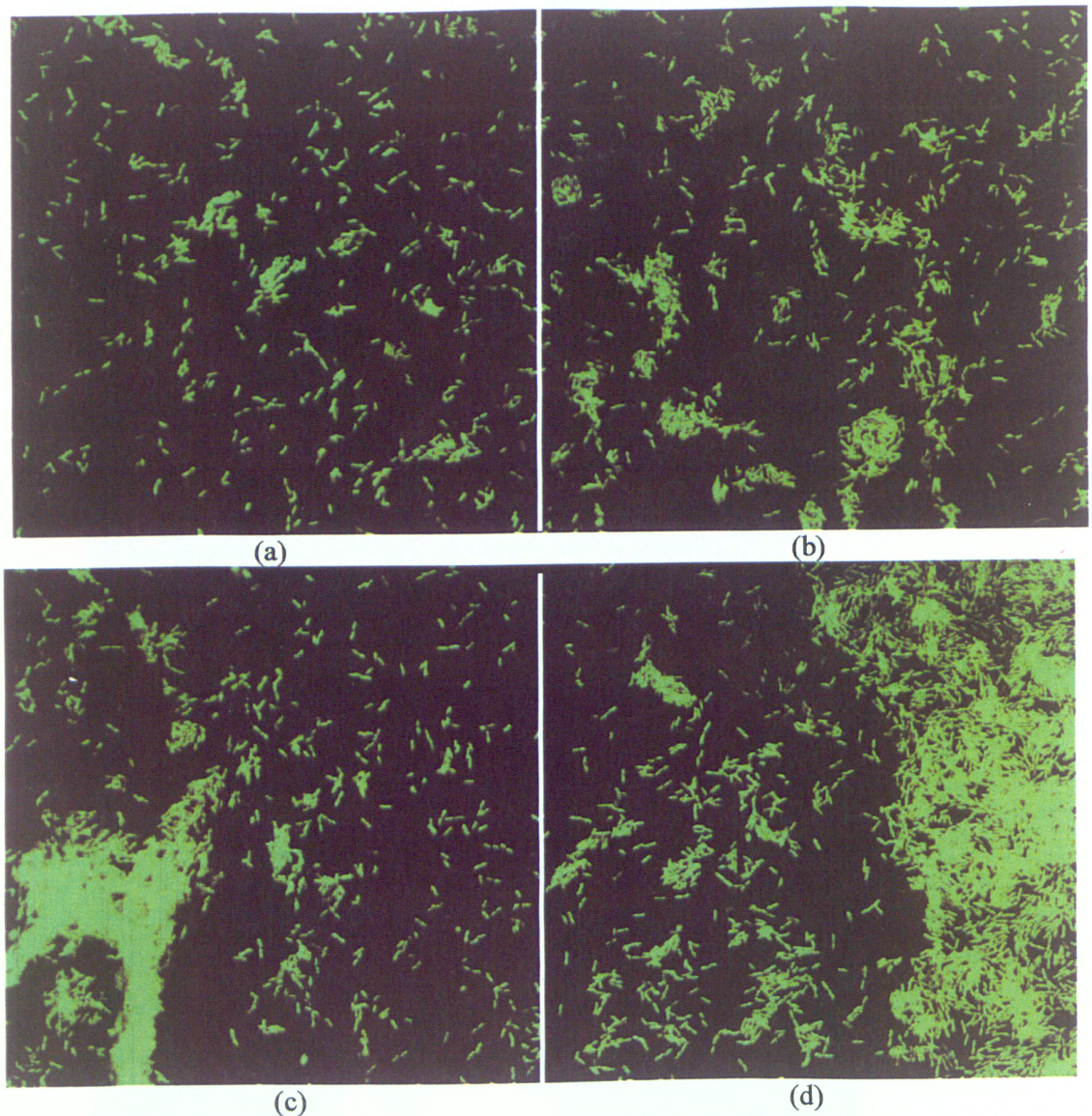

Figure 4.13. Confocal laser scanning microscope images of effluent samples from a PAO1:GFP biofilm, showing that the cells are released as single cells as well as duplets, and aggregates.

Cells detaching from biofilms cultivated under the three scenarios were also seen in both single and aggregate forms. Figure 4.14 shows an image obtained by confocal laser scanning microscopy from effluent of scenario 1 biofilms. In this image a small cluster of PAO1:GFP cells can be seen. Figure 4.15 is an example of effluent obtained from a scenario 2 biofilm that shows a large cluster containing PAO1:GFP and

community 1 cells. Images obtained from the effluent of scenario 3 biofilms are shown in figure 4.17. Epifluorescent images (figure 4.16.a and 4.16.b) show large clusters containing community 1 and PAO1:GFP cells. The image obtained by confocal laser scanning microscopy (figure 4.16.c) shows single cells of the community members as well as PAO1:GFP.

The presence of the mentioned large clusters in the effluent may afford protection to the test strain, not only in the form of existing as part of an aggregate, but also potential physical protection provided by community members.

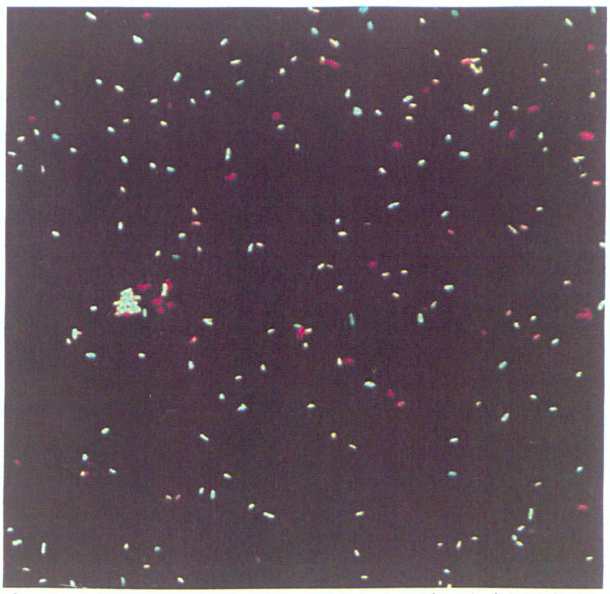

Figure 4.14. CLSM images from effluent of a scenario 1 biofilm, using community 2, stained with FM 4-64, showing single cells of PAO1:GFP (green) and community members (red) as well as a small aggregate of PAO1:GFP cells.

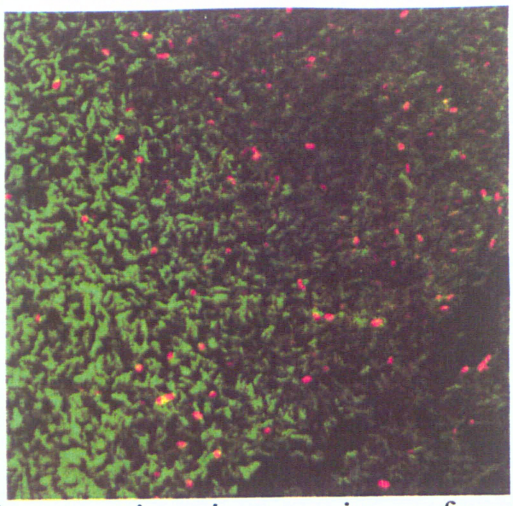

Figure 4.15. Confocal laser scanning microscope images from effluent of a scenario 2 biofilm. Red: community 1 cells stained with FM 4-64. Green: PAO1:GFP

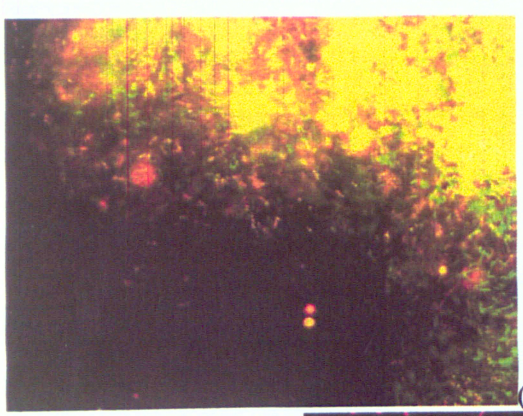

(a)

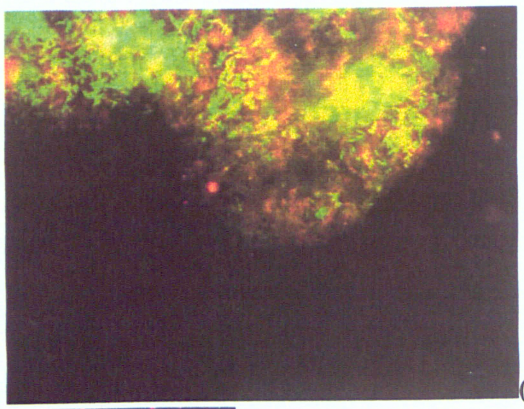

(b)

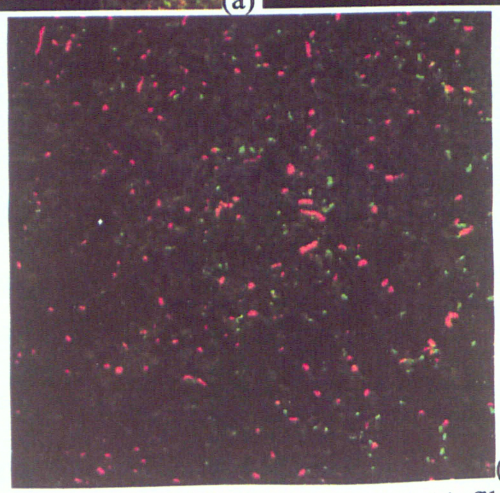

(c)

Figure 4.16. Examples of effluent samples of scenario 3 biofilms. Large clusters of cells (a) and (b) obtained by epifluorescent microscope, stained with nile red, and single cells (c) obtained by confocal laser scanning microscope. Community members are shown in red and PAO1:GFP cells are green.

4.2.2 Enumeration

Shown in figure 4.17 is the total number of cells released from the biofilms per ml of effluent over 7 days, starting from the time of flowcell inoculation, in scenario 2, and the time of community 1 inoculation in scenario 1 and PAO1:GFP inoculation in scenario 3. The number of detached cells from all biofilms throughout this period varied between 10^8 and 10^{11} cell/ml of effluent, and there was no significant difference between samples over time.

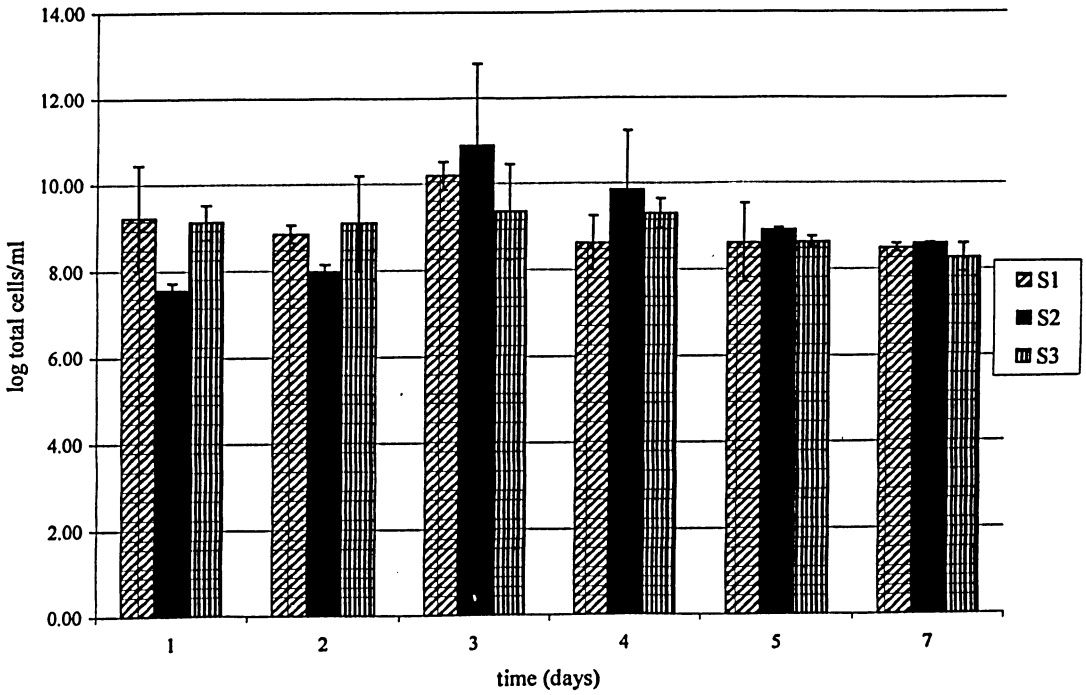

Figure 4.17. Cells released by biofilms, containing PAO1:GFP and community 1, in the three scenarios (S1, S2, and S3), over 7 days. t = 0 in S1: the time of community 1 inoculation, S2: inoculation of community members and PAO1:GFP, and S3: time of PAO1:GFP inoculation.

Figure 4.18 illustrates changes in ratio of PAO1:GFP in relation to the overall number of cells released from the mixed community biofilms in all three scenarios. Initially, the majority of cells released from the biofilms in scenario 1, where PAO1:GFP

was inoculated first, were PAO1:GFP cells. However, these numbers dropped rapidly to about 40% over 7 days. Conversely, cells detaching from a scenario 3 biofilm, where community 1 was inoculated first, were mainly from the community members. Although, the ratio of PAO1:GFP to drain cells fluctuated considerably over time, there seemed not to be a trend in the changes, nor did the PAO1:GFP portion of the detachment exceed 20% throughout the growth period. Scenario 2 was the most variable among the three. Even though the total number of released cells exhibited the same trends as scenarios 1 and 3, changes in the PAO1:GFP ratio did not follow a specific pattern while it changed drastically from one sampling time to the next.

It is important to point out that even though in many cases the relative number of PAO1:GFP decreased as the biofilm aged, because there are high numbers of cells being released (10^8 - 10^{11}), even a small percentage would represent large number of cells.

Naturally occurring biofilms usually grow for longer periods than what was tested in these experiments. Therefore, it is notable that the relative number of PAO1:GFP cells over time does not decrease to a point where these values are insignificant. For instance, a 12 day old scenario 2 biofilm was shown to release 5.8×10^8 cells/ml, of which 47% was PAO1:GFP.

These results lead to the conclusion that PAO1:GFP is very successful in incorporation and proliferation in a community context. Furthermore, from the high percentage of PAO1:GFP it may be concluded that this strain is likely to be one of the most dominant species in the mixed community after 7 days of growth, in all three scenarios.

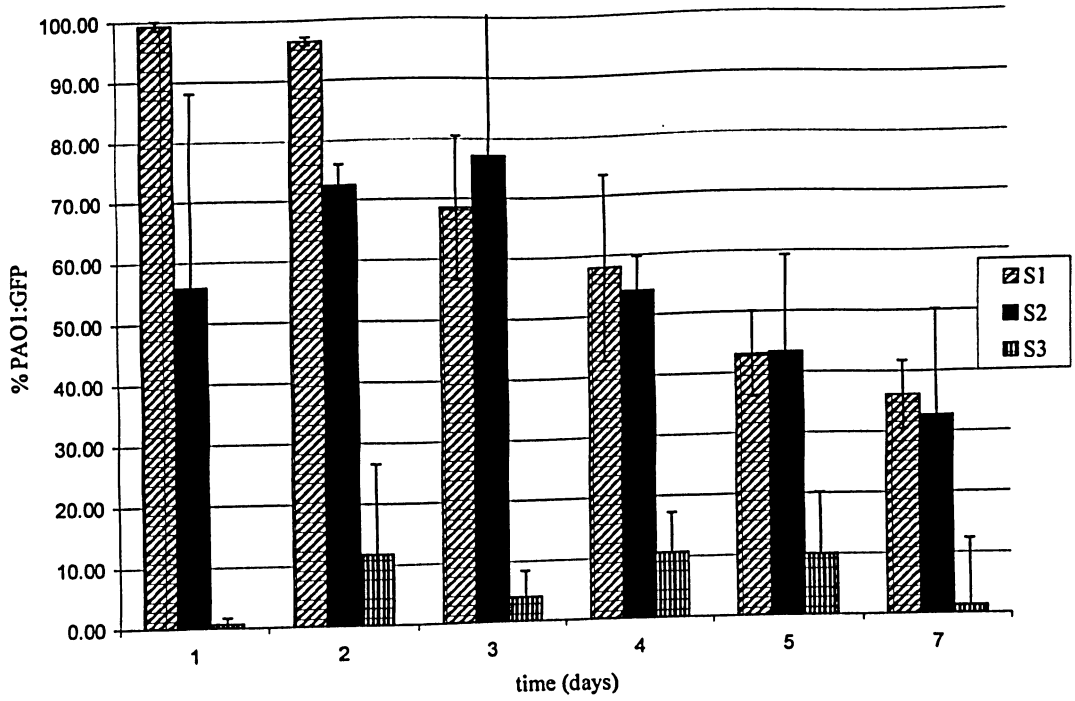

Figure 4.18. Changes in the percentage of PAO1:GFP cells in relation to the total number of released cells from the biofilms in each scenario, over 7 days. t = 0 in S1: the time of community 1 inoculation, S2: inoculation of community members and PAO1:GFP, and S3: time of PAO1:GFP inoculation.

When community 2 was used as a source of mixed species, in testing cell detachment from biofilms in the three scenarios, the same variability existed as was seen in the case of community 1 as a source of mixed species. As shown in figure 4.19, the total number of cells released by the biofilms varied between 10^8 and 10^{11}. These values did not change significantly over time.

Another notable observation is that the number of detaching cells did not seem to be correlated to biofilm thickness. For instance, confocal laser scanning microscopy images obtained from 7 day scenario 1 biofilms (figure 4.7.b) were consistently thinner than those of the other scenarios, under similar conditions (figures 4.9.b and 4.12.b),

however the number of released cells from the biofilms did not differ significantly. This observation may lead to the conclusion that biofilms seem to be effective sources of planktonic cells, regardless of thickness.

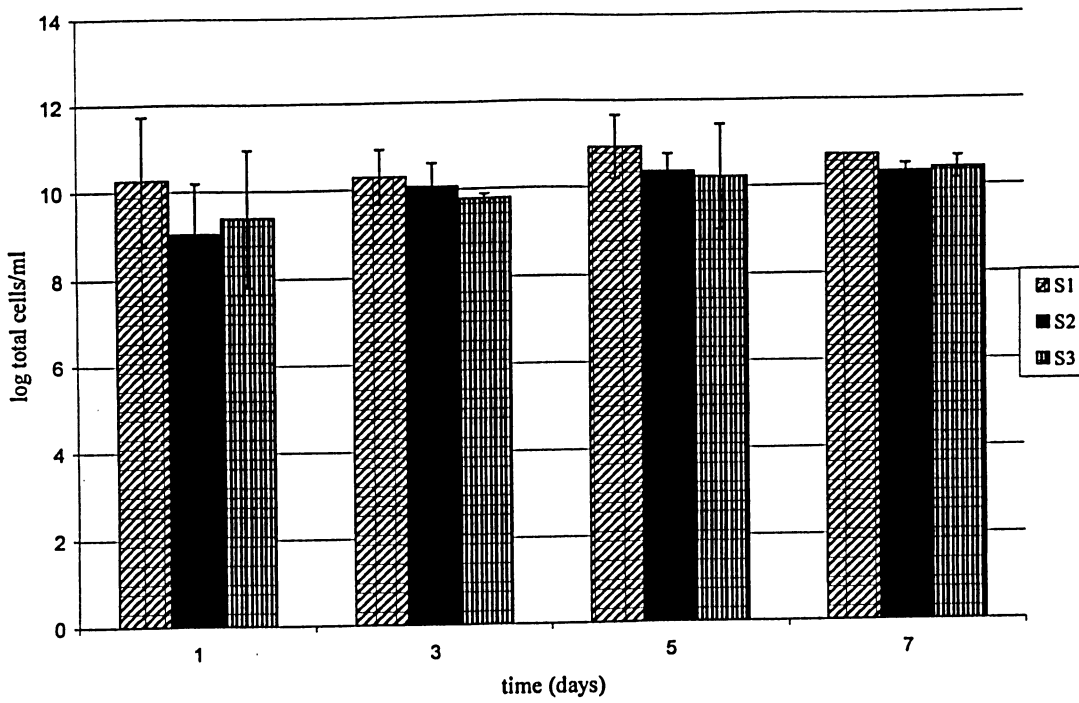

Figure 4.19. Cells released by biofilms, containing PAO1:GFP and community 2, in each scenario, over 7 days. t = 0 in S1: the time of community 2 inoculation, S2: inoculation of community members and PAO1:GFP, and S3: time of PAO1:GFP inoculation.

Figure 4.20 shows changes in the percentage of PAO1:GFP cell detachment from biofilms in the three scenarios. A high degree of variability existed among biofilms containing the same strains, cultivated under similar conditions, in terms of the ratio of PAO1:GFP cells released by the mixed species biofilms, as illustrated by the large error bars in figure 4.20. It thus appears that integration of PAO1 with community members is largely a random process; thus what can be concluded from these observations is that PAO1 successfully integrates into the community but this colonization does not occur in

a predictable fashion. This phenomenon is probably widespread among different microbial species and should be considered when microbial processes are modeled.

Despite the obvious inconsistency in replicate biofilms, certain trends were observed with respect to PAO1:GFP detachment over time, within each scenario. In scenario 1 (PAO1:GFP inoculated first), the percentage of PAO1:GFP cells in relation to the total cells released by the biofilm decreased with time, from more than 99.9% to 4% during 7 days. These results are consistent with the order of inoculation and show that PAO1:GFP, as an established biofilm, provided the majority of detached cells, when compared to the freshly inoculated community 2. However, as the layer of community members grew thicker, covering the older PAO1:GFP layer, the main form of detachment was observed to be mixed species.

The ratio of PAO1:GFP released from scenario 2 biofilms also decreased over time, although, the rate of decrease was not as high as in scenario 1. Although, both PAO1:GFP and community 2 were inoculated simultaneously, 24 hours following inoculation 97% ± 2 of released cells were PAO1:GFP. On day 7 following inoculation, PAO1:GFP represented 40% ± 5 of the total number of detached cells.

These results may be explained when compared to microscope images obtained from the producing biofilms. As seen in figures 4.6, 4.9 and 4.10, there existed a layer of community species covering PAO1:GFP biofilm cells in 7 day scenario 2 biofilms. This layer was speculated to be the result of a higher rate of growth of the mixed species. Therefore, it may be concluded that as the layer of community species grows thicker, the ratio of detaching PAO1:GFP cells decreases. This observation also provides an indication that the majority of cell detachment occurred at the outer biofilm layers,

possibly as a result of erosion.

Initial cell detachment from scenario 3 (community 2 inoculated first) was found to consist mainly of community members and only 3% ± 3 were PAO1:GFP. Although, the relative number of detaching test strains increased over time with a large degree of variability, the percentage of PAO1:GFP cell did not exceed 52% ± 20. In fact, these values appeared to have dropped from 52% ± 20 on day 5 to 45% ± 15 on day 7 following PAO1:GFP inoculation.

The increase in the ratio of PAO1:GFP cells may be the result of the growth of this strain as a layer covering other community members. These results indicate successful integration of PAO1:GFP into the mixed community in the form of a dominant member. On the other hand, the fact that the increase is gradual, could be explained through speculation that the mixed community, as a whole, grows at a higher rate compared to PAO1:GFP.

These observations point to a highly variable nature of biofilm form. Replicate experiments carried out under the same growth conditions, including nutrient, flow rate and inoculation period, resulted in considerable variations as is made obvious by the large error bars on the charts in figures 4.17, 4.18, 4.19 and 4.20. The complications caused by lack of biofilm reproducibility have been reported previously (Bester et al., 2005).

A study by Lewandowsky et al. (2004) intended to explain biofilm inconsistencies. They suggested that structural changes to the biofilms were caused by sloughing and re-growth cycles. They found biofilms to be reproducible only until the first sloughing event and questioned the existence of a steady state in biofilm reactors.

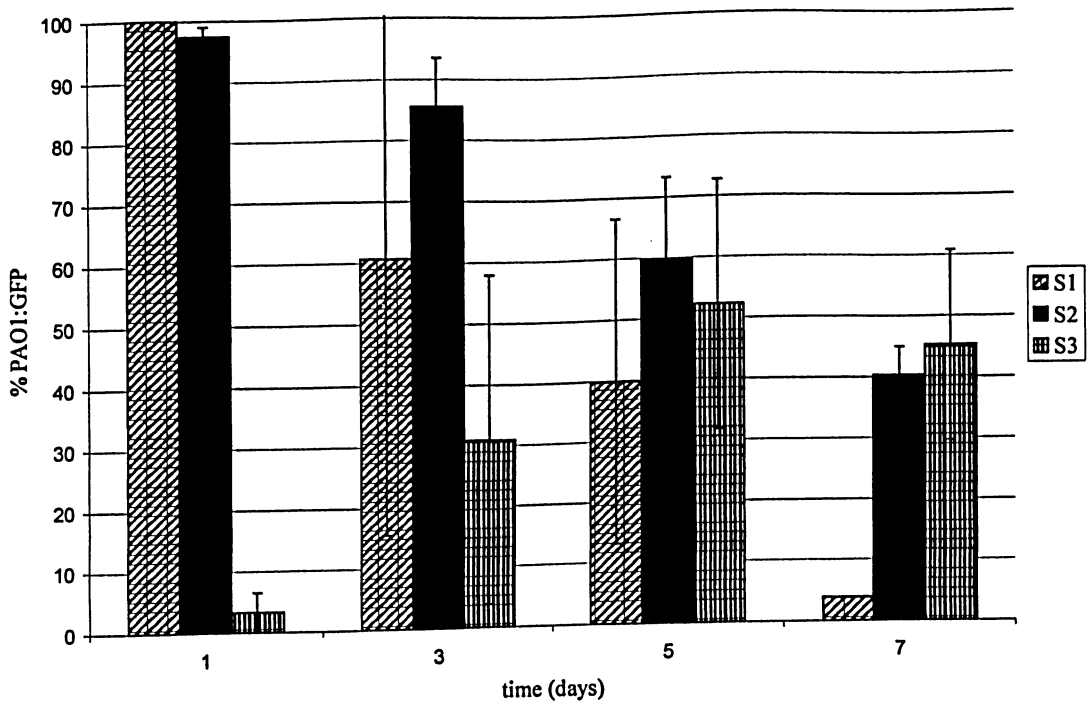

Figure 4.20. Changes in the percentage of PAO1:GFP cells in relation to the total number of released cells from the biofilms in each scenario, over 7 days. t = 0 in S1: the time of community 2 inoculation, S2: inoculation of community members and PAO1:GFP, and S3: time of PAO1:GFP inoculation.

In summary, PAO1:GFP cells are released from biofilms in all scenarios as single cells and as part of aggregates, which often included other community members. This form of dispersal may provide an advantage for the opportunistic pathogen to colonize new surfaces and ultimately cause infection in individuals with compromised immune systems.

Although the test strain was observed in the effluent of all three tested biofilm scenarios, its amount relative to that of the total released cells varied over time. This variation was often seen as a decrease in the relative PAO1:GFP numbers over the seven-

day experiments.

Visualization of the biofilms in the three scenarios helped explain these observations. PAO1:GFP cells were often found at the bottom of thick biofilms, which could have prevented dispersion to the same degree as community members at the outer layers.

4.3 Effect of antibiotic treatment

The susceptibility of planktonic PAO1:GFP to streptomycin was tested through determination of the minimal inhibitory concentration (MIC), which was found to be 7 μg/ml when grown in batch culture. Since biofilms have been found to have higher antibiotic resistance, the streptomycin concentration used for treating the biofilms was selected to be slightly higher than the MIC (8μl/ml).

When epifluorescent microscopy was used to analyze effluent samples obtained from a PAO1:GFP biofilm, before and after streptomycin (8μl/ml), very different images were produced (figure 4.21). Effluent images acquired prior to streptomycin addition showed single cells and aggregates in various sizes, while in those obtained following 2 hours of streptomycin exposure, only large clusters were observed.

It should be pointed out, however, that the there is no evidence supporting the possibility of streptomycin exposure inducing aggregate detachment. The lack of single cells observed by epifluorescent microscopy may be the result of a decrease in gfp expression in single cells as a result of streptomycin exposure, as has been reported previously (Collins et al., 1998). Since streptomycin is an inhibitory antibiotic that functions by targeting protein production, it is expected that it inhibited expression of gfp

in detaching single cells, while those present in aggregates seemed to be protected against streptomycin exposure and were consequently fluorescent. Since it had been shown previously that PAO1:GFP was released from mixed community biofilms as part of aggregates (section 4.2.1.4), it may be assumed that this strain would be able to spread and colonize new surfaces upon streptomycin exposure (8µl/ml) of mixed community biofilms in the three scenarios.

(a) (b)

Figure 4.21. Epifluorescent microscope images obtained from a PAO1:GFP biofilm, (a) before streptomycin exposure (8µl/ml) showing single cells and small clusters; and (b) after streptomycin (8 µg/ml) application, showing a large cluster.

Figures 4.22 and 4.23 are images from examples of PAO1:GFP biofilm, 48 hours after streptomycin treatment, stained with BacLight. They show a layer of dead cells covering live biofilm cells. As seen in figure 4.23, exposure to streptomycin (8 µg/ml) did not seem to significantly affect the structure of biofilms, as the microcolonies remained intact.

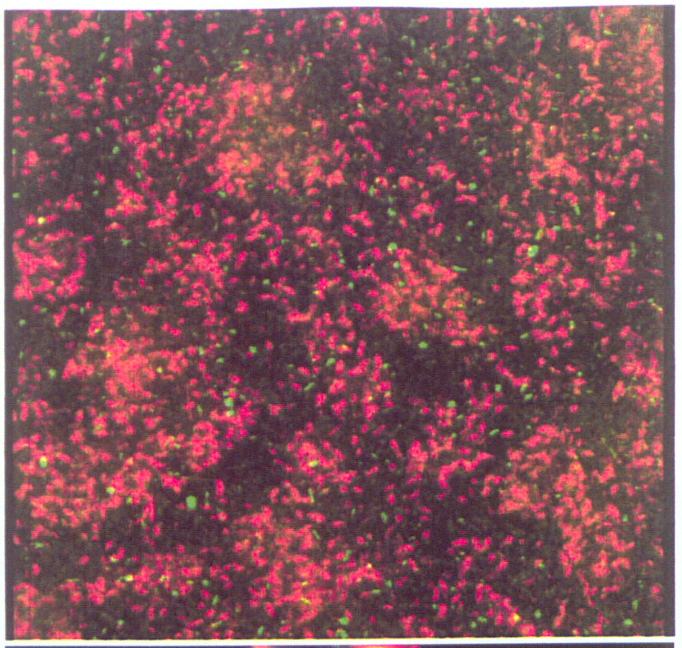

(a)

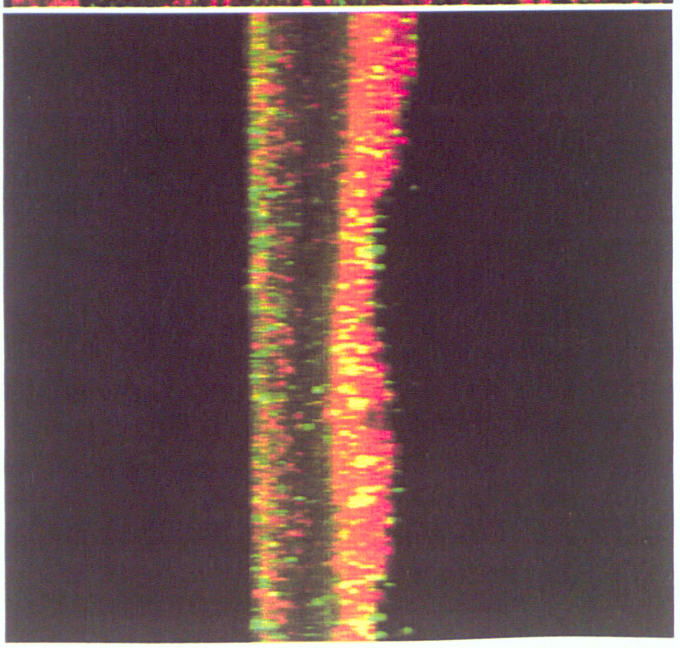

(b)

Figure 4.22 (a) Top view and (b) side-view from confocal laser scanning microscopye images obtained from a 7 day PAO1:GFP biofilm, 48 hours following treatment with streptomycin (8 µg/ml) for 2 hours, stained with propidium iodide (red, dead) and styo 9 (green, live) showing the majority of live cells closer to the biofilm base, covered by a layer of predominantly dead cells.

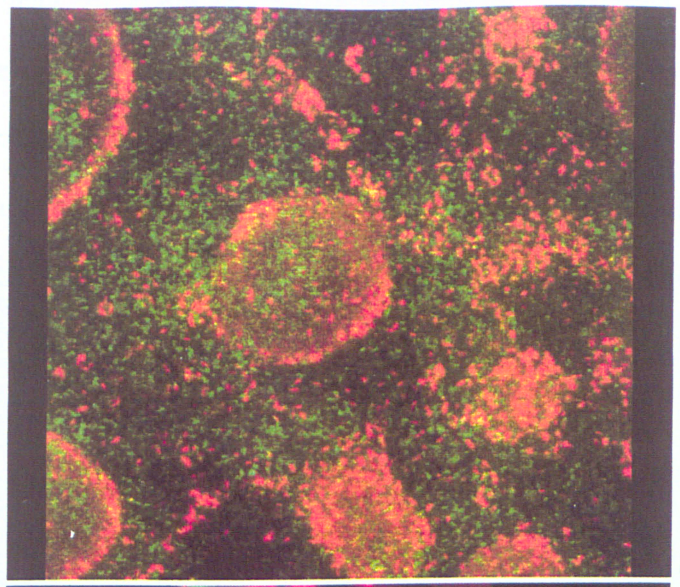

(a)

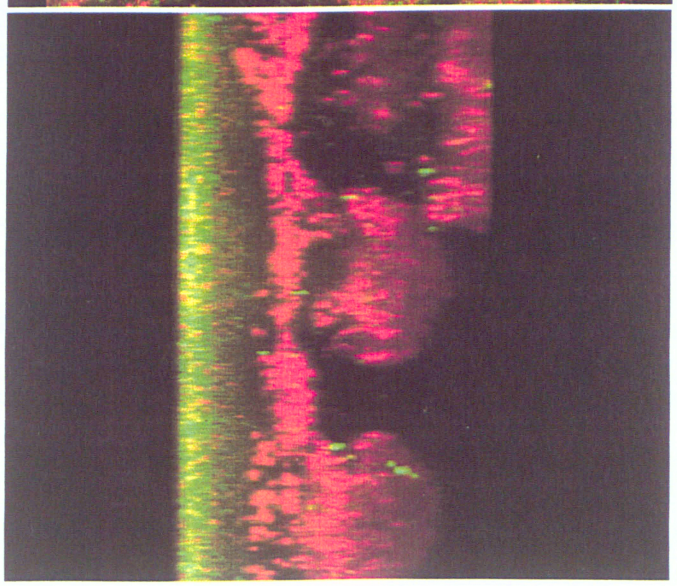

(b)

Figure 4.23 (a) Top view and (b) side-view from confocal laser scanning microscopy images obtained from a 7 day PAO1:GFP biofilm, 48 hours following treatment with streptomycin (8 µg/ml) for 2 hours, stained with propidium iodide (red, dead) and styo 9 (green, live), displaying the protected basal layer of the biofilm to consist mainly of live cells, while the 'heads' of the mushroom structures appear to be predominantly dead.

As seen in figure 4.24, addition of streptomycin to the mixed community biofilms, at a concentration of 8 µg/ml, increased the number of released cells from scenarios 1 and 3 during the exposure period, while it had no obvious effect on

detachment from the scenario 2 biofilm. Over the next 48 hours, the yield of scenario 1 dropped significantly, while in the case of scenarios 2 and 3 the total numbers of detached cells were restored to original levels. Overall, the pattern of changes in the number of released cells from the biofilms does not reveal a particular trend. Furthermore, the changes in cell detachment levels are not very extreme, as it does not exceed two orders of magnitude throughout the course of the experiment.

In contrast to scenarios 1 and 3, as seen in figure 4.24, a pure culture biofilm of PAO1:GFP reacted to streptomycin exposure with a significant drop in the number of released cells, initially. However, these numbers increased over the next 48 hours. The ability of the PAO1:GFP biofilms to restore their effluent levels may be explained with figures 4.22 and 4.23, which show only a thin upper layer of the biofilm seems to be affected by streptomycin treatment.

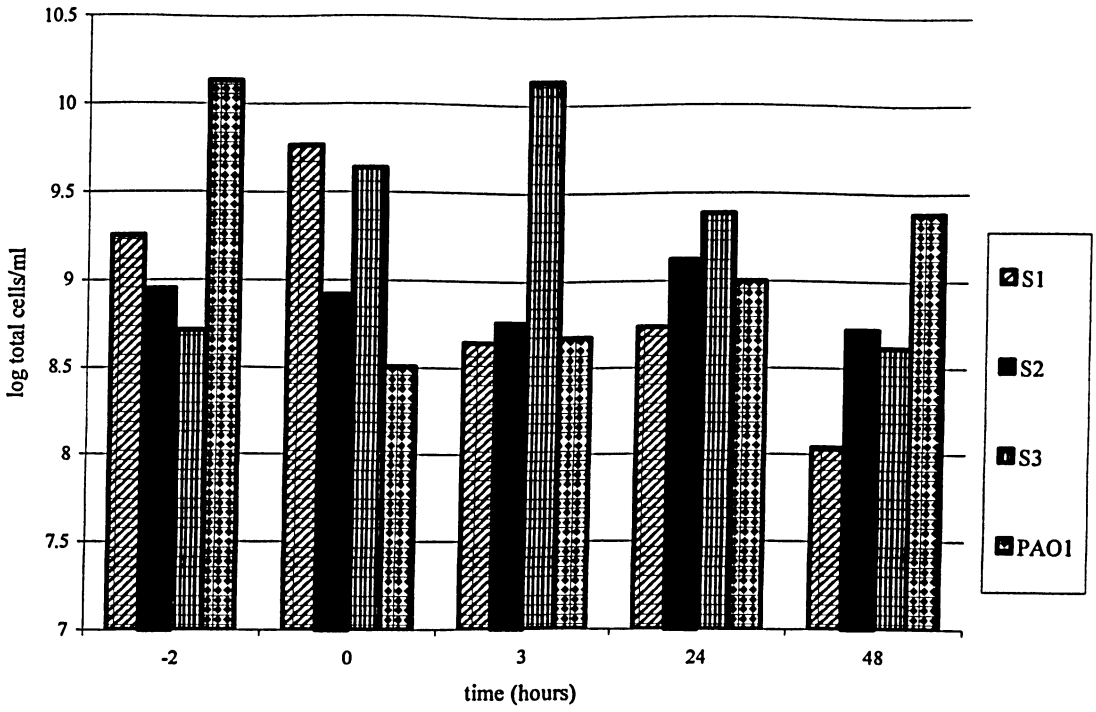

Figure 4.24. Changes in the total number of released cells from biofilms in the three scenarios (S1, S2, and S3) and pure culture PAO1:GFP in reaction to streptomycin (8 μg/ml) exposure (time -2 to 0)

The PAO1:GFP strain in these mixed community biofilms were affected by the streptomycin addition in a different manner compared to other strains. Figure 4.25, demonstrates a significant drop in the percentage of PAO1:GFP cells in all scenarios. Furthermore, these numbers did not increase drastically during the 48 hours following the treatment.

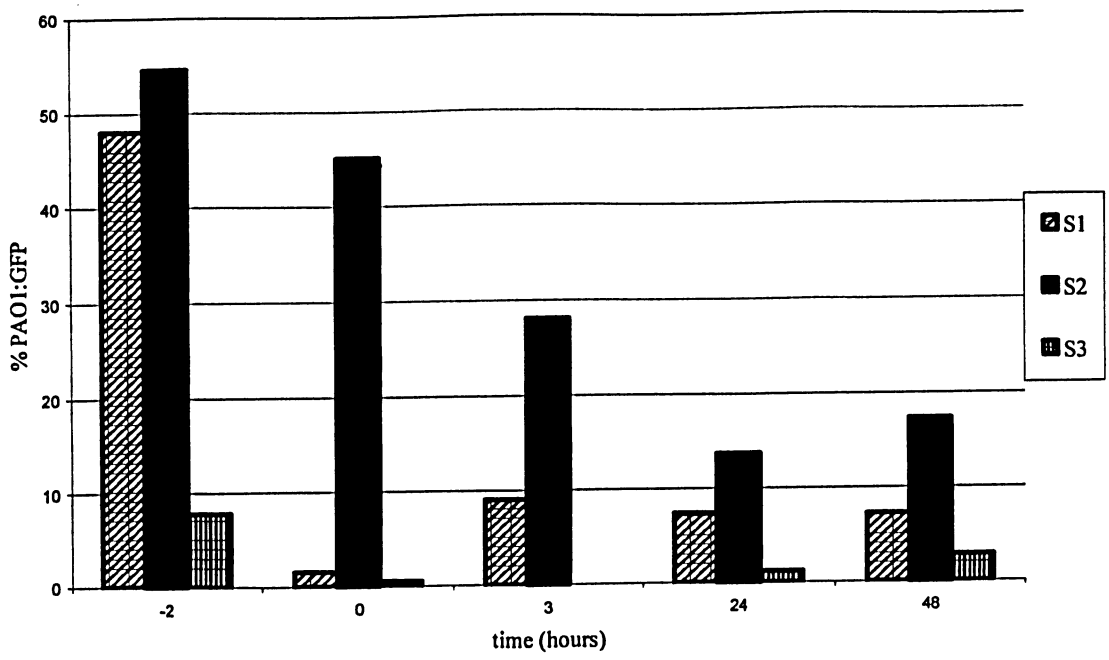

Figure 4.25. Changes in the percentage to PAO1:GFP cells released by the biofilms of the three scenarios upon streptomycin (8 μg/ml) exposure (time -2 to 0) in relation to the total detached cells

Scenario 1, which was shown to produce the thinnest biofilms with little protection from community members (figures 4.3, 4.4 and 4.7), seemed to be most vulnerable against streptomycin exposure, both in terms of total detachment of cells and release of the test strain.

Another biofilm that reacted similar to scenario1 was scenario 3. Although in this case biofilms were thicker, the position of PAO1:GFP cells (figure 4.11 and 4.12) provided for these cells to be readily exposed to the antibiotic.

It may be pointed out that the biofilm with the smallest decrease in the number of PAO1:GFP cells was that of scenario 2. An explanation for this observation may be the physical barrier offered by the drain community, as seen in figures 4.5, 4.6, 4.9 and 4.10.

It, therefore, seems possible that the association between an introduced species and a biofilm community may not be the sole determinant of the introduced species' response to hostile conditions such as antimicrobial treatment. In fact, the spatial positioning of the introduced cells may play a more important role.

Nevertheless, the large drop in the total number of released cells from scenario 1, which contained almost 50% PAO1:GFP cells before antibiotic treatment, as well as the significant reduction in the relative number of cells from the test strain, show that the biofilm of PAO1:GFP and its cell yield are more susceptible to this concentration of streptomycin compared to the community members.

Overall, it may be concluded that streptomycin exposure to a community biofilm, containing an opportunistic pathogen, was not an effective means of treatment, since the antibiotics only appear to have affected the upper layer of the biofilm, while there often existed a layer of community cells covering the test strain. This holds true even in the case that the test strain was more susceptible to the antibiotic compared to the mixed species. Therefore, a higher concentration of streptomycin should be tested in order to address this problem in an applied sense.

4.4 Effect of EDTA addition

EDTA exposure for 15 hours caused a 3 fold reduction in the number of cells released from two examples of scenario 2 biofilms (S2 A and S2 B), as seen in figure 4.26. The effect of EDTA on the biofilms did not seem to be immediate. During the first hour of exposure, there is no significant change in the number of released cells. This is confirmed by transmitted light microscopy images obtained from the S2 A biofilm during

the first 75 minutes of EDTA treatment (figure 4.27). The biggest drop in the number of cells occurred between 1 and 5 hours after the treatment was initiated, with little reduction during the next 10 hours.

When a pure culture PAO1:GFP biofilm was exposed to EDTA, a decrease in the number of detaching cells was observed during the first 5 hours, which was followed by an increase in detachment observed at 15 hours following initiation of EDTA addition (figure 4. 26). Furthermore, 2 hours after EDTA exposure was discontinued and nutrient flow was resumed, no biofilm was observed using confocal laser scanning microscopy. These observations indicate effective removal of PAO1:GFP biofilm by means of EDTA exposure.

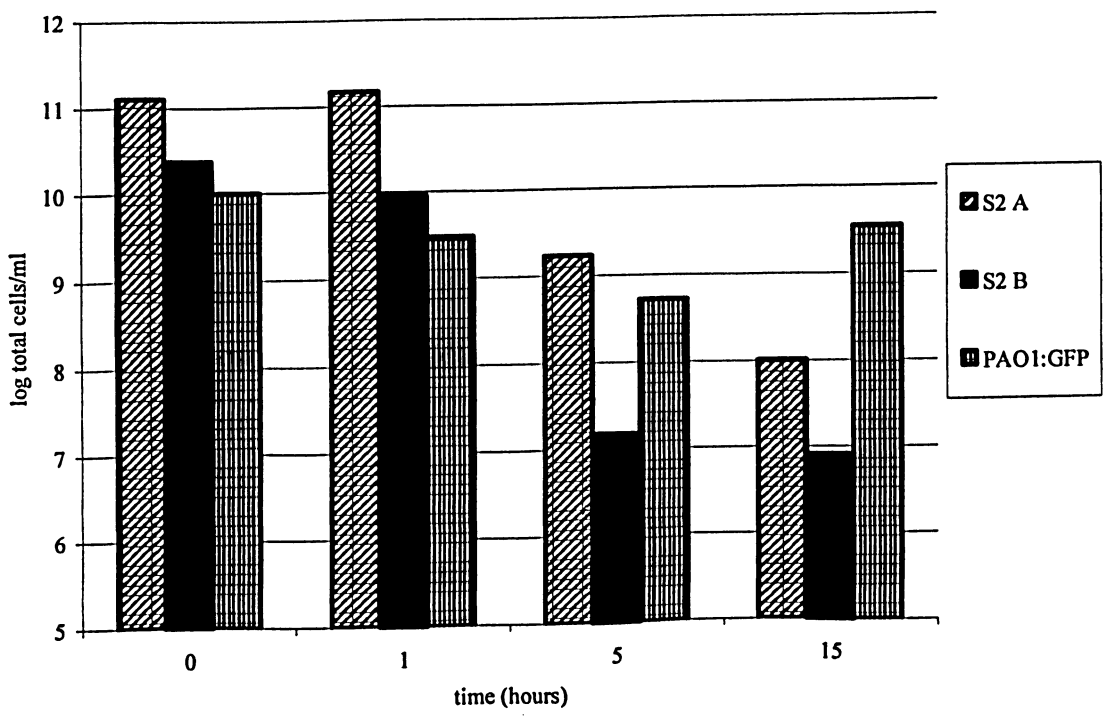

Figure 4.26. Changes in the number of cells released from duplicate scenario 2 biofilms (S2A and S2B) and a pure culture PAO1:GFP biofilm, over a 15 hour EDTA (40 mg/ml) exposure

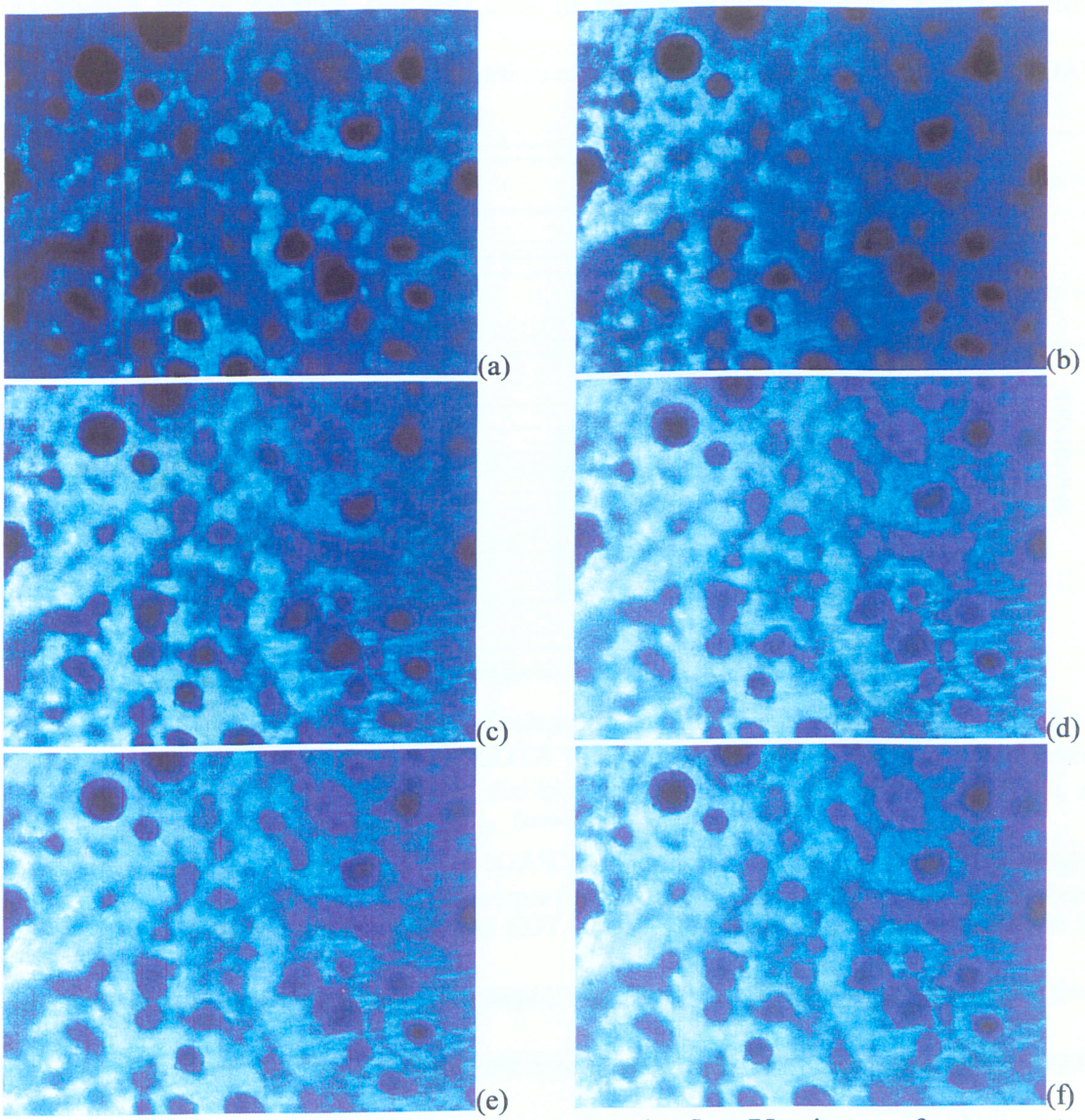

Figure 4.27. A scenario 2 biofilm (S2 A) during the first 75 minutes of exposure to EDTA (40 μg/ml). (a) t = 0 minutes (b) t = 5 minutes (c) t = 10 minutes (d) t = 30 minutes (e) t = 50 minutes (f) t = 75 minutes, showing no significant change in the microcolony structures but a noticeable reduction in biofilm density.

Although, the biofilm, as a whole, and the total number of released cells do not appear to be affected by the EDTA exposure during the first hour of treatment, the PAO1:GFP portion of the biofilm effluent was reduced to close to 0% during this period (figure 4.28). During the next 14 hours of continued treatment, the number of PAO1:GFP

cells increased slightly. It is important to note that this increase in the percentage PAO1:GFP over time does not correspond to a rise in actual numbers of released cells.

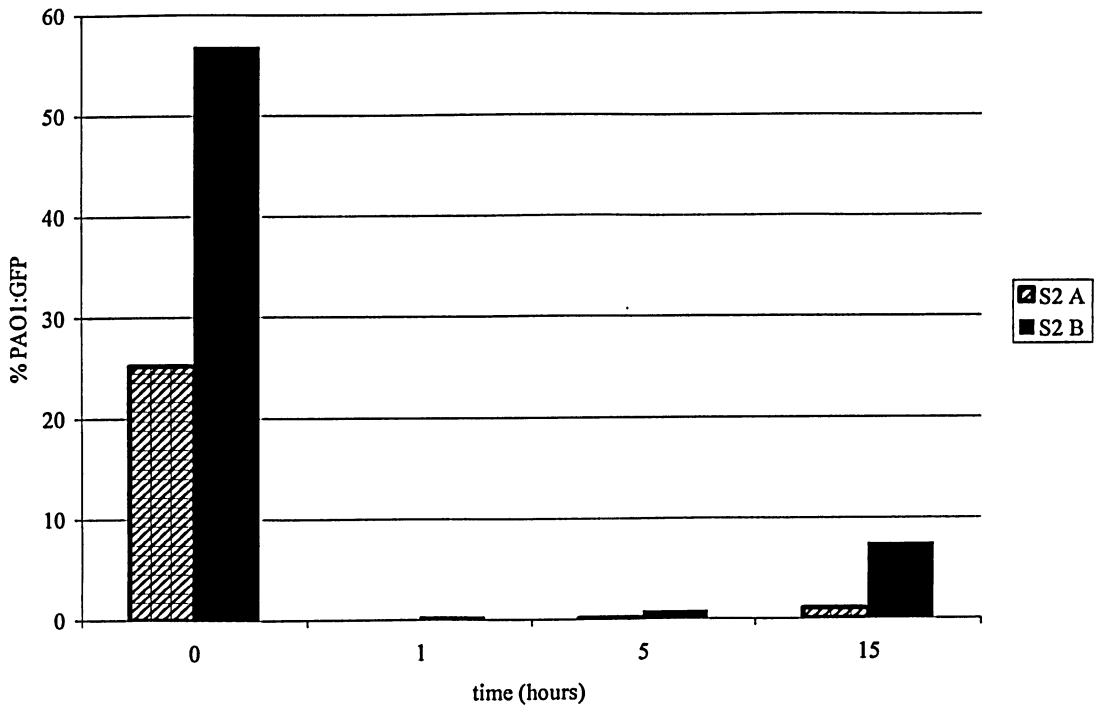

Figure 4.28. Changes in the percentage of PAO1:GFP cells detaching from scenario 2 biofilms during a 15 hour EDTA (40 mg/ml) exposure

As determined by plate counts, the average number of colony forming units of PAO1:GFP per ml of effluent from scenario 2 biofilms, was reduced from 2.27×10^{10} to 1.00×10^{7} during the first hour of EDTA exposure and did not change significantly during the following 14 hours of treatment. Conversely, the number of average detaching cells from community 1 members did not drop significantly during the first hour but did so thereafter, as illustrated in figure 4.29.

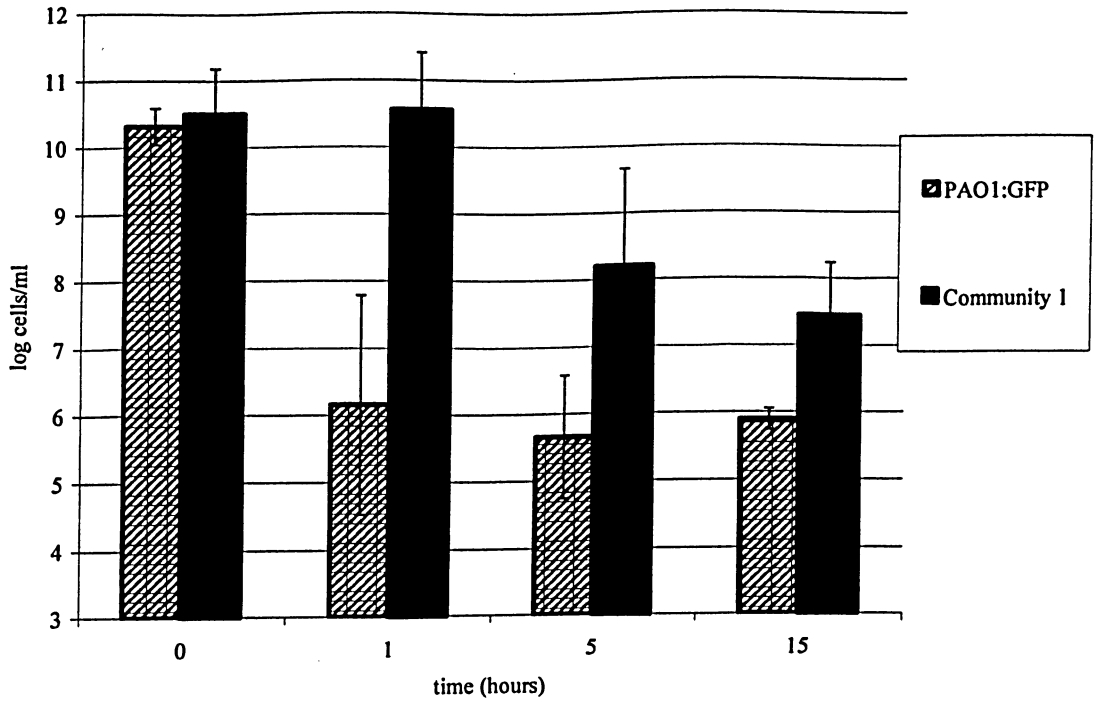

Figure 4.29. Changes in the number of released PAO1:GFP and community 1 cells from scenario 2 biofilms over a 15 hour EDTA (40 mg/ml) exposure, show a more severe impact on the PAO1:GFP portion of the biofilm, during the first hour of exposure, as determined by analysis of released cells.

Overall, these results show that EDTA exposure caused a substantial decrease in the yield of mixed community biofilms and it was more effective against PAO1:GFP than the rest of the community. This suggests that in the case of mixed community, there may be multiple forces, such as electrostatic and divalent cation interactions governing adherence compared to relatively fewer such forces in PAO1:GFP. Since EDTA is a chelating agent that affects adhesive properties of biofilms, it appears to be able to disrupt the biofilm matrix and cause detachment to large numbers of cells and clusters. Reductions in the number of culturable cells detaching from the biofilms showed that EDTA was also capable of effectively disrupting biofilm and its yielding cells.

With respect to the effect of EDTA on PAO1:GFP in a community setting in

comparison to a pure culture biofilm of PAO1:GFP, it may be concluded that the test strain does in fact benefit from existing as part of a mixed community, since the pure culture biofilm was completely eradicated following 15 hours of exposure, while a scenario 2 biofilms were still visible after treatment.

4.5 Biofilm erosion by flow rate increase

Figure 4.30 shows an increase in the speed of medium flowing through the flowcell chambers resulted in a significant increase in detachment from four examples of scenario 2 biofilms (S2 A, S2 B, S2 C, and S2 D). It can also be seen that the number of total released cells return to pre-disruption levels within 3 hours. S2 A and B were inoculated 5 days prior to flow rate increase, while S2 C and S2 C and D were 3 day old biofilms.

As shown in figure 4.30, similar effluent numbers in the 3 day old (S2C and S2D) and 5 day old (S2A and S2B) biofilms indicate steady state biofilms probably developed within 3 days following inoculation.

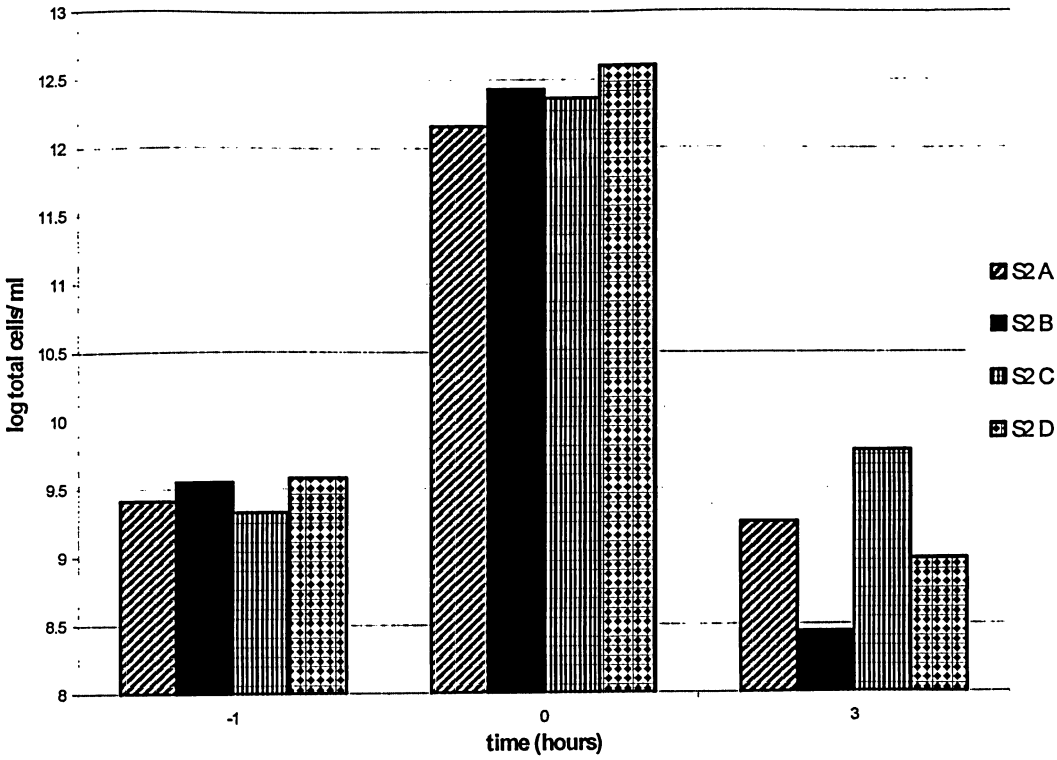

Figure 4.30. Changes in the number of detached cells from scenario 2 biofilms in response to flow rate increase (for 15 seconds at t=0). Effluent samples collected one hour prior to increasing flow rate (t=-1), during increased flow rate (t=0) and 5 hours following flow rate increase, show a significant increase in the number of released cells from the biofilm as a result of shear.

When flow rate was increased in flowcells containing PAO1:GFP biofilms, the same pattern was observed (figure 4.31). However, the PAO1 A biofilm, which was 5 days old, showed a higher increase in the number of detached cells. The PAO1 B biofilm was only 3 days old, so it was expected to be thinner and less complex, which explains why the high rate of flow did not disrupt it as it did in the case of the older biofilm with larger microcolonies (figure 4.32). In older biofilms, as illustrated in figure 4.32.a, mushroom-like structures are more frequently detached as a result of increased flow rate, resulting in larger number of cells in the effluent.

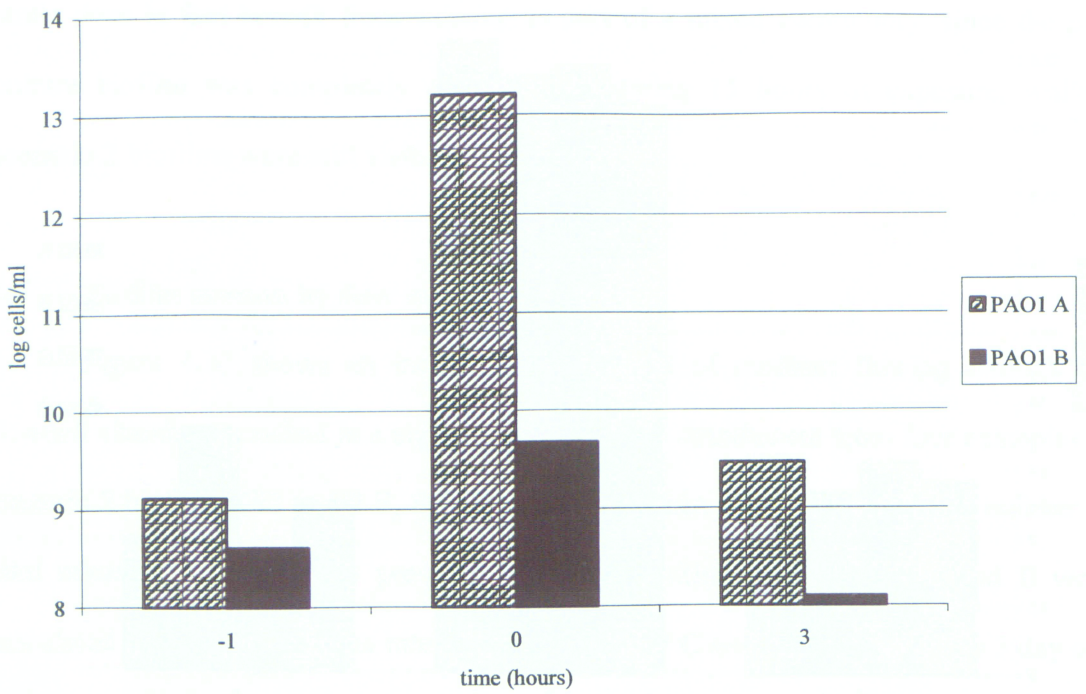

Figure 4. 31. Changes in the number of detached cells from PAO1:GFP biofilms (A: 5 days old and B: 3 days old) in response to flow rate increase (at t=0).

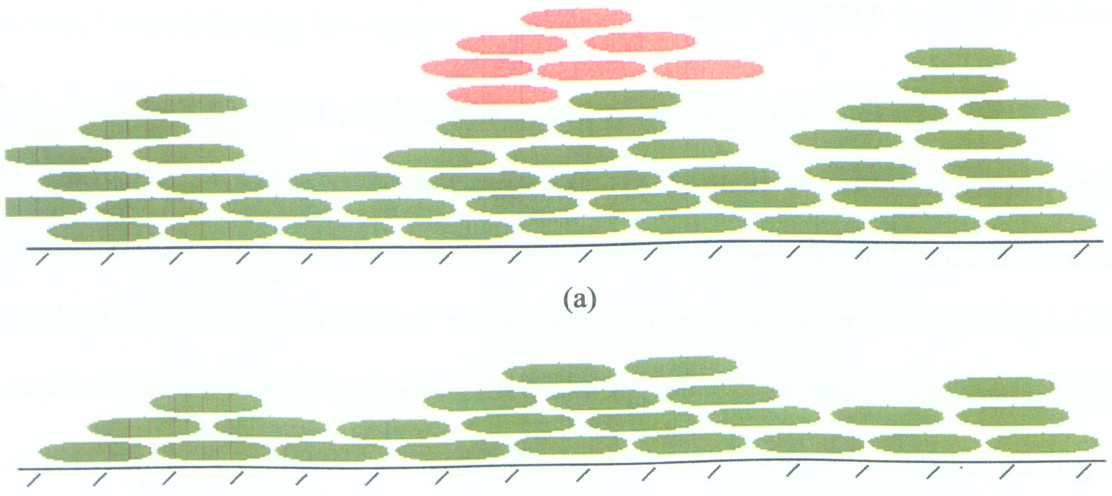

(a)

(b)

Figure 4.32. Schematic diagrams illustrating structural differences between 5 day old (a) and 3 day old (b) PAO1 biofilms. The large microcolonies in the older biofilms are more vulnerable to detachment by physical forces such as high flow conditions (orange section).

Shown in figure 4.33 is the changes in the relative amounts of PAO1:GFP during erosion caused by an increase in flow rate to scenario 2 biofilms. Changes caused by flow rate increase to these biofilms were extremely variable. Because the high liquid flow in the chambers physically removed large portions of the biofilm, that were seen with the naked eye in the effluent, the relative amounts of detached strains depend solely on the positioning of the cells within the biofilm. For instance, shear application to a large microcolony, in which PAO1:GFP is the main constituent at the time of shear application, is expected to cause a large portion of this microcolony to be collected in the effluent sample, resulting in a higher percentage of PAO1:GFP. This is expected to be the situation in the case of S2 B. Conversely, if the large microcolony consisted mainly of community members, the effluent sample would contain much lower PAO1:GFP ratios, as is expected to be the case of S2 A.

Another notable observation is the higher percentage of PAO1:GFP, three hours following flow rate increase, in both examples in comparison to pre-shear levels. An explanation that may be provided for this observation is that the force created by the high flow removes the cells from the biofilm interface, exposing the inner layer, which was seen to contain larger quantities of PAO1:GFP cells (figures 4.5, 4.6, 4.9 and 4.10).

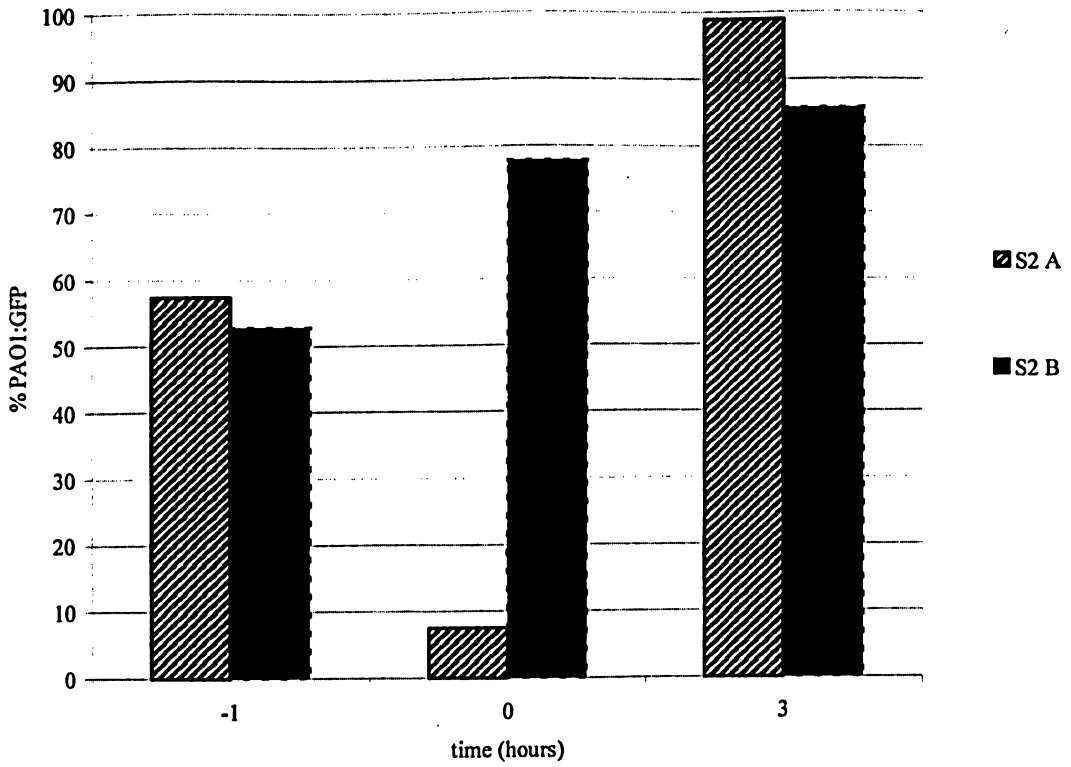

Figure 4.33. Changes in the percentage of PAO1:GFP released cells from two examples of 5 day old scenario 2 biofilms (S2 A and S2 B) eroded by a high flow rate (15 seconds at t=0), showing extreme variations between PAO1:GFP ratio of cell detachment from the two biofilms in response to increased flow rate.

As seen in figure 4.34, although S2 C and S2 D biofilms released cells in very different PAO1:GFP fractions, these values did not seem to be affected by the increase in flow rate. Unlike S2 A and S2 B, the younger biofilms S2 C and S2 D are more homogeneous. This results in cell yield that is more representative of the biofilms.

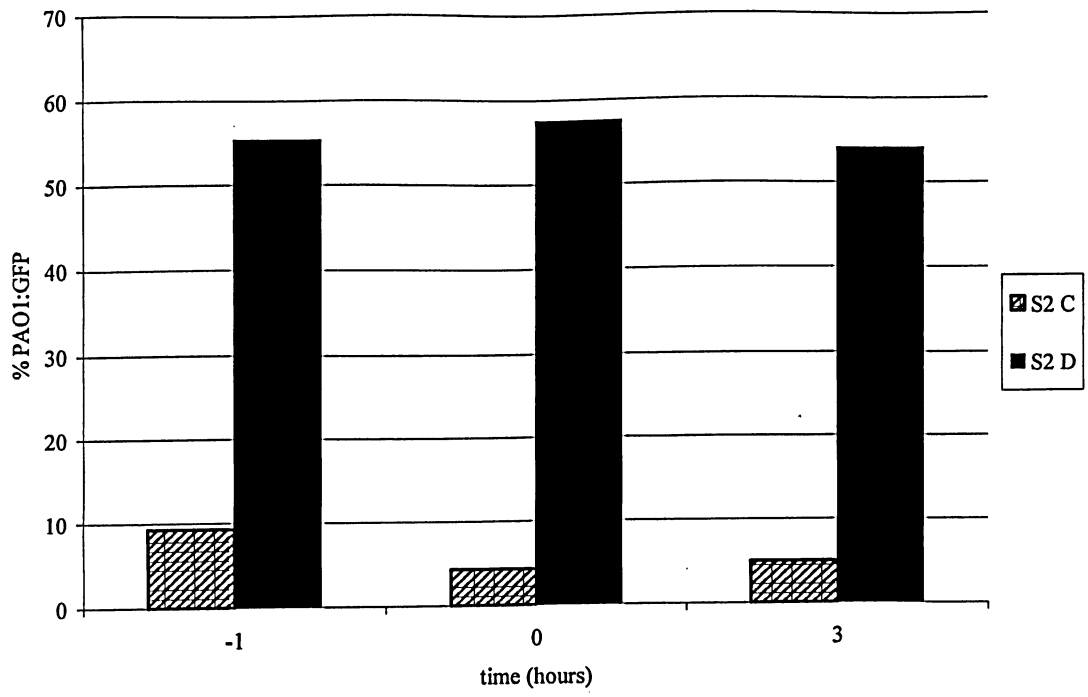

Figure 4.34. Changes in the percentage of PAO1:GFP released cells from two examples of 3 day old scenario 2 biofilms (S2 A and S2 B) eroded by a high flow rate (15 seconds at t=0), showing no significant change in the ratio of PAO1:GFP detachment in response to the flow rate increase.

Confocal laser scanning microscopy on the S2A biofilm showed a green mat of PAO1:GFP cells with a distribution of scattered cells and microcolonies of community members (figure 4.35). Furthermore, throughout the biofilm, there existed several zones with low cell densities, which are speculated to be the position of detached microcolonies.

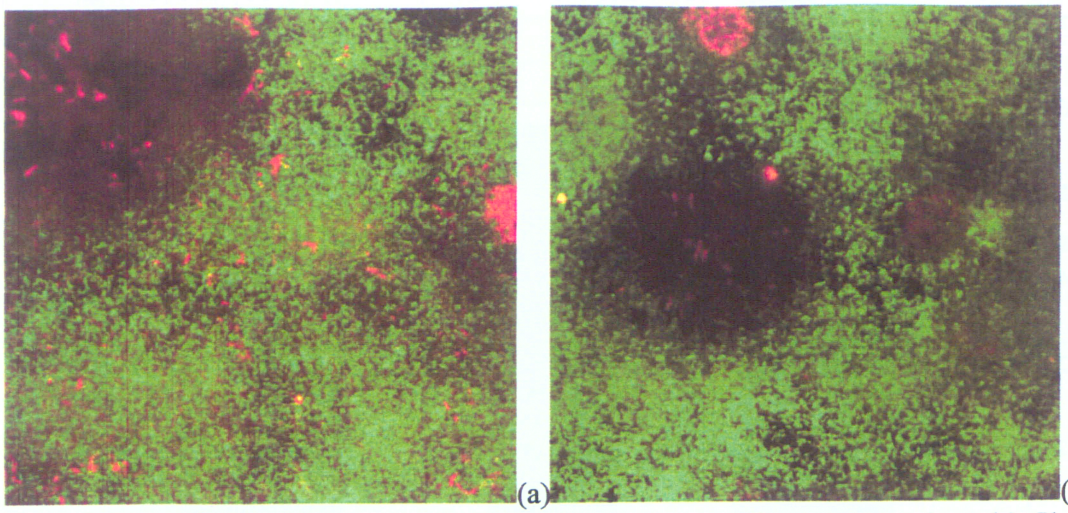

Figure 4.35. Confocal laser scanning microscope images from a scenario 2 biofilm, 3 hours following flow rate increase. Red: community 1 cells stained with Nile Red. Green: PAO1:GFP.

Considering these results, it is clear that shear force caused a dramatic increase in biofilm detachment. As is the case of the other treatments, it appears that high flow rate affected biofilms differently depending on their structural complexities, including the relative positioning of cells in the biofilm matrix. Essentially, a dramatic increase in the flow rate provides for a means of transporting bacterial cells in the form of large aggregates containing PAO1:GFP from the biofilm to other environments.

4.6 EPS matrix of PAO1:GFP and mixed-community biofilms

Light microscopy on colonies grown on agar, showed that the majority of strains in both communities 1 and 2, produce smooth, round colonies (figure 4.36.a), although there were a few rugose and irregular colonies also observed (figure 4.36.b). Strains that produce rugose colonies have been shown to produce biofilms with complex structures that are more resistant to environmental stress (Fong et al, 2007). PAO1:GFP colonies produced irregular colonies with seemingly high volume of EPS on the edges (figure

4.36.c).

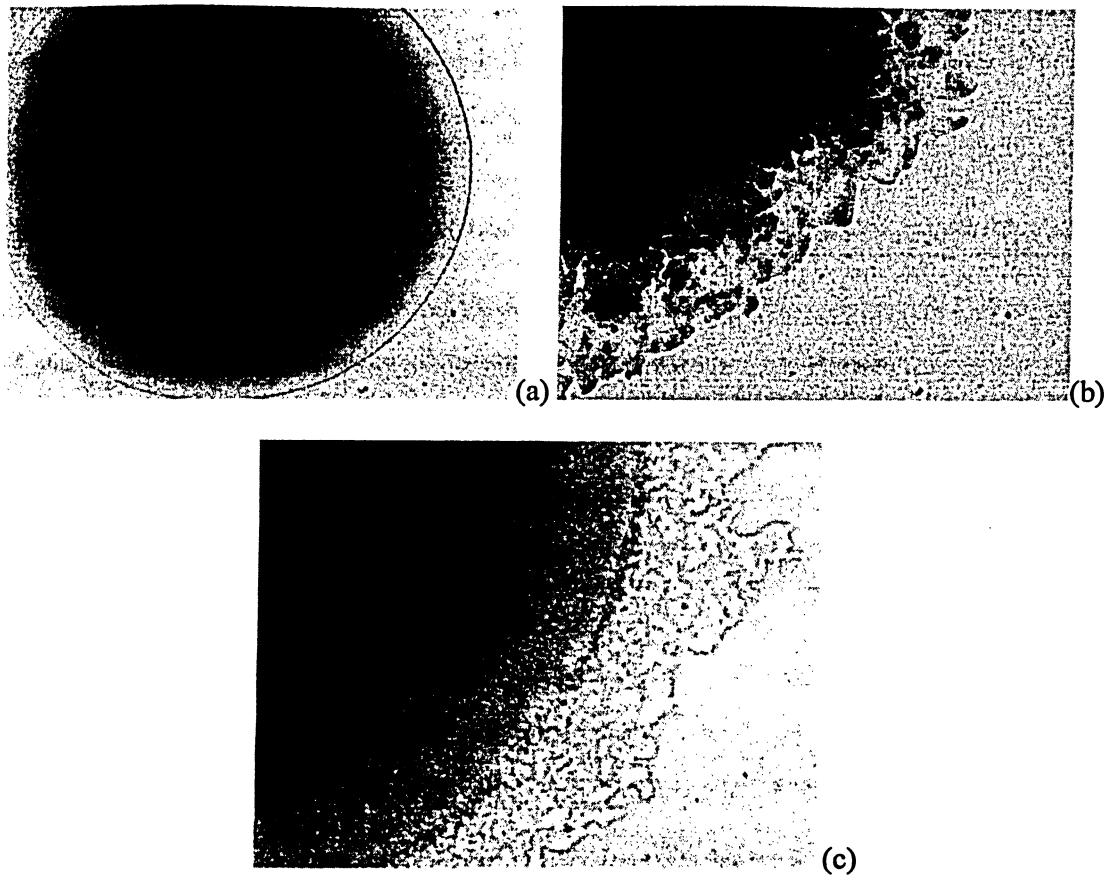

Figure 4.36. Examples of colony morohtypes from the mixed-species microbial communities (a) and (b), and PAO1 (c) viewed by light microscopy, at 10x magnification.

Confocal laser scanning microscopy images in figure 4.37 show a 7 day community 1 biofilm. In these mixed-species biofilms isolated microcolonies were observed, in addition to sections of flat multi-layers of cells. Figure 4.38 shows images of a 7 day PAO1:GFP biofilm, consisting mainly of mushroom-shaped microcolonies formed on top of a multilayered mat.

Both biofilms contain cells that did not appear to be directly connected to the biofilm, seemingly supported by EPS. In community 1 biofilms (figure 4.37.b) they appeared in the form of single cells, while in PAO1:GFP biofilms (figure 4.38.b), these cells were mainly filamentous. Following up on this observation, it was decided to apply a standard crude procedure for EPS extraction to compare the EPS produced by PAO1:GFP to that of the community.

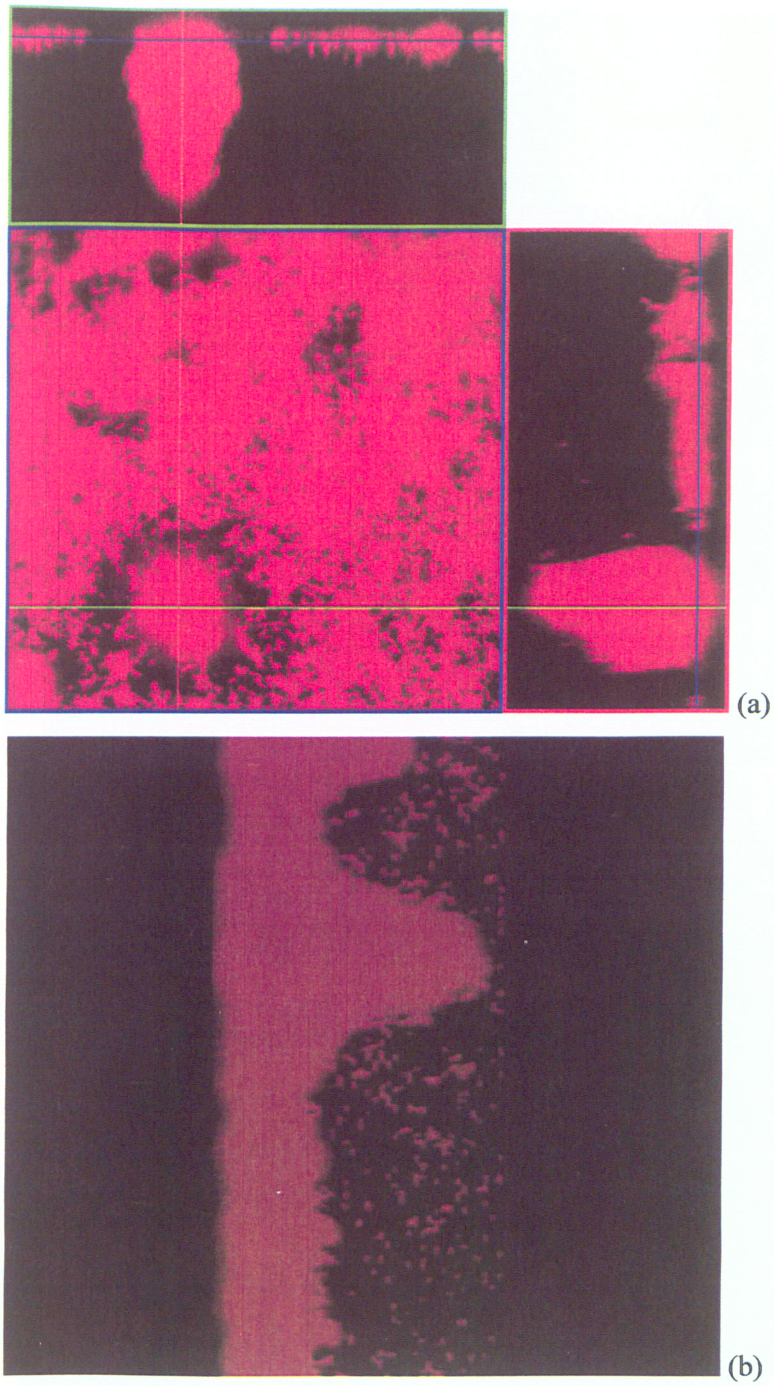

Figure 4.37. (a) Orthogonal sectioning and (b) through-view of confocal laser scanning microscopy images, obtained by 63 x 1.2 objective, from a 7 day community 1 biofilm, stained with FM 4-64, showing a multi-layered biofilm with a single microcolony.

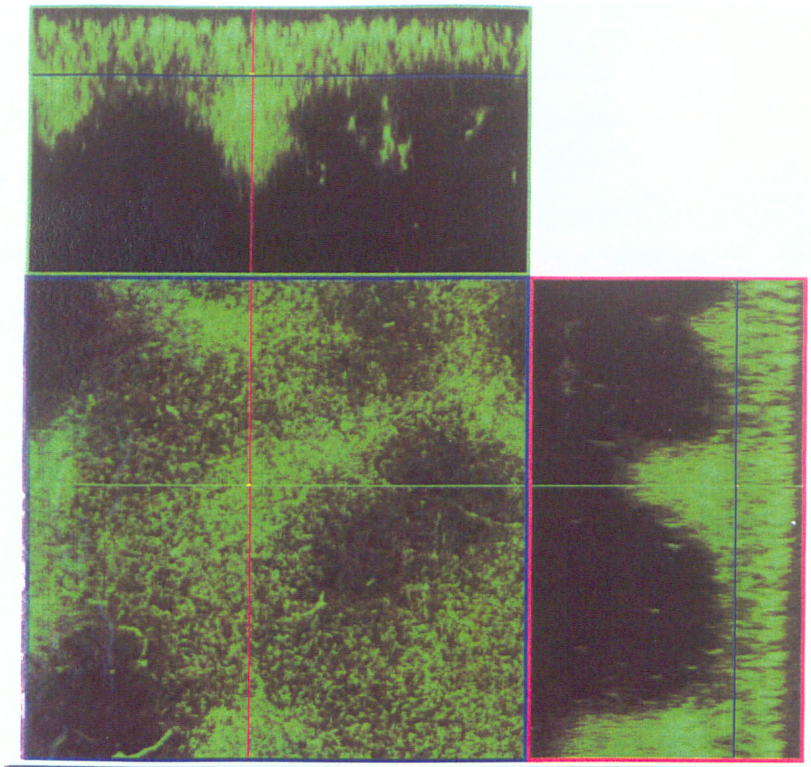

(a)

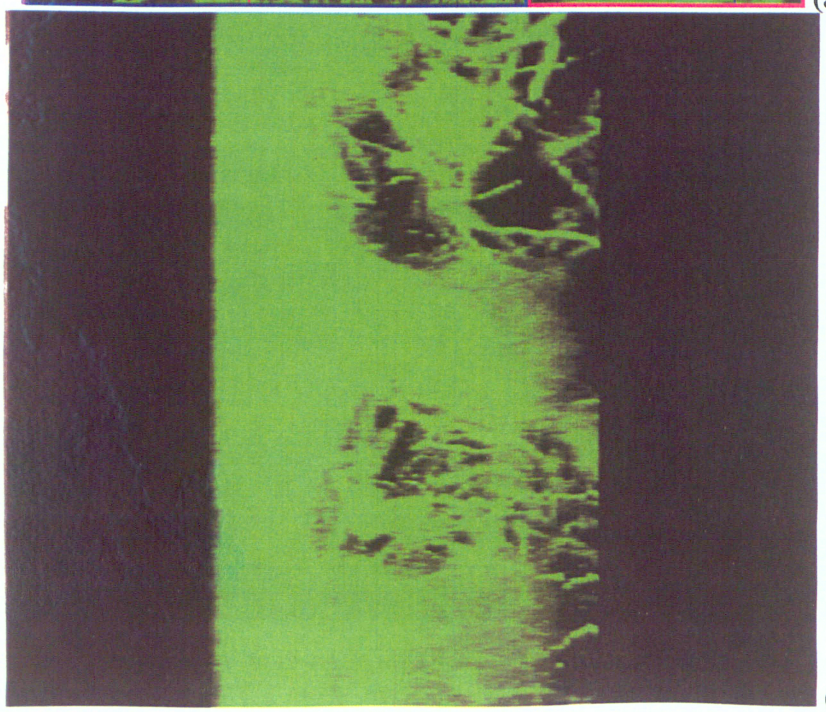

(b)

Figure 4.38. (a) Orthogonal sectioning and (b) through-view of confocal laser scanning microscopy images, obtained by 63 x 1.2 objective, showing several microcolonies and EPS-supported filamentous cells that make up the structure of a 7 day old PAO1:GFP biofilm.

Due to the appearance of higher EPS volumes in colonies of PAO1:GFP compared to that of community members, high-speed centrifugation for EPS extraction was performed on biofilms of pure culture PAO1:GFP and community 1.

Following centrifugation of the biofilm samples, the amount of EPS extracted from the mixed species biofilm was more than the extraction from the PAO1:GFP biofilm (result not shown). However, it was observed that the pellet from the second round of centrifugation did not consist of cells alone (Figure 4.39). In fact, it is speculated that a high fraction of the residue was EPS. From these observations it may be concluded that EPS of the PAO1:GFP biofilm has a higher affinity for the cells compared to the dominant portion of the mixed community.

(a)

(b)

Figure 4.39. Pellets resulting from high-speed centrifugation of (a) community 1 biofilm and (b) PAO1:GFP biofilm, showing that the two steps of centrifugation is inadequate in EPS extraction from the PAO1:GFP biofilm.

From these observations (colonies grown on agar, biofilm architecture and CLSM images of biofilms, it may be concluded that PAO1:GFP produces more extensive, higher affinity EPS, compared to community members.

Overall, although biofilm structures were found to be extremely variable, PAO1:GFP biofilms appeared to produce more complex structures with a higher surface area in comparison to structures seen in the case of mixed community biofilms.

4.7 Development of a protocol based on Flow Cytometry for the measurement of cell release by PAO1:GFP and mixed community biofilms

In order to optimize instrument settings, batch cultures of PAO1:GFP and community 1 were analyzed by flow cytometry. In the dot plots produced by the cytometer, green fluorescent levels were set on the x-axis, while the y-axis shows events based on their degree of red fluorescence. Therefore, the lower left quadrant in the dot plot contains events that do not fluoresce, the upper left quadrant shows red fluorescent events, in the lower right quadrant green fluorescent events are plotted and events in the upper right quadrant are those that exhibit both red and green fluorescence.

Figure 4.40.a is a dot plot of a sample containing cells from the mixed community stained with 2.5 μg/ml FM 4-64. According to this plot, 88.55% of the events in the sample are fluorescing red. The majority of the remaining events (11.33%) were observed in the lower left quadrant. These events represent small debris and cells that were not adequately stained.

In figure 4.40.b a sample of PAO1:GFP was analyzed and was found to have 90.56% green fluorescent events. The lower left quadrant contained 9.34% events, which represent small debris and non-fluorescent PAO1:GFP cells.

Figure 4.40.c shows a dot plot of the PAO1:GFP culture that has been stained with 2.5 μg/ml FM 4-64. It shows that 91.82% of the events fluoresce both red and green.

Furthermore, 5.74% of events were located in the upper left quadrant, which represent PAO1:GFP cells that do not fluoresce green but were stained with FM 4-64. Only 2.11% of the events were seen in the lower left quadrant, which are small debris and PAO1:GFP cells that are neither green fluorescent nor stained red. Since only 0.33% of events were found in the lower right quadrant, it was concluded that the vast majority of cells are stained with FM 4-64, thus it was assumed that the number of cells that were not stained with FM 4-64 were negligible.

From the results provided by these samples it may be concluded that almost 100% of cells are efficiently stained with FM 4-64, while about 92% of PAO1:GFP exhibit fluorescence that is detectable by the flow cytometer.

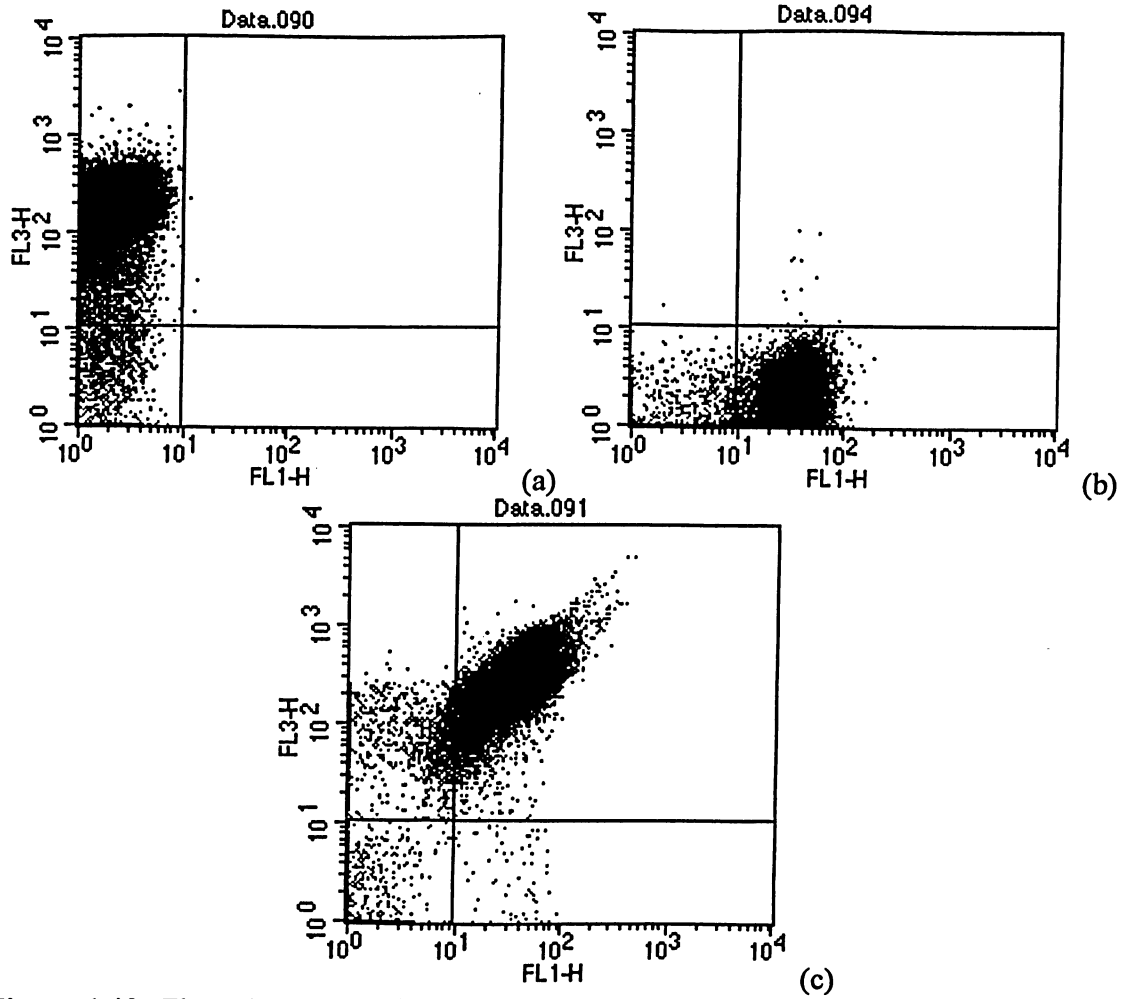

Figure 4.40. Flow Cytometry dot plots obtained from batch cultures of (a) FM 4-64 stained drain strains, (b) unstained PAO1:GFP, and (c) PAO1:GFP cells stained with FM 4-64. FL3-H represents the level of red fluorescence while FL1-H represents green fluoresce.

Since the effluent samples from scenario 2 biofilms were stained with FM 4-64, the majority of events appeared in the upper quadrants. The events in the upper left quadrant corresponded to drain cells and 8% of PAO1:GFP cells, which were stained red and the upper right quadrant contained events represented 92% PAO1:GFP cells, which fluoresced green and were stained red.

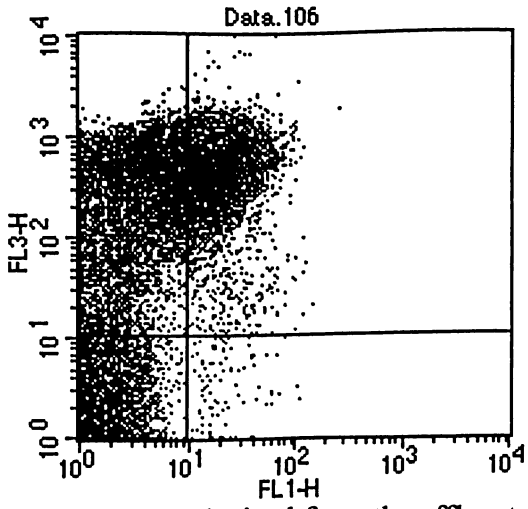

Figure 4.41. Flow cytometry dot plot obtained from the effluent of a 3 day old scenario2 biofilm, showing events representing community cells in the upper left quadrant and events representing PAO1:GFP cells in the upper right quadrant. FL3-H represents the level of red fluorescence while FL1-H represents green fluoresce.

Shown in figure 4.41 is an example of a dot plot obtained from an effluent sample of a 3 day old scenario 2 biofilm. As seen in table 4.1, flow cytometry on these samples showed that 36.5% ± 4.1 of the released cells were PAO1:GFP, while the result obtained by plate counting was 67%.

Table 4.1. Flow Cytometry results obtained for effluent of a 3 day old scenario 2 biofilm.

		Sample 1	Sample 2	Sample 3	Average	Standard deviation
Quadrant	UL	6257	5625	4766	5549	748.4
	UR	3568	3059	1970	2866	816.4
total events		9825	8684	6736	8415	1562.0
PAO1:GFP events		3878	3325	2141	3115	887.3
drain events		5947	5359	4595	5300	677.9
%PAO1:GFP		39.5	38.3	31.8	**36.5**	4.1

When an effluent sample from a 5 day old scenario 2 biofilm was examined using flow cytometry, the relative number of PAO1:GFP seemed to be very close to that of the 3 day old biofilm. As seen in figure 4.42 and table 4.2, 34.2% ± 1.0 of the events were

green fluorescent. At the same time, a plate count of the same effluent sample revealed 96.7% PAO1:GFP CFU.

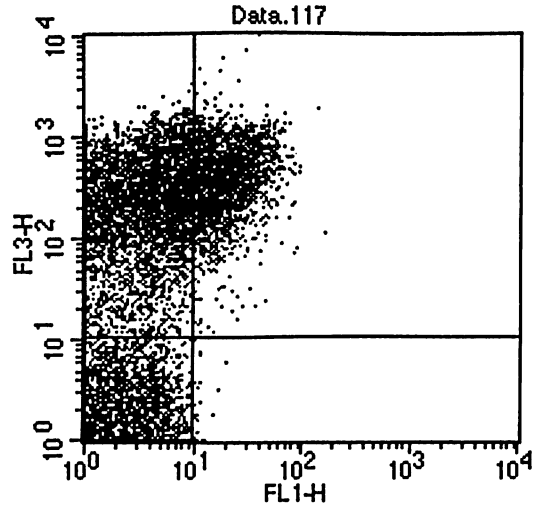

Figure 4.42. Flow Cytometry dot plot obtained from the effluent of a 5 day old scenario2 biofilm, showing events representing community cells in the upper left quadrant and events representing PAO1:GFP cells in the upper right quadrant. FL3-H represents the level of red fluorescence while FL1-H represents green fluoresce.

Table 4.2. Flow Cytometry results obtained for effluent of a 5 day old scenario 2 biofilm

		Sample 1	Sample 2	Sample 3	Average	Standard deviation
Quadrant	UL	4587	5410	4792	4930	428.4
	UR	2057	2421	2305	2261	185.9
total events		6644	7831	7097	7191	599.0
PAO1:GFP events		2236	2632	2505	2458	202.1
drain events		4408	5199	4592	4733	414.2
%PAO1:GFP		33.7	33.6	35.3	34.2	1.0

The scenario biofilm effluent was also tested 6 days after inoculation. As seen in the dot plot in figure 4.43 the relative number of PAO1:GFP events had dropped since previous samplings. Tables 4.3 and 4.4, show results obtained from two separate sampling periods. In this case, the PAO1:GFP events comprised 9.8% ± 0.9 of total events, while plate counts 63.1% PAO1:GFP.

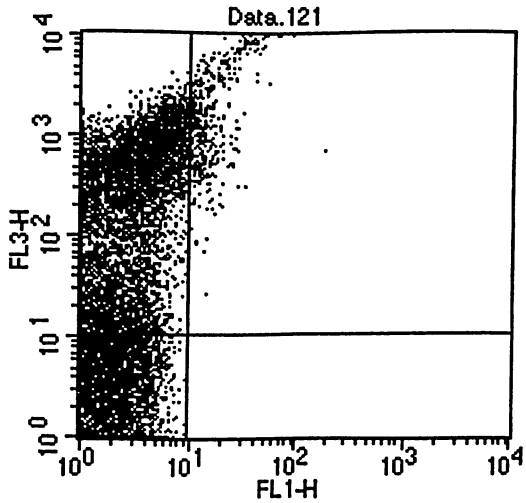

Figure 4.43. Flow Cytometry dot plot obtained from the effluent of a 6 day old scenario2 biofilm, showing events representing community cells in the upper left quadrant and events representing PAO1:GFP cells in the upper right quadrant. FL3-H represents the level of red fluorescence while FL1-H represents green fluoresce.

Table 4.3. Flow Cytometry results obtained for a 6 day old scenario 2 biofilm

		Sample 1	Sample 2	Sample 3	Average	Standard deviation
Quadrant	UL	3263	2658	2576	2832	375.2
	UR	289	276	273	279	8.5
total events		3552	2934	2849	3112	383.7
PAO1:GFP events		314	300	297	304	9.2
drain events		3238	2634	2552	2808	374.5
%PAO1:GFP		8.8	10.2	10.4	**9.8**	0.9

Table 4.4. Flow Cytometry results obtained for a 6 day old scenario 2 biofilm

		Sample 1	Sample 2	Sample 3	Average	Standard deviation
Quadrant	UL	6880	6233	6011	6375	451.5
	UR	432	463	461	452	17.3
total events		7312	6696	6472	6827	435.0
PAO1:GFP events		470	503	501	491	18.9
drain events		6842	6193	5971	6335	452.9
%PAO1:GFP		6.4	7.5	7.7	**7.2**	0.71

Effluent sampling from a 7 day old scenario 2 biofilm showed an extremely low green fluorescent detection by the flow cytometer, as seen in figure 4.44. According to

results shown in table 4.5, only 0.3% ± 0.14 of the total events were PAO1:GFP. It should be noted that a standard deviation for the number of events was not calculated since the sample acquisition was set for different lengths of time.

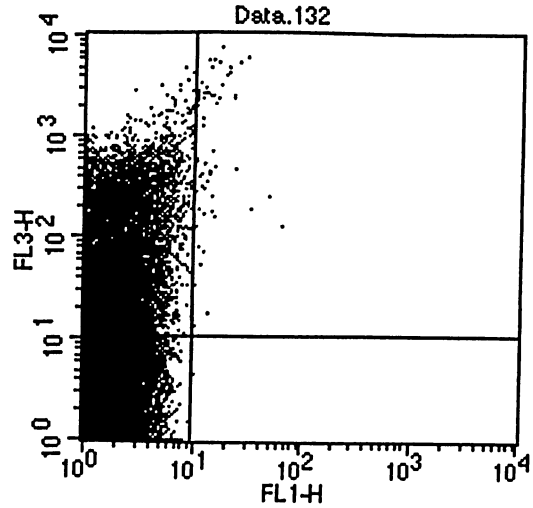

Figure. 4.44. Flow Cytometry dot plot obtained from the effluent of a 7 day old scenario2 biofilm. FL3-H represents the level of red fluorescence while FL1-H represents green fluoresce.

Table 4.5. Flow Cytometry results obtained for a 7 day old scenario 2 biofilm

		Sample 1	Sample 2	Sample 3	Average	Standard deviation
Quadrant	UL	1310	16305	4312	7309	N/A
	UR	2	54	17	24	N/A
total events		1312	16359	4329	7333	N/A
PAO1:GFP events		2	59	18	26	N/A
drain events		1310	16300	4311	7307	N/A
%PAO1:GFP		0.2	0.4	0.4	**0.3**	0.14

Results obtained by flow Cytometry show a decrease in the PAO1:GFP percentage in relation to the total number of cells yielding from the biofilm. However, plate counting on the effluent of these biofilms showed variability, as had been observed previously (section 4.2.2). As seen in figure 4.45, the PAO1:GFP levels obtained by flow cytometry were considerably lower than those found by plate counting. In order to

explain these observations it is important to consider how results are achieved with respect to each method and to assess their accuracy in representation of the strains.

In flow Cytometry, every object with a diameter of 0.2 to 50 μm is counted as an 'event'. Therefore no distinction can be made between viable and non-viable cells, or single cells and small clusters. Although plate counting is also unable to show the form of detachment, whether single cells or in clusters, it only accounts for viable and culturable cells. Since FM 4-64 is a non-specific stain, it stains both live and dead cells from community and PAO1:GFP, which would explain the lower relative number of green fluorescent events obtained by this method.

Epifluorescent microscopy and BacLight staining were used to determine the relative quantities of dead cells in scenario 2 and PAO1:GFP biofilm effluent. It was found that 21% ± 9 of the cells detaching from the scenario 2 biofilms were dead, with no obvious change in these values over time. In the effluent of PAO1:GFP a significantly lower level of dead cells was observed, 5% ± 3.

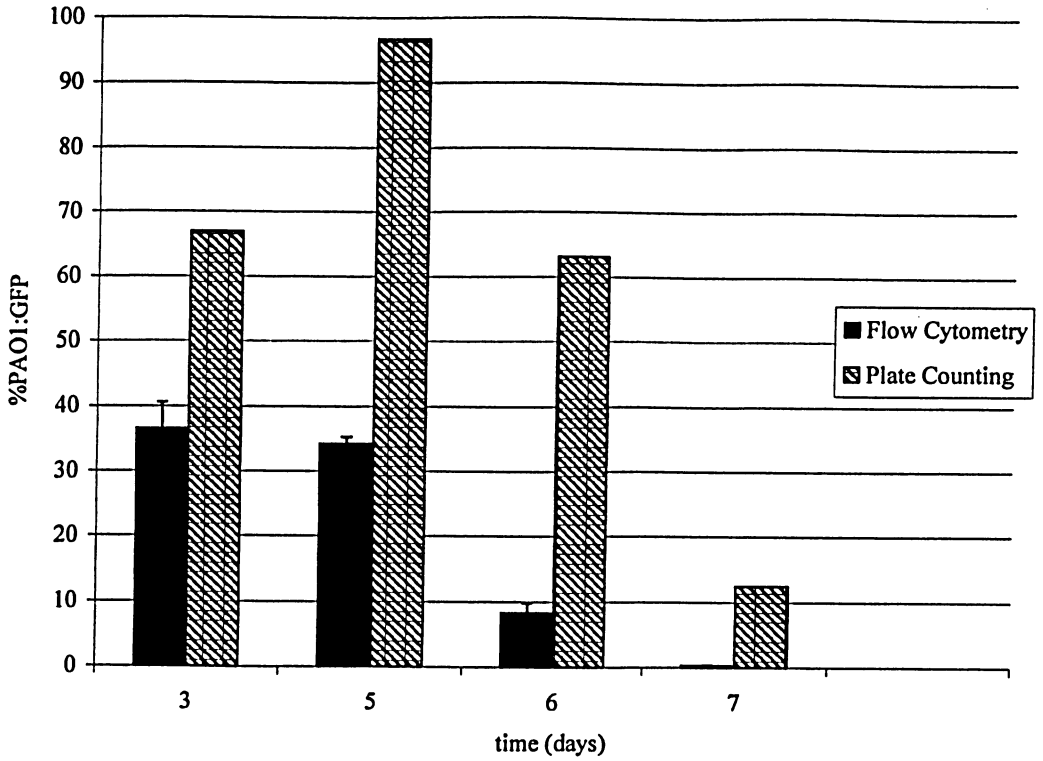

Figure 4.45. Changes in the percentage of PAO1:GFP cells detached by a scenario 2 biofilm over time, obtained by flow Cytometry and plate counting.

In conclusion, flow cytometry provides for a means of determining relative amounts of bacterial cells, depending on their size, internal complexities and fluorescence. In contrast to plate counting, which requires days of growth, flow cytometry is a fast and efficient method. Furthermore, unlike plate counting, it is able to account for both culturable and non-culturable bacteria.

A complication of flow cytometry is that it is unable to distinguish between single cells and aggregates released by the biofilm; however, this is also a disadvantage of plate counting. Furthermore, the flow cytometer is only capable of detecting objects up to 50 μm in diameter, which would result in larger aggregates to be unaccounted for. Another disadvantage of flow cytometry is that it only provides relative amounts of cells, whereas

with plate counting, absolute number of cells released with respect to effluent volume can be determined. Overall, the results obtained with this study show that careful analysis would be needed for flow cytometry to become a reliable, accurate substitute for conventional plate counts, especially when working with small cells such as bacteria.

CHAPTER 5 CONCLUSIONS AND RECOMMENDATIONS

In the course of this study the ability of an opportunistic pathogen to survive and proliferate within a mixed-species biofilm, was examined. The test strain used in this study was *P. aeruginosa* PAO1, and the chosen mixed communities were acquired from sink drains (communities 1 and 2). In order to determine whether the environment created by the community would exclude the test strain or provide protection against disturbance factors, the biofilms were subjected to high flow rate, exposed to an antibiotic and treated using a chelating agent. Furthermore, biofilm detachment was studied in order to determine the nature of released cells, whether single cells or in the form of aggregates.

Effects of varying the order of introduction of the test strain to the mixed-community was studies by inoculating PAO1 3 days before (scenario 1), along with (scenario 2) or 3 days after (scenario 3) inoculation of the mixed species. Microscopy on these biofilms revealed that the rate of biofilm accumulation in the community was higher than the test strain, resulting in layered growth within the biofilm. This type of growth provided a blanket effect, physically protecting the test strain against environmental stress, except for the case of scenario 3.

Studies on biofilm detachment showed that cells were released from the biofilms in all three scenarios as single cells, duplets and clusters in various sizes. In some cases, clusters included PAO1 and community members. This form of dispersal allows for the opportunistic pathogen to enjoy advantages of existing as part of an aggregate while being transported to colonize new surfaces.

Exposure of the biofilms in the three scenarios to streptomycin, at a concentration of 8 μg/ml, was found to be relatively ineffective in eradiation of the test strain from the

biofilms. This conclusion was reached in light of results suggesting limited penetration of the antibiotic into the biofilms, while the test strain was often physically shielded by other community members. This shows that antibiotic concentrations significantly higher than the MIC determined for planktonic cells are needed to control the biofilm mode of growth.

EDTA treatment of scenario 2 biofilms was shown to cause a substantial decrease in the biofilm yield. This chelating substance, unlike the antibiotic, proved to be an effective treatment option by affecting adhesive properties of biofilm, causing disruption of the matrix.

Application of a high flow rate to scenario 2 biofilms resulted in a dramatic increase in the number of detaching cells, providing a means of transportation of the opportunistic pathogen to surrounding environments.

Flow cytometry was found to be a fast and easy method for determining relative quantities of biofilm-derived planktonic cells, based on size, internal complexities and fluorescence. When compared to conventional plate counting, this method was found to be advantageous in its ability to account for both culturable and non-culturable bacterial cells. On the other hand, flow cytometry does not allow for distinguishing between live and dead cells.

Overall, it may be stated that a mixed community biofilm, does indeed serve as a receptive matrix for the test strain to survive and proliferate. The protection offered by the mixed species biofilms was observed for the test strain, against environmental stress within the biofilm as well as upon its release from the biofilm, which was often observed

to occur as part of aggregate of community members.

In order to improve upon and expand this study, the following approaches are recommended:

- Since no trend was observed in changes of the total and relative number of detached cells, the experiments could be run for 30 days to ensure that the obtained results hold true for more mature biofilms.
- Due to the inability of streptomycin at a concentration of 8 μg/ml to effectively penetrate the biofilm and kill cells in the deeper sections of the biofilm, it is recommended that antibiotic concentrations several folds higher than the MIC for cells in the planktonic phase be tested, since biofilms have been reported to be up to 10,000 folds greater than planktonic cells (Mah et al., 2003).
- Although EDTA was found to be effective against the pure culture biofilms of the test strain, it was unable to completely eradicate mixed community biofilms even after continuous exposure for 15 hours. Therefore it may be helpful to couple this chelating agent with a physical tool such as ultrasonication (Oulahal et al., 2004) an antibiotic (Raad et al., 2002) or other chemical agents such as Tween 20 (Chen et al., 2000) for a possible synergic effect on treatment.
- In order to maximize accuracy of effluent analysis for studies involving detaching cell counts, it is recommended that the effluent samples be subjected to sonication in order to break up aggregates (Banas et al., 2007), as vortexing did not seem to be completely effective.

CHAPTER 6 REFERENCES

Abraham, W., Lünsdorf, H., C Strömpl, B Nogales, E. R. B. Moore, K. N. Timmis (2003) Microbial Communities in Composite Biofilms Participating in the Degradation of PCB. *Water, Air, & Soil Pollution.* 3(3):57-64.

Allison, D. G., Ruiz, B., SanJose, C., Jaspe, A., and Gilbert, P. (1998) Extracellular products as mediators of the formation and detachment of *Pseudomonas fluorescens* biofilms. *FEMS Microbiology Letters.* 167(2): 179-184.

Alonso, J. L., Mascellaro, S., Moreno, Y., Ferrús, M. A., and Hernández, J., (2002) Double-Staining Method for Differentiation of Morphological Changes and Membrane Integrity of *Campylobacter coli* Cells. *Appl. Environ. Microbiol.* 68(10): 5151-515.

Antonios, V., Berbari, E., and Osmon, D. (2005) Treatment protocol of infections of orthopedic devices. *In:* J. L. Pace, M. E. Rupp, and R. G. Finch (eds), Biofilms, infection, and antimicrobial therapy. CRC Press: Boca Raton.

Banas, J. A., Miller, J. D., Fuschino, M. E., Hazlett, K. R. O., Toyofuku, W., Porter, K. A., Reutzel, S. B., Florczyk, M. A., McDonough, K. A., and Michalek, S. M. (2007) Evidence that Accumulation of Mutants in a Biofilm Reflects Natural Selection Rather than Stress-Induced Adaptive Mutation. *Appl. Environ. Microbiol.* 73(1):357-361.

Baty, A. M., B. Frolund, G.G. Geesey, S. Langille, E.J. Quintero, P.A. Suci, and R.M. Weiner, (1996) Adhesion of Biofilms to Inert Surfaces: A Molecular Level Approach Directed at the Marine Environment, Biofouling, 10(1-3): 111-121

Beech, I. B., Tapper, R. C., and Gubner, R. J., Microscopy methods for studying biofilms. *In:* L. V. Evans (ed.), Biofilms: Recent advances in their study and control. Harwood Publishers.

Beeken, K. E., Blevins, J. S., and Smeltzer, M. S. (2003) Mutation of *sarA* in *Staphylococcus aureus* limits biofilm formation. *Infection and Immunity.* 71(7): 4206-4211.

Bester, E., Wolfaardt, G., joubert, L., Garny, K., and Saftic, S. (2005) Planktonic-cell yield of a pseudomonad biofilm. *Appl. Env. Microbiol.* 71(12): 7792-7798.

Bryers, D. (1992) Mixed population biofilms. *In:* L. F. Melo, T. R. Bott, M. Fletcher and B. Capdeville, Biofilms – science and technology. Singer: Durhan, North Carolina. pp.277-278.

Braxton, E. E. Jr, Ehrlich, G. D., Hall-Stoodley, L., Stoodley, P., Veeh, R., Fux, C., Hu, F. Z., Quigley, M. and J.C. Post. 2005. Role of biofilms in neurosurgical device-

related infections. *Neurosurg Rev.* 28 (4): 249-255.

Burmølle, M., Webb, J. S., Rao, D., Hansen, L. H., Sørensen, S. L., and Kjelleberg, S. (2006) Enhanced Biofilm Formation and Increased Resistance to Antimicrobial Agents and Bacterial Invasion Are Caused by Synergistic Interactions in Multispecies Biofilms. *Appl Environ Microbiol.* 72(6): 3916–3923.

Cabral, D. A., Loh, B. A. and Speert, D. P., (1987) Mucoid Pseudomonas aeruginosa Resists Nonopsic Phagocytosis by Human Meurophils and Macrophages, *Pediatric Research*, 22: 429-431.

Capdeville, B. and Rols, J. L. (1992) Introduction to biofilms in water and wastewater treatment. *In:* L. F. Melo, T. R. Bott, M. Fletcher, and B. Capdeville (eds) Biofilms - science and technology. NATO Advanced Studies Institute Series Vol. 223: Netherlands. p. 13.

Ceri, H., Olson, M. E., Morck, D. W., and Storey, D. G. (2005) Minimal biofilm eradication concentration (MBEC) assay: Susceptibility testing for biofilms. *In:* J. L. Pace, M. E. Rupp, and R. G. Finch (eds) Biofilms, infection, and antimicrobial therapy. CRC Press, Florida. pp. 257-270.

Chandra, J., and Ghannoum, M. A. (2004) Fungal biofilms. *In:* M. A. Ghannoum and G. A. O'Toole (eds) Microbial biofilms. ASM Press: Washington, DC. p. 30.

Chen, X., and Stewart, P. S. (2000) Biofilm removal caused by chemical treatment. *Water Resources.* 34(17): 4229-4233.

Cho, W., Lee, E. H., Shim, E. H., Kim, J., Hee, W. R., and Cho, K. S., (2005) Bacterial communities of biofilms sampled from seepage groundwater contaminated with petroleum oil. *J. Microbiol. Baiotechnol.* 15(5):952-964.

Collins, L. A., Torrero, M. N., and Franzblau, S. G. (1998) Green fluorescent protein reporter microplate assay for high-throughput screening of compounds against *Micobacterium tuberculosis. Antimicrob. Agents Chemother.* 42(2): 344-347.

Costerton, J. W., and Anwar, H. (1996) *Pseudomonas aeruginosa*: the microbe and pathogen. *In:* Baltch, A. L., and Smith, R. P. (eds), *Pseudomonas aeruginosa:* infections and treatment. Marcel Dekker, Inc. pp. 1-17

Cramton, S. E., Gerke, C., Schnell, N. F., Wright, W. N., and Götz, F. (1999) The Intercellular Adhesion (*ica*) Locus Is Present in *Staphylococcus aureus* and Is Required for Biofilm Formation. *Infection and Immunity.* 67(10): 5427-5433.

Danese, P. N., Pratt, L. A., Kolter, R. (2000) Exopolysaccharide production is required for development of *Escherichia coli* K-12 biofilm architecture. *J. Bacteriol.* 182(12): 3593-3596.

Davey, H. M., and Kell, D. B. (1997) Fluorescent brighteners: Novel stains for the flow cytometric analysis of microorganisms. *Cytometry.* 28(4): 311-315.

Davies, D. G. (1999) Regulation of matrix polymer in biofilm formation and dispersion. *In:* J. Wingender, T. R. Neu, and H. C. Flemming (eds) Microbial extracellular polymeric substances: characterization, structure and function. Springer-Verlag: Berlin Heidelberg, Germany, pp. 104-110.

Decho, A. W. (2000) Microbial biofilms in intertidal systems: an overview. *Continental Shelf Research.* 20: 1257-127

Donlan, R. M. (2002) Biofilms: microbial life on surfaces. Emerging Infectious Diseases. Vol. 8. No. 9. http://www.cdc.gov/ncidod/eid/vol8no9/02-0063_app.htm

Drenkard, E., and Ausubel, F. M., (2002), Pseudomonas Biofilm Rormation and Antibiotic Resistance are Linked to Phenotypic Variation, *Nature.* 18;416(6882):740-3.

Du, H., Fuh, R. A. Li, J., Corkan, A., Lindsey, J. S. (1998) PhotochemCAD: A computer-aided design and research tool in photochemistry, *Photochemistry and Photobiology.* 68: 141-142.

Fath, A, Bethke, P. C., and Jones, R. L. (2001) Enzymes that scavenge reactive oxygen species are down-regulated prior to gibberellic acid-induced programmed cell death in barley aleurone, *Plant Physiol.* 126(1): 156–166.

Freitas dos Santos, L. M., Pavasant, P., Strachan, L. F., Pistokopolos, L. N., and Livingston, A. G., (1997) Membrane Attached Biofilms for Waste-Treatment Fundamentals and Applications, *Pure & Appl. Chem.*, 69(11): 2459-2469

Flemming, H. C., Wingender, J., Griebe, T., and Mayer, C. (2000a) Physio-chemical properties of biofilms. *In:* L. V. Evans (ed) Biofilms: recent advances in their study and control. Harwood Academic Publishers. Singapore. pp. 19-34.

Flemming, H. C., Wingender, J., Mayer, V., Korstgens, V., and Borchard, W. (2000b) Cohesiveness in biofilm matrix polymers. *In:* D. G. Allison, P. Gilbert. H. M. Lappin-Scott and M. Wilson (eds) Community structure and co-operation in biofilms. Cambridge University Press: Cambridge. pp. 87-106.

Flemming, H. C., and Wingender, J. (2003) The crucial role of extracellular polymeric substances in biofilm. *In:*S. Wuertz, P. L. Bishop, and P. A. Wildere (eds) Biofilms in wastewater treatment: An interdisciplinary approach. pp. 178-202

Fong, C. N. J. and Yildiz, F. H. (2007) The *rbmBCDEF* Gene Cluster Modulates Development of Rugose Colony Morphology and Biofilm Formation in *Vibrio*

cholerae. J. Bacteriol. 189(6): 2319-2330.

Fowler, S. D., and Greenspan, P. (1985) Application of Nile-Red, a fluorescent hydrophobic probe, for the detection of neutral lipid deposits in tissue sections: comparison with oil red O. *Journal of Histochemistry and Cytochemistry.* 33 (8): 833-836

Fux, C. A., Shirtliff, M., Stoodeley, P., and Costerton, J. W. (2005) Can laboratory reference strains mirror 'real-world ' pathogenesis? *Trends Microbiol.* 13(2):58-63.

Gandhi, P. A., Sawant, A. D., Wilson, L. A., and Ahearn, D. G. (1993) Adaptation and growth of Serratia marcescens in contact lens disinfectant solutions containing chlorhexidine gluconate. *Appl. Env.l Microbiol.* 59(1): 183-188.

Gavín, R., Rabaan, A. A., Merino, S., Tomás, J. M., Gryllos, I., and Shaw, J. G. (2002) Lateral flagella of *Aeromonas* species are essential for epithelial cell adherence and biofilm formation. *Mol. Microbiol.* 43(2): 383-397.

Geldreich, E. E. (1996) Microbial quality of water supply in distribution systems. Lewis Publishers: Boca Rata, Florida. p. 110.

Gilbert, P., Maira-Litran, Tomas, McBain, A. J., Rickard, A. H., and Whyte, F. W. (2002) The physiology and collective recalcitrance of microbial biofilm communites. *Adv. Microb. Physiol.* 46: 203-256.

Greenspan, P., Mayer, E. P., and Fowler, S. D. (1985) Nile red: a selective fluorescent stain for intracellular lipid droplets. *J. Cell Biol.* 100 (3): 965-73

Hall-Stoodley, L., Costerton, J. W., and Stoodley, P. (2004) Bacterial biofilms: from the natural environment to infectious diseases. *Nature Reviews, Microbiology.* 2: 95-107

Hall-Stoodley, L. and P. Stoodley. (2005) Biofilm formation and dispersal and the transmission of human pathogens. *Trends Microbiol.* 13(1): 7-10.

Heilmann, C., Gerke, C., Perdreau-Remington, F., and Götz, F. (1996) Characterization of Tn917 insertion mutants of Staphylococcus epidermidis affected in biofilm formation. *Infection and Immunity.* 64(1): 277-282.

Holah, J., and Gibson, H. (2000) Food industry biofilms. *In:* L. V. Evans (ed) Biofilms: Recent advances in their study and control. Harwood Academic Publishers. Singapore. pp. 211-236.

Hu, J. Y., Yu. B., Feng, Y. Y., Tan, X, L., Ong, S. L., Ng, W. J., and Hoe, W. C. (2005) Investigation into biofilms in a local drinking water distribution system. *Biofilms*, 2: 19-25.

Kosaric, N., and Blaszczyk, R. (1990) The morphology and electron microscopy of microbial aggregates. *In:* R. D. Tyagi, and K. Vembu (eds) Wastewater treatment by immobilized cells. CRC Press: Boca Raton, FL. p. 80

Lancini, G. L., Parenti, F., and Gallo, G. G. (1995) Antibiotics: A multidisciplinary approach. Plenum Publishing Corporation: Mascaretti, Netherlands. p. 68.

Lam, J., Chan, R., Lam, K., and Costerton, J. W. (1980) Production of mucoid microcolonies by *Pseudomonas aeruginosa* within infected lungs in cystic fibrosis. *Infection and Immunity.* 28(2): 546-556.

Lawrence, J. R., Korber, D. R., Hoyle, B. D., Costerton, J. W., and Caldwell, D. E. (1991) Optical sectioning of microbial biofilms. *J Bacteriol.* 173(20): 6558-6567.

Lee, B., Haagensen, J. A. J., Ciofu, O., Andersen, J. B., Høiby, N., and Molin, S. (2005) Heterogeneity of Biofilms Formed by Nonmucoid *Pseudomonas aeruginosa* Isolates from Patients with Cystic Fibrosis. *J. Clin. Microbiol.* 43(10):5247-5255.

Leriche, V., Briandet, R., and Carpentier, B. (2003) Ecology of mixed biofilms subjected daily to a chlorinated alkaline solution: spatial distribution of bacterial species suggests a protective effect of one species to another. *Environ. Microbiol.* 5(1): 64-71.

Lewandowski, Z., Avci, R., Geiser, M., Shi, X., Braughton, K., and Yurt, N. (2002) Biofouling and Corrosion of Stainless Steels in Natural Waters, *Wat. Sci. Tech.* 2(4):65–72.

Lewandowski, Z., Beyenal, H., and Stookey, D. (2004) Reproducibility of biofilm processes and the meaning of steady state in biofilm reactors. *Wat. Sci. Tech.* 49(11): 359-364.

Li, J., Helmerhost, E. J., Leone, C. W., Troxer, R. F., Yaskell, T., Haffajee, A. D., Socransky, S. S., Oppenheim, F. G. (2004) Identification of early microbial colonizers in human dental biofilm. *J. Appl. Microbiol.* 97(6): 1311-1318.

Lin, J. J. (1995) Electroporation of *Agrobacterium. In:* J. A. Nickoloff (ed) Electroporation protocols for microorganisms. Humana Press: New Jersey. pp. 171-178.

Lynch, M. J., Swift, S., Kirke, D. F., Keevil, C. F., Dodd, C. E., and Williams, P. (2002) The regulation of biofilm development by quorum sensing in *Aeromonas hydrophila. Environ. Microbiol.* 4(1): 18-28.

Mack, D., Fischer, W., Krokotsch, A., Leopold, K., Hartmann, R., Egge, H., and Laufs, R. (1996) The intercellular adhesion involved in biofilm accumulation of

Staphylococcus epidermidis is a linear beta-1,6-linked glucosaminoglycan: purification and structural analysis. *J. Bacteriol.* 178(1): 175-183.

Madigan, M. T., Martinko, J. M., and Parker, J., (1997) Brock Biology of Microorganism. Eighth edition. Prentice Hall, Inc.: New Jersey.

Mah, T. F., Pitts, B., Pellock, B., Walker, G. C., Stewart, P. S., and O'Toole, G. A. (2003) A genetic basis for *Pseudomonas aeruginosa* biofilm antibiotic resistance. *Nature.* 426(6964):306-310.

Manahan, S. E. (2005) Environmental chemistry. Eight edition. CRC Press: Boca Raton, FL. pp. 67-69.

Marsh, P. D. (2005) Dental plaque: biological significance of a biofilm and community life-style. *J Clin Periodontol.* 32(supplement 6):7–15.

Marsh, P. D. and Bowden, G. H. W. (2000) Microbial community interactions in biofilms. *In:* D. G. Allison, P. Gilbert. H. M. Lappin-Scott and M. Wilson (eds) Community structure and co-operation in biofilms. Cambridge University Press: Cambridge. pp. 167-198.

Matsuno, A., Itoh, J., Nagashima, T., Osamura, R. Y., and Watanabe, K. (2001) Confocal Laser Scanning Microscopy. *In:* R. V. Lloyd (ed). Morphology methods: Cell and molecular biology techniques. Humana Press: Newark. pp. 165-167.

McBain, A. J., Bartolo, R. G., Catrenich, C. E., Charbonneau, D., Ledder, R. G., Rickard, A. H., Symmons, A. A., and Gilbert, P. (2003) Microbial characterization of biofilms in domestic drains and the establishment of stable biofilm microcosms. *Appl. Env. Microbiol.* 69(1):177-185.

Micklos, D. and Feyer, G. A., (200) DNA Science: A first course in DNA technology, CSHL Publishing: New York. p. 174.

Mitchell, R. (1992) Environmental Microbiology. Wiley-Liss, Inc.: New York, NY.

Moller, S., Pedersen., A. R., Poulsen, L. K., Arvin, E., and Molin, S. (1996) Activity and three-dimensional distribution of toluene-degrading *Pseudomonas putida* in a multispecies biofilm assessed by quantitative in situ hybridization and scanning confocal laser microscopy. *Appl. Env. Microbiol.* 62(12): 4632-4640.

Moore, G. F., Dunsmore, B. C., Jones, S. M., Smejkal, C. W., Jass, J., Stoodley, P., and Lappin-Scott, H. M. (2000) Microbial detachment from biofilms. *In:* D. G. Allison, P. Gilbert. H. M. Lappin-Scott and M. Wilson (eds) Community structure and co-operation in biofilms. Cambridge University Press, p. 110.

Morin, A. (1998) Screening of polysaccharide-producing microorganism, factors

influencing the production, and recovery of microbial polysaccharides. *In:* S. Dumitriu (Ed) Polysaccharides: Structural diversity and functional versatility. Marcel Dekker Inc.: New York. pp. 275 -296.

Mulcahy, R. (1996) Diseases: Finding the cure, The Oliver Press: Minneapolis. pp. 85-100.

Nickel, J. C., Ruseka, I., Wright, J. B., and Costerton, J. W. (1985) Tobramycin resistance of Pseudomonas aeruginosa cells growing as a biofilm on urinary catheter material. *Antimicrobial Agents and Chemotherapy.* 27(4): 619-624.

Nielsen, P. H., and Jahn, A. (1999) Extraction of EPS. *In:* J. Wingender, H. C. Flemming, and T. R. Neu. (eds) Microbial Extracellular Polymeric substances: Characterization, structure, and function. Springer: Berlin. pp. 49-69.

Oulahal, N., Martial-Gros, A., Bonneau, M, and Blum, L. J. (2004) Combined effect of chelating agents and ultrasound on biofilm removal from stainless steel surfaces. Application to *Escherichia coli* milk and *Staphylococcus aureus* milk biofilms. *Biofilms.* 1:65-73.

O'Toole, G. A., and Kolter, R. (1998) Initiation of biofilm formation in *Pseudomonas fluorescens* WCS365 proceeds via multiple, convergent signaling pathways: a genetic analysis. *Mol. Microbiol.* 28(3): 449-461.

Pai, T. Y., Chauang, S. H., Tsai, Y. P., and Ouyang, C. F. (2004) Modeling a combined anaerobic/anoxic oxide and rotating biological contactors process under dissolved oxygen variation by using an activated sludge-biofilm hybrid model. Journal of Environmental Engineering. 130(12): 1433-1441.

Palleroni, N. J., and Moore, E. R. B. (2006) Taxonomy of *Pseudomonads*: environmental approaches. *In:* Ramos, J. L. (ed) Pseudomonas: genomics, lifestyle and molecular architecture, Springer: New York. pp. 3-6.

Parsek, M. R., and Singh, P. K. (2003) Bacterial Biofilms: An Emerging Link to Disease Pathogenesis, *Annu. Rev. Microbiol.* 57:677-701.

Phinny, D. J., and Halstead, J. H. (2004) Delmar's Dental Assisting: A Comprehensive Approach, 2nd Edition, Thomson Learning, Inc.: Clifton Park, New York.

Pratt, L. A., and Kolter, R. (1998) Genetic analysis of *Escherichia coli* biofilm formation: roles of flagella, motility, chemotaxis and type I pili. *Mol. Microbiol.* 30(2): 285-293.

Raad, I. I., Chatzinikolaou, I., Chaiban, G., Hanna, H., Hachem, R., Dvorak, T., and Shrerertz, R. (2002) In Vitro and Ex Vivo Activity of Minocycline and EDTA (M-

EDTA) against Microorganisms Embedded in Biofilm on Catheters. *Abstr Intersci Conf Antimicrob Agents Chemother Intersci Conf Antimicrob Agents Chemother.* 42: abstract no. K-75.

Rao, D., Webb, J. S., and Kjelleberg, S. (2005) Competitive interactions in mixed-species biofilms containing the marine bacterium Pseudoalteromonas tunicate. *Appl Environ Microbiol.* 71(4): 1729-36.

Rice, A. S., Koh, K. S., Queck, S. Y., Labbate, M., Lam, K. W., and Kjelleberg, S. (2005) Biofilm formation and sloughing in *Serratia marcescens* are controlled by quorum sensing and nutrient cues. *J. Bacteriol.* 187(19): 2477-3485.

Richet, H. (2000) A strategy to control the emergence of antimicrobial resistance. *In:* R. C. Mahajan, and A. Therwath. (eds) Multi-Drug Resistance in Emerging and Re-emerging Diseases. Indian National Science Academy: Narosa Pub. House: New Delhi. pp. 219-222.

Sá-Correia, I., and Fialho, A. M. (2000) Electrotransformation of *Sphingomonas pancimobilis. In:* N. Eynard, and J. Teissie (eds) Electrotransformation of bacteria. Springer: Berlin. pp. 108-118.

Sauer, K., Camper, A. K., Ehrlich, G. D., Costerton, J. W., and Davies, D.G. (2002) *Pseudomonas aeruginosa* Displays Multiple Phenotypes during Development as a Biofilm. *J. Bacteriol.* 184(4): 1140-1154.

Sklar, A. S. (2005) Flow Cytometry for Biotechnology, Oxford University Press: London. pp. 4-5.

Spaeth, R. and Wuertz, S. (2000) Extraction and quantification of extracellular polymeric substances from wastewater. *In:* H. Flemming, U. Szewzyk, and T. Griebe (eds) Biofilms: Investigative methods and Application. Technomic Publishing Co.: Lancaster. pp. 51-65.

Spencer, P. Greenman, J., McKenzie, C., Gafan, G., Spratt, D., and Flanagan, A. (2007) In vitro biofilm model for studying tongue flora and malodour. *J. Appl. Microbiol.* 103(4): 985-992.

Starkey, M., and Gray, K. A. (2004) A sticky business: the extracellular polymeric substance matrix of bacterial biofilms. *In:* Ghannoum, M., and O'Toole, G. A. (eds) Microbial biofilms. ASM Press: Washington, DC. pp.174-191.

Steen, H. B., Boye, E. (1980) Bacterial growth studied by flow cytometry. *Cytometry.* 1(1): 32-36.

Stoodley, P., Wilson, S., Hall-Stoodley, L., Boyle, J.D., Lappin-Scott, H.M. and J.W. Costerton. (2001). Growth and detachment of cell clusters from mature mixed species

biofilms. *Appl. Env. Microbiol.* 67(12): 5608-13.

Stover, C. K., Pham, X. Q., Erwin, A. L., Mizoguchi, S. D., Warrener, P., Hickey, M. J., Brinkman, F. S., Hufnagle, W. O., Kowalik, D. J., Lagrou, M., Garber, R. L., Goltry, L., Tolentino, E., Westbrock-Wadman, S., Yuan, Y., Brody, L. L., Coulter, S. N., Folger, K. R., Kas, A., Larbig, K., Lim, R., Smith, K., Spencer, D., Wong, G. K., Wu, Z., Paulsen, I. T., Reizer, J., Saier, M. H., Hancock, R. E., Lory, S., and Olson, M. V., (2000) Complete genome sequence of Pseudomonas aeruginosa PA01, an opportunistic pathogen. *Nature.* 406(6799): 959-964.

Sturman, P.J., Stewart, P. S., Cunningham, A. B., Bouwer, E. J. and Wolfram, J. H., (1995) Engineering Scale-up of In Situ Bioremediation Processes: A Review, J. *Contaminant Hydrology*, 19:171-203.

Squier, C., Yu, V. L., and Stout, J. E. (2000) Waterborne noscomial infections. *Current Infectious Disease Reports.* 2(6): 490-496.

Suller, M. T. E., and Lloyd, D. (1999) Fluorescence monitoring of antibiotic-induced bacterial damage using flow cytometry. *Cytometry.* 35(3): 235-241.

Tait, K., and Sutherland, I. W. (2002) Antagonistic interactions amongst bacteriocin-producing enteric bacteria in dual species biofilms, *J Appl Microbiol.* 93(2): 345-52.

Takena, S., Iwaku, M., and Hoshino, E. (2003) Artificial *Pseudomonas aeruginosa* biofilms and confocal laser scanning microscopic analysis. *J Infect Chemother.* 7:87-93.

Talaro, K. P, and Talaro, A. (2003) Foundations in Microbiology: Basic Principles, 5th edition, McGraw Hill: Boston. pp. 1-12.

Tsuneda, S., Aikawa, H., Hayashi, H., Yuasa, A., and Hirata, A. (2003) Extracellular polymeric substances responsible for bacterial adhesion onto solid surface. *FEMS Microbiology Letters.* 223: 287-292.

Valle, J., Da Re, S., Henry, N., Fontaine, T., Balestrino, D., Latour-Lambert, P., and Ghigo, J. M. (2006) Broad-spectrum biofilm inhibition by a secreted bacterial polysaccharide. *Proc Natl Acad Sci.* 103(33): 12558–12563

Varnam, A. H., and Evans, M. G., (2000), Environmental Microbiology, Manson Publishing Ltd.: London. p. 8.

Vida, T. A. and Emr, S. D. (1995) A new vital stain for visualizing vacuolar membrane dynamics and endcytosis in yeast. *J. Cell Biol.* 128 (5):779-92.

Watson, J. V., (1991) Introduction to Flow Cytometry, Cambridge University Press,: Cambridge. p. 2.

Weaver, J. C. (1995) Electroporation theory: concepts and mechanisms. *In:* J. A. Nickoloff (Ed.) Electroporation protocols for microorganisms. Humana Press: Tottowa, New Jersey. pp. 1-26.

Wingender, T. Neu, R., and Flemming, H. C., (1999) Microbial Extracellular Polymeric Substances: Characterization, Structure and Function, Springer-Verlag: Berlin Heidelberg, Germany, pp 1-15.

Zhang, J., Campbell, R. E., Ting, A. Y., and Tsien, R. Y. (2002) Creating new fluorescent probes for cell biology. *Nat. Rev. Mol. Cell. Biol.* 3: 906-918.

Zhang, X., Bishop, P. L., and Kinkle, B. K. (1999) Comparison of extraction methods for quantifying extracellular polymers in biofilms. *Water Science and Technology.* 39(7): 211-218.

Zhang, Y., Vilcheze, C., and Jacobs, W. R., (2005) Mechanisms of Drug Resistance in *Mycobacterium tuberculosis. In:* Cole, S. T., Eisenach, K. D., McMurray, D. N., and Jacobs, W. R. (eds) Tuberculosis and the Tubercle Bacillus. ASM Press: Washington, DC. p. 129.

Appendices

Appendix A – CLSM configurations

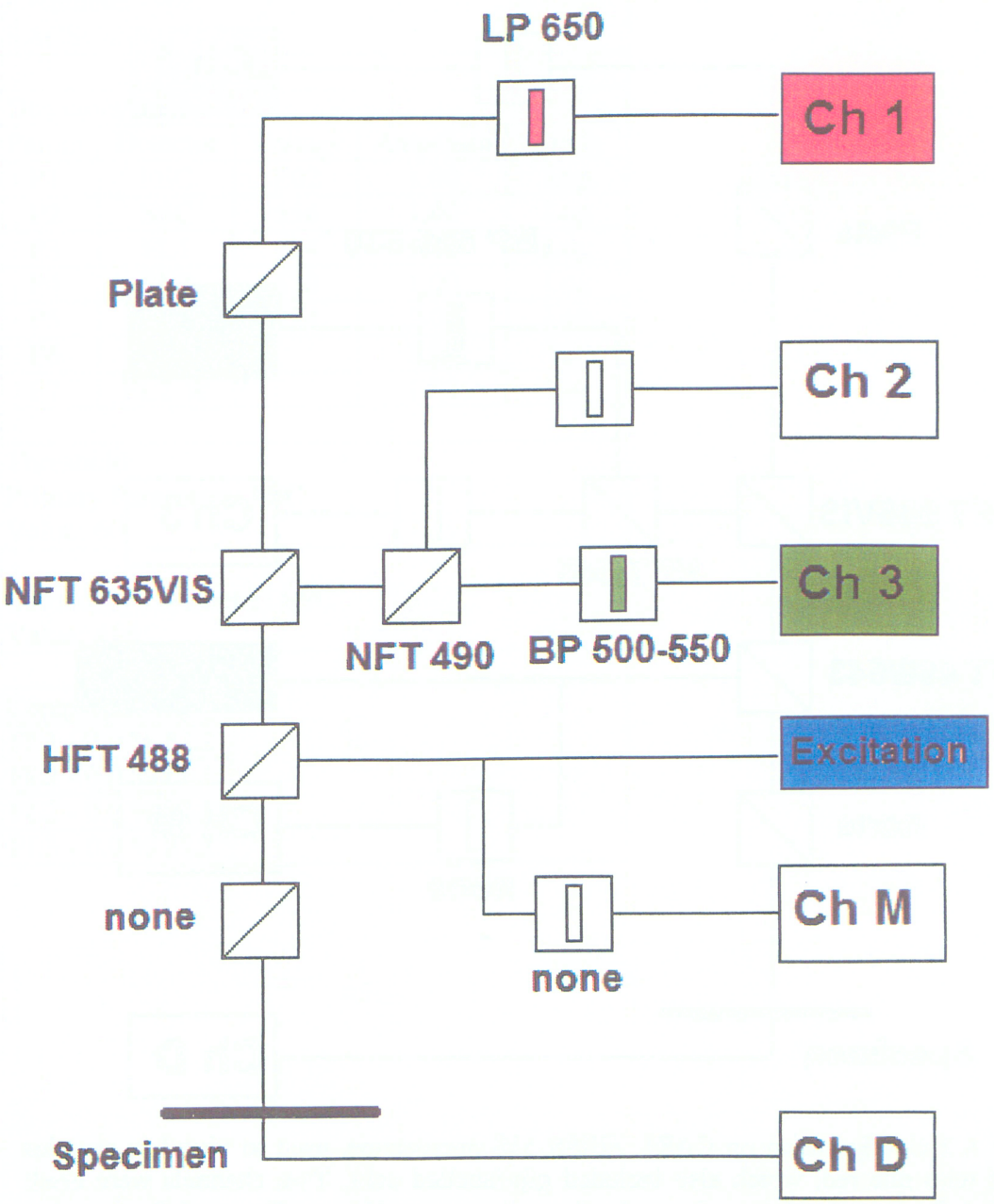

Figure A.1. Configuration on CARL ZEISS 510 microscope, used to visualize samples stained with FM 4-64, which also included gfp-labelled cells. Two channels were used; cells that fluoresced red were imaged using a long pass 650 nm filter and fluorescence from gfp-tagged cells was imaged using a band pass 500-550 nm filter.

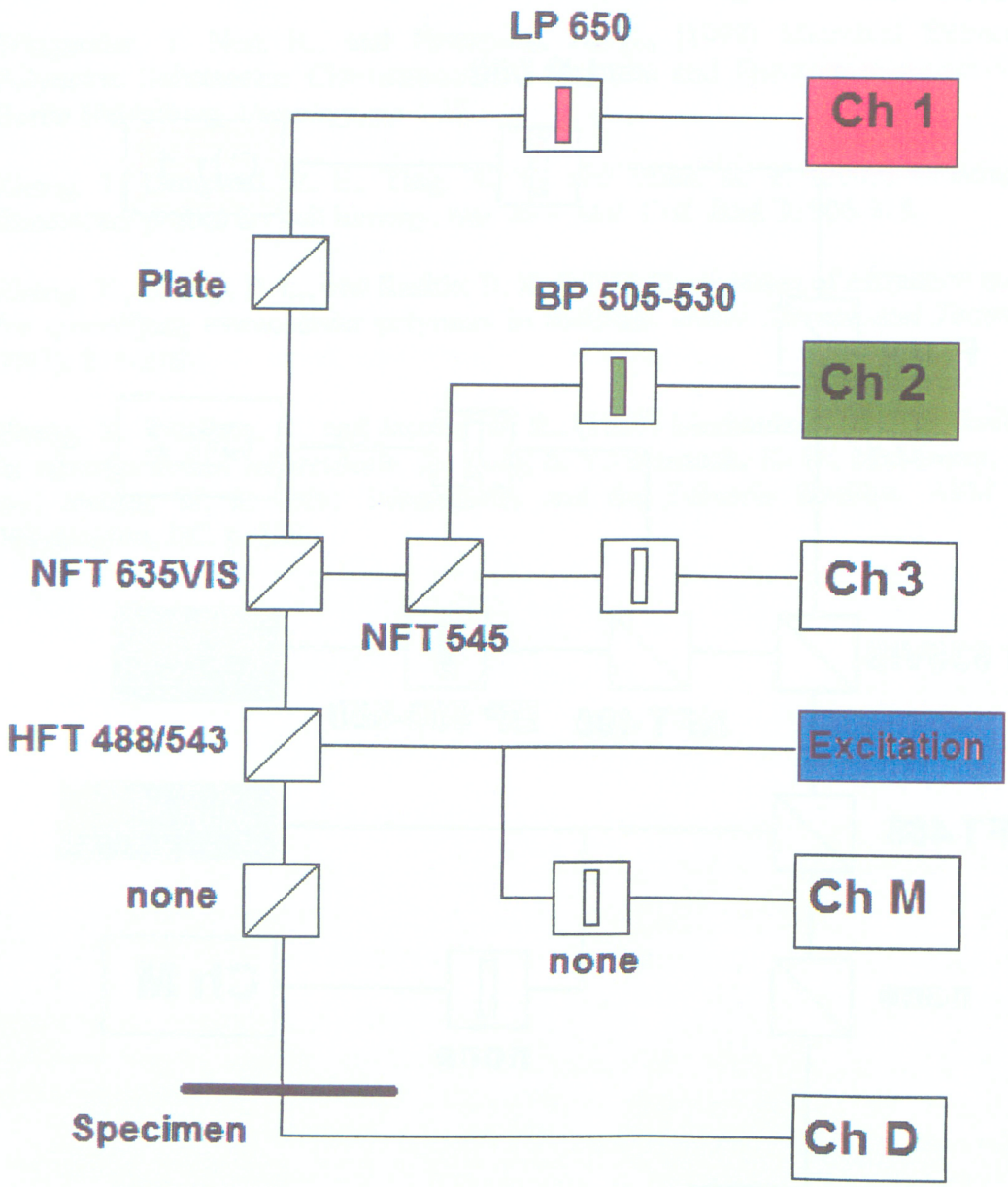

Figure A.2 Configuration on CARL ZEISS 510 microscope, used to visualize samples stained with nile red, which also included gfp-labelled cells. Two channels were used; cells that fluoresced red were imaged using a long pass 650 nm filter and fluorescence from gfp-tagged cells was imaged using a band pass 500-530 nm filter.

Appendix B - Flow cytometry instrument settings

Table B.1 Instrument settings used for flow cytometry on biofilm effluent samples containing gfp-fluorescent cells and community 1 cells stained with FM 4-64.

Cytometer type:
FACSCalibur

Detectors/Amps:

Param	Detector	Voltage	AmpGain	Mode
P1	FSC	E02	1.00	Log
P2	SSC	556	1.00	Log
P3	FL1	724	1.00	Log
P4	FL2	570	1.00	Log
P5	FL3	724	1.00	Log
P6	FL2-A		1.00	Lin
P7	FL2-W		1.00	Lin

Threshold:
Primary Parameter: FSC
Value: 60

Secondary Parameter: SSC
Value: 416

Compensation:

FL1 - 0.0 % FL2
FL2 - 0.0 % FL1
FL2 - 0.0 % FL3
FL3 - 0.0 % FL2